Hydrographic Observations at the Woods Hole Oceanographic Institution Hawaii Ocean Time-series Site: 2011 – 2012 Data Report #8

Fernando Santiago-Mandujano, Daniel McCoy, Cameron Fumar, Craig Nosse, Albert Plueddemann, Robert Weller, Roger Lukas, Jefrey Snyder, Sean Whelan, Jeffrey Lord, Nan Galbraith and Ethan Roth

March, 2015

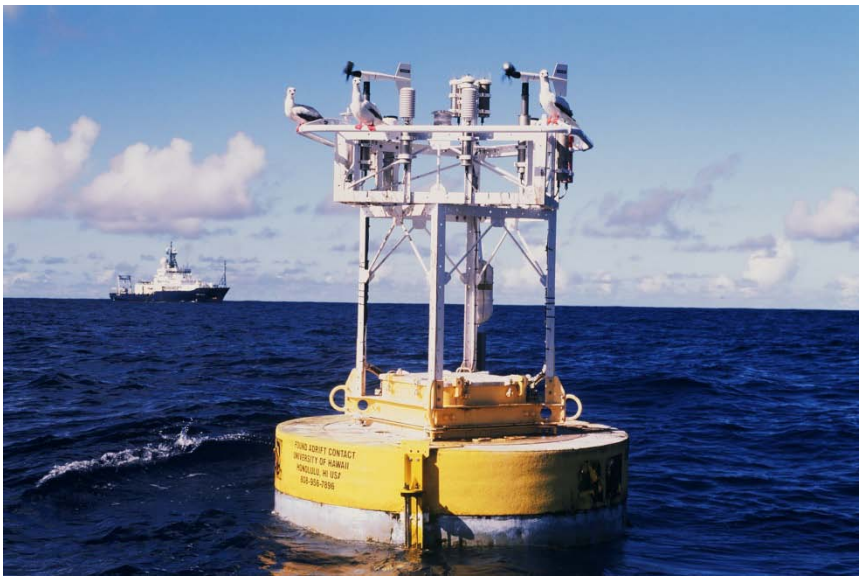

SCHOOL OF OCEAN AND EARTH SCIENCE AND TECHNOLOGY
UNIVERSITY OF HAWAI'I AT MĀNOA
SOEST Publication # 9296

Acknowledgments

Many people participated in the WHOTS mooring deployment/recovery cruises. They are listed in Table 2-1 and Table 2-4. We gratefully acknowledge their contributions and support. Thanks are due to all the personnel of the Upper Ocean Processes Group (UOP) at WHOI who prepared the WHOTS buoy's instrumentation and mooring; to Alison Andrews, Jennifer George, David Hashisaka, Branden Nakahara, and Nicholas Seymour for their technical assistance with the moored and shipboard instrumentation; to Kellie Terada for her excellent project support, and to Joseph Gum for his shore-based support. We gratefully acknowledge the support from the colleagues at Sea-Bird for helping us maintain the quality of the CTD data. We would also like to thank the captains and crew of the Ship *Hi'ialakai* and especially the University of Hawaii (UH) Marine Center staff for their efforts. The WHOTS Ocean Reference Station mooring is funded by the National Oceanic and Atmospheric Administration (NOAA) through the Cooperative Institute for Climate and Ocean Research (CICOR) under Grant No. NA09OAR4320129 to the Woods Hole Oceanographic Institution. Support for preparation and processing of subsurface instrumentation at WHOI is via a subcontract from the UH NSF project (OCE-0926766).

Table of Contents

1. Introduction

In 2003, Robert Weller (Woods Hole Oceanographic Institution [WHOI]), Albert Plueddemann (WHOI) and Roger Lukas (University of Hawaii [UH]) proposed to establish a long-term surface mooring at the Hawaii Ocean Time-series (HOT) Station ALOHA (22°45'N, 158°W) to provide sustained, high-quality air-sea fluxes and the associated upper ocean response as a coordinated part of the HOT program, and as an element of the global array of ocean reference stations supported by the National Oceanic and Atmospheric Administration's (NOAA) Office of Climate Observation.

With support from NOAA and the National Science Foundation (NSF), the WHOI HOT Site (WHOTS) surface mooring has been maintained at Station ALOHA since August 2004. The objective of this project is to provide long-term, high-quality air-sea fluxes as a coordinated part of the HOT program and contribute to the goals of observing heat, fresh water and chemical fluxes at a site representative of the oligotrophic North Pacific Ocean. The approach is to maintain a surface mooring outfitted for meteorological and oceanographic measurements at a site near Station ALOHA by successive mooring turnarounds. These observations are being used to investigate air-sea interaction processes related to climate variability and change.

The original mooring system is described in the mooring deployment/recovery cruise reports (Plueddemann et al., 2006; Whelan et al., 2007). Briefly, a Surlyn foam surface buoy is equipped with meteorological instrumentation including two complete Air-Sea Interaction Meteorological (ASIMET) systems (Hosom et al. (1995), Colbo and Weller (2009)) measuring air and sea surface temperatures, relative humidity, barometric pressure, wind speed and direction, incoming shortwave and longwave radiation, and precipitation. Complete surface meteorological measurements are recorded every minute, as required to compute air-sea fluxes of heat, freshwater and momentum. Each ASIMET system also transmits hourly averages of the surface meteorological variables via the Argos satellite system and via iridium. The mooring line is instrumented in order to collect time series of upper ocean temperatures, salinities and velocities with the surface forcing record. This includes vector measuring current meters, conductivity, salinity and temperature recorders, and two Acoustic Doppler current profilers (ADCPs). See the WHOTS-8 mooring diagram in Figure 1-1.

The subsurface instrumentation is located vertically to resolve the temporal variations of shear and stratification in the upper pycnocline to support study of mixed layer entrainment. Experience with moored profiler measurements near Hawaii suggests that Richardson number estimates over 10 m scales are adequate. Salinity is clearly important to the stratification, as salt-stratified barrier layers are observed at HOT and in the region (Kara et al., 2000), so we use Sea-Bird MicroCATs with vertical separation ranging from 5-20 m to measure temperature and salinity. We use an RDI ADCP to obtain current profiles across the entrainment zone and another in the mixed layer. Both ADCPs are in an upward-looking configuration, one is at 125 m, using 4 m bins, and the other is a 47.5 m using 2 m bins. To provide near-surface velocity (where the ADCP estimates are less reliable) we deploy two Vector Measuring Current Meters (VMCMs). The nominal mooring design is a balance between resolving extremes versus typical annual cycling of the mixed layer (see WHOTS Data Report 1-2, Santiago-Mandujano et al., 2007).

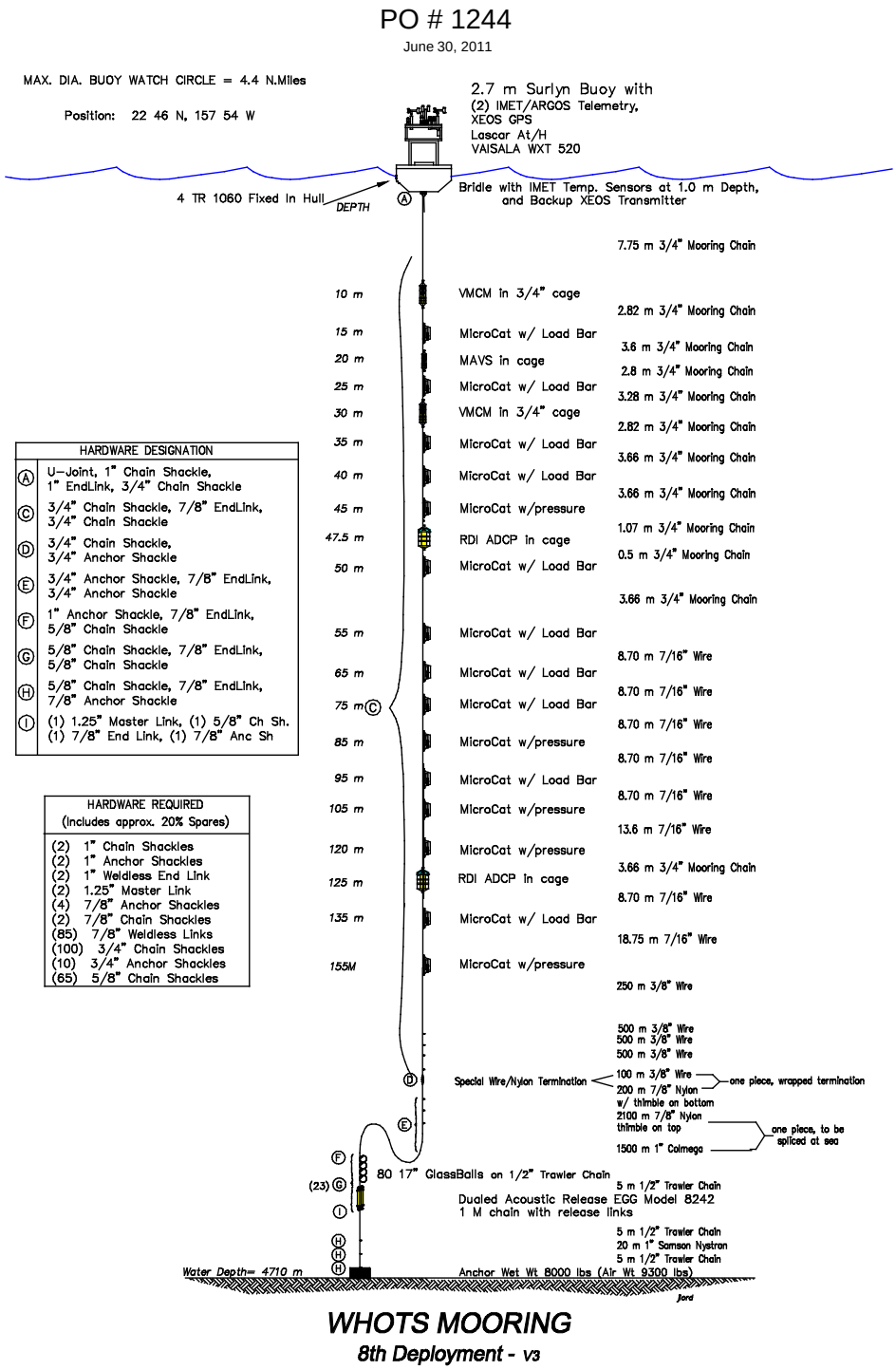

Figure 1-1. WHOTS-8 mooring design.

The eighth WHOTS mooring (WHOTS-8 mooring) was deployed in July 2011, and it was recovered in June 2012 during an 8-day cruise (WHOTS-9 cruise), both cruises aboard the NOAA Ship *Hi'ialakai*. A ninth mooring was deployed during the WHOTS-9 cruise; to be recovered July 2013.

This report documents and describes the oceanographic observations made on the WHOTS-8 mooring during a period of nearly one year, and from shipboard during the two cruises when the mooring was deployed and recovered. Sections 2 and 3, respectively, include a detailed description of the cruises and the mooring. Sampling and processing procedures of the hydrographic casts, thermosalinograph, and shipboard ADCP data collected during cruises are in Section 4. Section 5 includes the processing procedures for the data collected by the moored instruments: SeaCATs, MicroCATs, VMCMs, and moored ADCP. Plots of the resulting data and a preliminary analysis are included in Section 6.

2. Description of the WHOTS-8 Mooring Cruises

A. WHOTS-8 Cruise: WHOTS-8 Mooring Deployment

The Woods Hole Oceanographic Institution Upper Ocean Processes Group (WHOI/UOP), with the assistance of the UH group conducted the eighth deployment of the WHOTS mooring on board the NOAA Ship *Hi'ialakai* during the WHOTS-8 cruise between 5 and 14 July 2011. The WHOTS-8 mooring was deployed at HOT Station 52 on 07 July 2011 at 01:08 UTC. The scientific personnel that participated during the cruise are listed in Table 2-1.

Table 2-1. Scientific personnel on Ship Hi'ialakai *during the WHOTS-8 deployment cruise.*

Cruise	**Name**	**Title or function**	**Affiliation**
WHOTS-8	Plueddemann, Albert	Chief Scientist	WHOI
	Lukas, Roger	Professor/PI	UH
	Whelan, Sean	Senior Engineering Assistant	WHOI
	Pietro, Ben	Engineering Assistant	WHOI
	Snyder, Jefrey	Marine Technician	UH
	Fumar, Cameron	Research Associate	UH
	McCoy, Daniel	Research Associate	UH
	Roth, Ethan	Marine Technician	UH
	George, Jennifer	Volunteer	UH
	Nakahara, Branden	Volunteer	UH
	Wolfe, Dan	Scientist	NOAA/CIRES

The shipboard oceanographic observations during the cruise were conducted by the UH group. A complete description of these operations is available in the WHOTS-8 cruise report (Whelan *et al*., 2012).

A Sea-Bird CTD (conductivity, temperature and depth) system was used to measure T, S, and O_2 profiles during eleven CTD casts. The time, location, and maximum CTD pressure for each of the profiles are listed in Table 2-2.

One cast was conducted to 1020 dbar at a test site near Oahu. Five CTD casts were conducted at Station 50 near the WHOTS-7 mooring for comparison with subsurface instruments before its recovery; each cast was to 500 dabr except the last one which was to 1020 dbar. Five CTD casts were made at Station 52 near the WHOTS-8 mooring for comparison with subsurface instruments after the WHOTS-8 mooring deployment; each cast was to 500 dbar. These casts were sited approximately 200 to 500 m from the buoys and consisted of 4 yo-yo cycles between 10 dbar and 200 dbar and then to 500 dbar (5th yo-yo cycle of each cast) except for the last cast at Station 50 which went to 1020 dbar. Four to five salinity samples were taken from each cast to calibrate the conductivity sensors used for the CTD profiling.

Additionally, five more CTD casts were conducted on July 12th as part of a survey through an anti-cyclonic eddy that had been monitored during the cruise while on station. The survey utilized five stations (Figure 2-1). Station 51 was located northeast of the WHOTS mooring sites in an attempt to assess the center of the eddy. Station 53 was located southwest of the WHOTS 16 mooring sites to assess the area outside of the eddy. Station 2 is the center of Station ALOHA; the primary site for HOT cruise work and will be re-occupied by a HOT cruise on July 19th.

Stations 50 and 52 were the same sites used for the comparison work conducted July 7-10, 2011 and provided an opportunity for a temporal comparison of both the eddy and subsurface instruments on the WHOTS-8 mooring. All CTD casts conducted as part of the eddy survey were to 1020 dbars.

Table 2-2. CTD stations occupied during the WHOTS-8 deployment cruise

Station/cast	Date	Time (UTC)	Location	Max pressure (dbar)
Test	7/6/11	06:05	21° 27.98´ N, 158° 20.70´ W	1036
52 / 1	7/7/11	16:07	22° 40.57´ N, 157° 58.97´ W	498
52 / 2	7/7/11	19:36	22° 40.65´ N, 157° 59.03´ W	502
52 / 3	7/7/11	23:45	22° 40.88´ N, 157° 59.14´ W	502
52 / 4	7/8/11	03:50	22° 40.93´ N, 157° 59.14´ W	510
52 / 5	7/8/11	07:31	22° 40.49´ N, 157° 59.66´ W	506
50 / 1	7/9/11	15:43	22° 46.56´ N, 157° 55.95´ W	504
50 / 2	7/9/11	19:37	22° 46.57´ N, 157° 56.01´ W	504
50 / 3	7/9/11	23:36	22° 47.00´ N, 157° 55.87´ W	504
50 / 4	7/10/11	03:42	22° 47.00´ N, 157° 55.66´ W	508
50 / 5	7/10/11	07:32	22° 46.84´ N, 157° 55.90´ W	1022
51 / 1	7/12/11	16:15	22° 47.85´ N, 157° 49.96´ W	1022
50 / 6	7/12/11	18:06	22° 46.90´ N, 157° 56.09´ W	1014
2 / 1	7/12/11	19:47	22° 44.95´ N, 158° 00.00´ W	1018
52 / 6	7/12/11	21:46	22° 40.97´ N, 157° 59.02´ W	1016
53 / 1	7/12/11	23:53	22° 40.02´ N, 158° 05.04´ W	1024

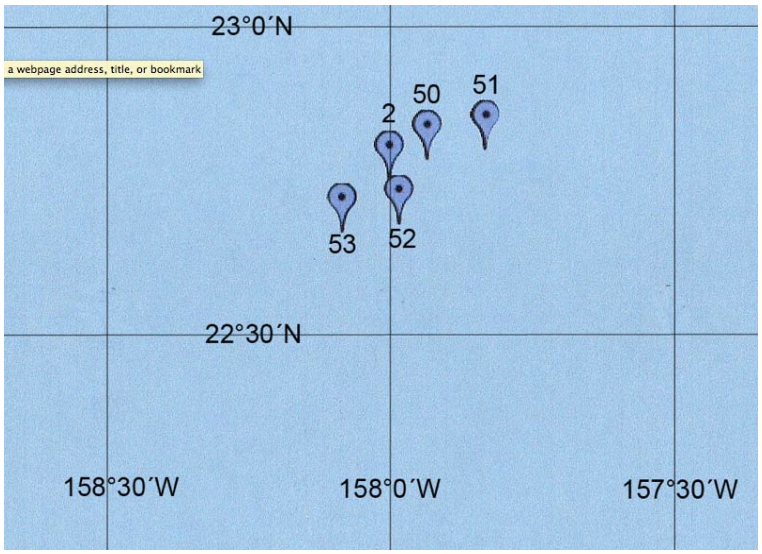

Figure 2-1. General map of hydrographic survey on 12 July 2011.

In addition, continuous acoustic Doppler current profiler (ADCP) and near surface thermosalinograph (TSG) data were obtained while underway.

The NOAA Ship *Hi'ialakai* was equipped with an RD Instruments Ocean Surveyor 75 kHz ADCP, set to function in broadband and narrowband configurations. Configurations for each system are shown in Table 2-3. The ADCP used input from a S.G. Brown gyrometer and a Furuno GP 90 GPS receiver to establish the heading and attitude of the ship while an Applanix POSMV4 system archived attitude data for use in post-processing.

Table 2-3. Configuration of the Ocean Surveyor 75kHz ADCP on board the NOAA Ship Hi'ialakai during the WHOTS-8 deployment cruise.

	OS75BB*	OS75NB
Sample interval (s)	900	900
Number of bins	80	60
Bin Length (m)	8	16
Pulse Length (m)	8	16
Transducer depth (m)	5	5
Blanking length (m)	16	24

*Broadband mode unavailable for WHOTS-8

Near-surface temperature and salinity data for WHOTS-8 cruise were acquired through a thermosalinograph (TSG) system aboard NOAA Ship *Hi'ialakai.* The system was comprised of a Sea-Bird model SBE-21 measuring temperature and conductivity from the ship's flow through system. These instruments were set to record data every 60 seconds. NOAA Ship *Hi'ialakai* has a thermosalinograph intake depth of 2 m below the sea surface in the bow thruster room. The data were acquired continuously during the WHOTS-8 deployment cruise, with salt calibration

samples taken roughly three times per day from an outlet in the flow through system located less than 0.5 m from the TSG.

B. WHOTS-9 Cruise: WHOTS-8 Mooring Recovery

The WHOI/UOP Group conducted the mooring turnaround operations during the WHOTS-9 cruise between 12 and 19 June 2012 aboard the NOAA Ship *Hi`ialakai*. The WHOTS-9 mooring was deployed at Station 50 on 14 June 2012 at 02:23 UTC.

The scientific personnel that participated during the cruise are listed in Table 2-4.

Table 2-4. Scientific personnel on Ship Hi`ialakai *during the WHOTS-9 cruise (WHOTS-8 recovery).*

Cruise	**Name**	**Title or function**	**Affiliation**
WHOTS-9	Plueddemann, Albert	Chief Scientist	WHOI
	Ryder, James	Scientist	WHOI
	Pietro, Ben	Engineering Assistant	WHOI
	Smith, Jason	Senior Engineering Assistant	WHOI
	Duncombe Rae, Chris	Scientist	WHOI
	Lukas, Roger	Professor/Co-PI	UH
	Nosse, Craig	Marine Research Associate	UH
	Snyder, Jefrey	Marine Electronics Technician	UH
	Fumar, Cameron	Research Associate	UH
	Andrews, Alison	Marine Technician	UH
	Hashisaka, David	Marine Research Associate	UH
	Roth, Ethan	Marine Research Engineer	UH
	Seymour, Nicholas	Marine Technician	UH
	Barteau, Ludovic	Scientist	CIRES
	Park, Sang-Jong	Scientist	KOPRI

The shipboard oceanographic observations during the cruise were conducted by the UH group. A complete description of these operations is available in the WHOTS-9 cruise report (Plueddemann *et al*., 2013).

A Sea-Bird CTD (conductivity, temperature and depth) system was used to measure T, S, and O_2 profiles during ten CTD casts. The time, location, and maximum CTD pressure for each of the profiles are listed in Table 2-5. One cast was conducted at a test site near Oahu to 1020 dbar. Four CTD casts were conducted at Station 52 near the WHOTS-8 mooring for comparison with subsurface instruments before its recovery; each cast was to 500 dbar. Five CTD casts were made at Station 50 near the WHOTS-9 mooring for comparison with subsurface instruments after the WHOTS-9 mooring deployment; each cast was to 500 dbar. Four salinity samples were taken from each 500 dbar cast to calibrate the conductivity sensors used for the CTD profiling.

Table 2-5. CTD stations occupied during the WHOTS-9 Deployment cruise

Station	Date	Time (GMT)	Location	Maximum pressure (dbar)
Test	6/13/12	06:03	21° 28.06' N, 158° 21.13' W	1024
50/1	6/14/12	15:49	22° 47.78' N, 157° 54.04' W	502
50/2	6/14/12	19:47	22° 47.66' N, 157° 53.81' W	502
50/3	6/14/12	23:52	22° 47.66' N, 157° 53.72' W	500
50/4	6/15/12	03:50	22° 47.66' N, 157° 53.66' W	502
50/5	6/15/12	07:50	22° 47.66' N, 157° 53.50' W	516
52/1	6/16/12	03:51	22° 41.96' N, 157° 56.38' W	502
52/2	6/16/12	07:51	22° 41.66' N, 157° 56.65' W	502
52/3	6/16/12	11:50	22° 41.75' N, 157° 56.79' W	502
52/4	6/16/12	15:51	22° 41.92' N, 157° 56.74' W	502

In addition, continuous acoustic Doppler current profiler (ADCP) and near surface thermosalinograph (TSG) data were obtained while underway.

The NOAA Ship *Hi'ialakai* was equipped with an RD Instruments Ocean Surveyor 75 kHz ADCP, set to function in broadband and narrowband configurations. Configurations for each system are shown in Table 2-6. The ADCP used input from a S.G. Brown gyrometer and a Furuno GP 90 GPS receiver to establish the heading and attitude of the ship while an Applanix POSMV4 system archived attitude data for use in post-processing.

Table 2-6. Configuration of the Ocean Surveyor 75kHz ADCP on board the NOAA Ship Hi'ialakai during the WHOTS-9 deployment cruise.

	OS75BB*	OS75NB
Sample interval (s)	900	900
Number of bins	80	60
Bin Length (m)	8	16
Pulse Length (m)	8	16
Transducer depth (m)	5	5
Blanking length (m)	16	24

*Broadband mode unavailable for WHOTS-9

Near-surface temperature and salinity data during the WHOTS-9 cruise were acquired through the use of a thermosalinograph (TSG) system aboard NOAA Ship *Hi'ialakai.* The system was comprised of a model SBE-21. These instruments were set to record data every 60 seconds. NOAA Ship *Hi'ialakai* has a thermosalinograph intake depth of 2 m. Since the thermosalinograph sensor is located inside the ship, sea water traveling through the intake plumbing is subjected to the environmental temperature of the ship. Therefore, as the thermosalinograph temperature data could be affected by heating or cooling of the ship, it should be considered suspect. The data were acquired continuously during the WHOTS-9 cruise, with salt calibration samples taken roughly three times per day from an outlet in the flow through

system located less than 0.5 m from the TSG. In addition, the temperature and salinity records were checked against the CTD station data.

3. Description of WHOTS-8 Mooring

The WHOTS-8 mooring, deployed on 7 July 2011 from NOAA's Ship *Hi'ialakai*, was outfitted with two complete sets (L09 and L10) of ASIMET sensors on the buoy and underneath, and subsurface instruments from 10 to 155 m depth (Figure 1-1). The WHOTS-8 recovery on 16 June 2012 resulted in 345 days on station.

The buoy tower also contains a radar reflector, two marine lanterns, and two independent Argos satellite transmission systems that provide continuous monitoring of buoy position. A Xeos Melo Global Positioning System (GPS) receiver, a SBE-39 temperature sensor adapted to measure air temperature and a Vaisala WXT-520 multi-variable (temperature, humidity, pressure, wind and precipitation) were also mounted on the tower. A fourth positioning system (SiS Argos transmitter) was mounted beneath the hull. Several other instruments were mounted on the buoy. A pCO_2 system, a pumped SBE-16 CTD and a SAMI-2 pH sensor were mounted to the underside of the buoy. The SHB-16 hosted turbidity and dissolved oxygen sensors. Five radiometers and a chlorophyll fluorometer were also mounted in one of the buoy access tubes.

Four internally-logging RBR TR-1060 temperature sensors and two SBE-37 MicroCATs were bolted to the underside of the buoy hull measuring sea surface temperature (SST) and salinity. The RBRs measured SST once every 60 sec between 80-95 cm below the surface, and the MicroCATs were at 1.55 m.

Instrumentation provided by UH for the WHOTS-8 mooring included 15 SBE-37 Microcats, an RDI 300 kHz Workhorse ADCP, an RDI 600 kHz Workhorse ADCP, and a Nobska MAVS acoustic velocity sensor. The Microcats all measured temperature and conductivity, with five also measuring pressure. WHOI provided two Vector Measuring Current Meters (VMCMs).

Table 3-1 provides a listing of the WHOTS-8 subsurface instrumentation at their nominal depths on the mooring, along with serial numbers, sampling rates and other pertinent information. Also included in the table are the four RBR TR-1060 and two MicroCATs from WHOI bolted to the underside of the buoy hull. A cold water spike was induced to the UH Microcats before deployment and after recovery by placing an ice pack in contact with their temperature sensor to check for any drift in their internal clock. Data from the SBE-16 (SN 6568) are analyzed elsewhere.

The RDI 300 kHz Workhorse Sentinel ADCP, SN 4891, with an additional external battery pack, was deployed at 125 m with transducers facing upwards. The instrument was set to ping at 4-second intervals for 160 seconds every 10 minutes. This burst sampling was designed to minimize aliasing by occasional large ocean swell orbital motions. Bin size was set for 4 m. The total number of ensemble records was 27,197. The first ensemble was at 7/06/2011 05:20:00Z, and the last was at 1/11/2012 01:59:59Z. This instrument also measured temperature.

The RDI 600 kHz Workhorse Sentinel ADCP, SN 1825, with an additional external battery pack, was deployed at 47.5 m with transducers facing upwards. The instrument was set to ping at 2-second intervals for 160 seconds every 10 minutes. This burst sampling was designed to minimize aliasing by occasional large ocean swell orbital motions. Bin size was set for 2 m. The total number of ensemble records was 24,443. The first ensemble was at 7/06/2011 05:20:00, and the last was at 12/22/2011 23:00:00. This instrument also measured temperature.

The two VMCMs, SN 016 and 019 were deployed at 10 m and 30 m depth respectively. The instruments were prepared for deployment by the WHOI/UOP group and set to sample at 1-minute intervals. These instruments also measured temperature.

A Nobska MAVS SN 10260 acoustic velocity sensor was deployed a 20 m in a downward orientation. The instrument was set to ping at 2-second intervals for 160 seconds every 30 minutes. This burst sampling was designed to minimize aliasing by occasional large ocean swell orbital motions. The deployment of the MAVS was largely unsuccessful, as one of the instrument's four transducers failed soon after the deployment.

All WHOTS-8 instruments were successfully recovered; post-deployment information for the C-T instruments is shown in Table 3-2.

Table 3-1. WHOTS-8 mooring subsurface instrument deployment information. All times are in UTC.

SN	Instrument	Depth	Pressure SN	Sample Interval (sec)	Start Logging Data (UTC)	Cold Spike-IN (UTC)	Cold Spike-OUT (UTC)	Time in Water (UTC)
20565	RBR 1060	1	N/A	60	6/28/11 22:01	N/A	N/A	7/6/11 18:55
20566	RBR 1060	1	N/A	60	6/28/11 22:01	N/A	N/A	7/6/11 18:55
20567	RBR 1060	1	N/A	60	6/28/11 22:01	N/A	N/A	7/6/11 18:55
20568	RBR 1060	1	N/A	60	6/28/11 22:01	N/A	N/A	7/6/11 18:55
6568	SBE-16	1	N/A	60	N/A	N/A	N/A	7/6/11 18:55
1835	Microcat	1.5	N/A	60	7/9/11 03:00	6/29/11 18:52	6/29/11 18:52	7/6/11 18:55
1727	Microcat	1.5	N/A	60	7/9/11 03:00	6/29/11 18:52	6/29/11 18:52	7/6/11 18:55
16	VMCM	10	N/A	60	7/7/11 3:00	N/A	N/A	7/6/11 18:34
6893	Microcat	15	N/A	150	6/30/11 0:00	7/1/11 23:30	7/2/11 0:00	7/6/11 18:29
10260	MAVS	20	N/A	1800	7/6/11 0:00	7/6/11 2:15	7/6/11 3:15	7/6/11 18:27
6894	Microcat	25	N/A	150	6/30/11 0:00	7/1/11 23:30	7/2/11 0:00	7/6/11 18:24
19	VMCM	30	N/A	60	7/7/11 3:00	N/A	N/A	7/6/11 18:21
6895	Microcat	35	N/A	150	6/30/11 0:00	7/1/11 23:30	7/2/11 0:00	7/6/11 18:18
6896	Microcat	40	N/A	150	6/30/11 0:00	7/1/11 23:30	7/2/11 0:00	7/6/11 18:15
6887	Microcat	45	2651319	180	6/30/11 0:00	7/1/11 23:30	7/2/11 0:00	7/6/11 18:12
1825	600 kHz ADCP	47.5	N/A	600	7/6/11 0:00	7/6/11 1:26	7/6/11 1:56	7/6/11 19:17
6897	Microcat	50	N/A	150	6/30/11 0:00	7/1/11 23:30	7/2/11 0:00	7/6/11 19:22
6898	Microcat	55	N/A	150	6/30/11 0:00	7/1/11 23:30	7/2/11 0:00	7/6/11 19:27
6899	Microcat	65	N/A	150	6/30/11 0:00	7/1/11 23:30	7/2/11 0:00	7/6/11 19:30
3618	Microcat	75	N/A	150	6/30/11 0:00	7/2/11 0:05	7/2/11 0:35	7/6/11 19:36
6888	Microcat	85	2651320	180	6/30/11 0:00	7/2/11 0:05	7/2/11 0:35	7/6/11 19:39
3617	Microcat	95	N/A	150	6/30/11 0:00	7/2/11 0:05	7/2/11 0:35	7/6/11 19:41
6889	Microcat	105	2651321	180	6/30/11 0:00	7/2/11 0:05	7/2/11 0:35	7/6/11 19:44
6890	Microcat	120	2651322	180	6/30/11 0:00	7/2/11 0:05	7/2/11 0:35	7/6/11 19:47
4891	300 kHz ADCP	125	N/A	600	7/6/11 0:00	7/6/11 0:55	7/6/11 1:25	7/6/11 19:50
3634	Microcat	135	N/A	150	6/30/11 0:00	7/2/11 0:05	7/2/11 0:35	7/6/11 19:53
6891	Microcat	155	2651323	180	6/30/11 0:00	7/2/11 0:05	7/2/11 0:35	7/6/11 19:59

Table 3-2. WHOTS-8 MicroCAT Recovery Information. All times stated are in UTC.

Depth (meters)	Seabird Serial #	Time out of water	Time of Spike	Time Logging Stopped	Samples Logged	Data Quality	File Name raw data
15	37SM31486-6893	06/17/2012 04:55	06/17/2012 19:37:00	06/17/2012 22:22:00	369,536	good	6893_recovery.cap
25	37SM31486-6894	06/17/2012 05:02	06/17/2012 19:37:00	06/17/2012 22:11:15	369,529	good	6894_recovery.cap
35	37SM31486-6895	06/17/2012 05:08	06/17/2012 19:37:00	06/17/2012 22:19:15	369,534	good	6895_recovery.cap
40	37SM31486-6896	06/17/2012 05:13	06/17/2012 19:37:00	06/18/2012 16:26:00	370,259	good	6896_recovery.cap
45	37SM31486-6887	06/17/2012 05:19	06/17/2012 19:37:00	06/18/2012 16:34:00	370,264	good	6887_recovery.cap
50	37SM31486-6897	06/17/2012 03:31	06/17/2012 19:37:00	06/18/2012 16:44:00	370,271	good	6897_recovery.cap
55	37SM31486-6898	06/17/2012 03:28	06/17/2012 19:37:00	06/17/2012 22:15:10	369,532	good	6898_recovery.cap
65	37SM31486-6899	06/17/2012 03:24	06/17/2012 19:37:00	06/17/2012 22:50:00	369,555	good	6899_recovery.cap
75	37SM31486-3618	06/17/2012 03:21	06/17/2012 19:37:00	06/17/2012 22:55:15	203,878	one bad time stamp	3618_recovery.cap
85	37SM31486-6888	06/17/2012 03:17	06/17/2012 19:37:00	06/17/2012 21:06:00	369,486	good	6888_recovery.cap
95	37SM31486-3617	06/17/2012 03:14	06/17/2012 19:37:00	06/17/2012 23:21:15	203,888	good	3617_recovery.cap
105	37SM31486-6889	06/17/2012 03:11	06/17/2012 19:37:00	06/17/2012 21:02:15	369,483	good	6889_recovery.cap
120	37SM31486-6890	06/17/2012 03:07	06/17/2012 19:37:00	06/17/2012 20:57:30	369,480	good	6890_recovery.cap
135	37SM31486-3634	06/17/2012 03:01	06/17/2012 19:37:00	06/17/2012 23:24:30	203,890	good	3634_recovery.cap
155	37SM31486-6891	06/17/2012 02:56	06/17/2012 19:37:00	06/17/2012 21:09:05	369,487	good	6891_recovery.cap

The data from the upward-looking 300 kHz ADCP at 125 m ends in January 2012. The instrument was not pinging upon recovery. Examination of the connectors on both the transducer and battery units showed corrosion. It appears that water may have leaked through those connectors and possibly caused the ADCP to stop recording data. This issue was seen previously for the WHOTS-7 deployment.

The data from the upward-looking 600 kHz ADCP at 47.5 m ends in December 2011. The instrument was not pinging upon recovery. Examination of the connectors on both the transducer and battery units showed corrosion. It appears that water may have leaked through those connectors and possibly caused the ADCP to stop recording data. This issue was seen previously for the WHOTS-7 deployment.

4. WHOTS-8 and -9 cruises shipboard observations

The hydrographic profile observations made during WHOTS cruises were obtained with a Sea-Bird CTD (conductivity, temperature and depth) instrument with duplicate temperature and conductivity, and oxygen sensors. Measurements were made to better than 0.01°C in temperature, 0.01 for salinity, and 1.5 µmol/kg in dissolved oxygen below 5 m. The CTD was installed on a rosette-sampler with 5-L Niskin bottles for calibration water samples. In addition, the NOAA Ship *Hi'ialakai* came equipped with a thermosalinograph system which provided a continuous depiction of temperature and salinity of the near-surface layer. Horizontal currents over the depth range of 30-1000 m were measured from the shipboard 75 kHz Ocean Surveyor ADCP (narrowband) with a vertical resolution of 16 m for the WHOTS-8 cruise. Broadband mode for the OS75 was available for WHOTS-9, with additional horizontal current data over the range of 20-650 m with a vertical resolution of 8 m.

A. Conductivity, Temperature and Depth (CTD) profiling

Continuous measurements of temperature, conductivity, dissolved oxygen and pressure were made with the UH Sea-Bird SBE-9/11Plus CTD underwater unit #09P43777-0850 (referred to as #0850) during the WHOTS-8 and WHOTS-9 cruises. The CTD was equipped with an internal Digiquartz pressure sensor and pairs of external temperature, conductivity, and oxygen sensors.

Each of the temperature-conductivity sensor pairs used a Sea-Bird TC duct which circulated seawater through independent pump and plumbing installations. The CTD configuration also included two oxygen sensors, installed in the plumbing for each sensor set. In both cruises, the CTD was mounted in a vertical position in the lower part of a rosette sampler, with the sensors' water intakes located at the bottom of the 12-place rosette.

The package was deployed on a conducting cable, which allowed for real-time data acquisition and display. The deployment procedure consisted in lowering the package to 10-15 dbar and waiting until the CTD pumps started operating. The CTD was then raised until the sensors were close to the surface to begin the CTD cast. The time and position of each cast was obtained via a GPS connection to the CTD deck box. Six Niskin bottles were used on the rosette. Four salinity samples were taken on each cast for calibration of the conductivity sensors.

1. Data acquisition and processing.

CTD data were acquired at the instrument's highest sampling rate of 24 samples per second. Digital data were stored on a laptop computer and, for redundancy, the analog signal was recorded on VHS video tapes. Backups of CTD data were made onto USB storage cards.

The raw CTD data were quality controlled and screened for spikes as described in the WHOTS Data Report 1 (Santiago-Mandujano et al., 2007). Data alignment, averaging, correction and reporting were done as described in Tupas *et al*. (1993). Spikes in the data occur when the CTD samples the disturbed water of its wake. Therefore, samples from the downcast were rejected when the CTD was moving upward or when its acceleration exceeded 0.5 m s^{-2} in

magnitude. The data were subsequently averaged into 2-dbar pressure bins after calibrating the CTD conductivity with the bottle salinities.

The data were additionally screened by comparing the T-C sensor pairs. These differences permitted identification of problems with the sensors. The data from only one T-C pair, whichever was deemed most reliable, is reported here. Only data from the downcast are reported, as upcast data are contaminated by rosette wake effects.

Temperature is reported in the ITS-90 scale. Salinity and all derived units were calculated using the UNESCO (1981) routines; salinity is reported in the practical salinity scale (PSS-78). Oxygen is reported in μmol kg^{-1}.

2. CTD sensor calibration and corrections

Pressure

The pressure calibration strategy for CTD pressure transducer SN 101430 used during WHOTS-8 and WHOTS-9 cruises employed a high-quality quartz pressure transducer as a transfer standard. Periodic recalibrations of this lab standard were performed with a primary pressure standard. The only corrections applied to the CTD pressures were a constant offset determined at the time that the CTD first enters the water on each cast. In addition, a span correction determined from bench tests on the sensor against the transfer standard was applied.

Transfer Standard Calibration

The transfer standard is a Paroscientific Model 760 pressure gauge equipped with a 10,000-PSI transducer. This instrument was purchased in March 1988, and was originally calibrated against a primary standard. Subsequent recalibrations have been performed every 2.5 years on average either at the Northwest Regional Calibration Center, at the Scripps Institute of Oceanography or at Fluke Electronics (DH Instruments Division). The latest calibrations were conducted at the Scripps Institute of Oceanography in April 1999, May 2001, May 2003, and July 2005; and at Fluke in July 2009 and November 2012.

CTD Pressure Transducer SN 51412 Bench Tests

CTD pressure transducer bench tests were done using an Ametek T-100 pump and a manifold to apply pressure simultaneously to the CTD pressure transducer and to the transfer standard. All these tests generated calibration data at six pressure levels between 0 and 4500 dbar, for both increasing and decreasing pressures. Pressure sensor SN 101430 was used during the WHOTS-8 and WHOTS-9 cruises. The results of the bench tests on this sensor are shown in Table 4-1. The 0-dbar offset is near zero and decreased slightly between 2011 and 2012, however, a more accurate offset was later determined for the time that the CTD first enters the water on each cast. The hysteresis from the bench tests has been small. A linear pressure dependent offset is applied during data collection to correct for the 0-4500 dbar span offset of about 1.24 dbar (Table 4-1).

Table 4-1. CTD pressure sensor #101430 calibrations against the transfer standard

Calibration Date	Offset @ 0 dbar	0-4500 dbar offset	Hysteresis
7 August 2012	-0.10	1.15	0.09
8 February 2012	0.00	1.19	0.06
12 August 2011	0.04	1.32	0.05
20 January 2011	0.15	1.20	0.10
12 August 2010	0.20	1.20	0.15
8 January 2010	0.20	1.30	0.16
9 September 2009	0.21	1.30	0.13
7 January 2009	0.28	1.10	0.10
26 August 2008	0.31	1.20	0.09
4 January 2008	0.27	1.10	0.12
24 July 2007	0.19	1.10	0.10
28 February 2007	0.05	1.00	0.08

Temperature

Two Sea-Bird SBE-3-Plus temperature transducers (#1416, #2454) were used during WHOTS-8 and -9 cruises, and were calibrated at Sea-Bird before and after each cruise to an accuracy better than 0.5 x 10^{-3}°C. Calibration coefficients obtained at Sea-Bird are listed in Table 4-2. These coefficients were used in the following formula that gives the temperature (in °C) as a function of the frequency signal (*f*):

$$Temperature = 1/\{a+b[ln(fo/f)]+c[ln^2(fo/f)+d[ln^3(fo/f]\}-273.15$$

For each sensor, we calculated the 0-30°C average offset for each calibration relative to the oldest one, and applied a linear fit to these offsets. A single baseline calibration was chosen and a temperature-independent offset relative to the baseline calibration was applied to the data to remove the temporal trend due to the sensor drift. The maximum drift correction for WHOTS cruises was less than 1.0 x 10^{-3}°C. The baseline calibration was selected as the one for which the trend-corrected average from 0-5°C was nearest to the ensemble mean of these averages.

Table 4-2. Calibration coefficients for Sea-Bird temperature sensors. RMS residuals from calibration give an indication of calibration quality.

SN	*Date yymmdd*	*f0*	*a*	*b*	*c*	*d*	*RMS (m°C)*
1416	130418	6233.46	3.68120966e-03	6.01717330e-04	1.46100832e-05	1.78997011e-06	0.28
1416	121221	6233.51	3.68120975e-03	6.01723831e-04	1.46108158e-05	1.78360634e-06	0.28
1416	120907	6233.47	3.68120979e-03	6.01715632e-04	1.46341513e-05	1.81681657e-06	0.28
1416	120512	6233.55	3.68121004e-03	6.01736349e-04	1.46939412e-05	1.86140829e-06	0.24
1416	120211	6233.55	3.68120995e-03	6.01726937e-04	1.46850658e-05	1.86458252e-06	0.28
1416	111208	6233.66	3.68120871e-03	6.01722327e-04	1.47288631e-05	1.91968969e-06	0.27
1416	110804	6233.73	3.68121041e-03	6.01714830e-04	1.46343735e-05	1.81119240e-06	0.25
1416	110331	6233.80	3.68120909e-03	6.01701993e-04	1.46000054e-05	1.77202876e-06	0.25
1416	101204	6233.82	3.68120939e-03	6.01690903e-04	1.45809993e-05	1.76471840e-06	0.23
1416	100819	6233.89	3.68121043e-03	6.01712719e-04	1.46569680e-05	1.83503331e-06	0.25
1416	100527	6233.99	3.68121240e-03	6.01740404e-04	1.47151496e-05	1.87272026e-06	0.23
1416	100204	6233.95	3.68121390e-03	6.01743750e-04	1.47499468e-05	1.90683091e-06	0.23
1416	91013	6233.99	3.68121278e-03	6.01744647e-04	1.47226360e-05	1.86894629e-06	0.22
1416	90611	6233.99	3.68121282e-03	6.01745306e-04	1.47625576e-05	1.91288383e-06	0.21
1416	90204	6234.05	3.68121253e-03	6.01759392e-04	1.47837598e-05	1.93393674e-06	0.20
2454	130420	2885.22	3.68121227e-03	6.02207569e-04	1.67735805e-05	2.36654472e-06	0.03
2454	121221	2885.27	3.68121226e-03	6.02202954e-04	1.67688028e-05	2.36839058e-06	0.03
2454	120907	2885.31	3.68121227e-03	6.02196110e-04	1.67816598e-05	2.39435289e-06	0.04
2454	120511	2885.36	3.68121173e-03	6.02194844e-04	1.67937787e-05	2.40818966e-06	0.04
2454	120216	2885.37	3.68121225e-03	6.02188034e-04	1.67634669e-05	2.37714945e-06	0.02
2454	111208	2885.40	3.68121094e-03	6.02190055e-04	1.67787094e-05	2.39362837e-06	0.02
2454	110803	2885.43	3.68121237e-03	6.02181187e-04	1.67431280e-05	2.36267504e-06	0.02
2454	110331	2885.53	3.68121054e-03	6.02184632e-04	1.67414323e-05	2.35175902e-06	0.04

A small residual pressure effect on the temperature sensors documented in Tupas et al. (1997) has been removed from measurements obtained with our sensors. Another correction to our temperature measurements was for the viscous heating of the sensor tip due to the water flow past it (Larson and Pederson, 1996). This correction is thoroughly documented in Tupas et al. (1997).

Dual sensors were used during all casts of the WHOTS-8 and -9 cruises. Sensors #1416 and #2454 were used during both cruises. The temperature differences between sensor pairs were calculated for each cast to evaluate the quality of the data, and to identify possible problems with the sensors. All sensors performed correctly during the cruises, showing temperature differences within expected values. The mean temperature difference in the water column was typically less than 2×10^{-3} °C in the 1000 m casts, with a standard deviation of less than 0.5×10^{-3} °C below 500 dbar. The largest variability in temperature difference between sensor pairs was observed in the thermocline, where the standard deviation reached nearly 1×10^{-2} °C. These differences are not unexpected, since each sensor has independent water intakes it is possible that when the CTD passes through this steep gradient region each sensor measures water from slightly different levels, yielding significant temperature differences.

Temperature sensor #1416

This sensor was used during the WHOTS-8 and -9 cruises. This sensor has maintained a stable drift for a long time. The calibrations from February 2009 through May 2012 yielded a sensor drift of 3.64 x 10^{-6} ºC day^{-1}, with an intercept of 2.7 x 10^{-4} ºC and a RMS residual of 4.1 x 10^{-4} ºC, which was used to obtain the drift correction for cruise WHOTS-8. When corrected for linear drift to 10 July 2011 (the mid-date when the sensor was used), the 8 December 2011 calibration gave the smallest deviation in the 0-5 ºC temperature range from the set of all calibrations (also corrected for linear drift to 10 July 2011). A drift correction was obtained using this calibration as a baseline. The resulting drift correction for the cruise was -0.55 m°C, and deemed insignificant. (Table 4-3).

The calibrations from February 2009 through April 2013 (Table 4-2) yielded a sensor drift of 3.80 x 10^{-6} ºC day^{-1}, with an intercept of 5.7 x 10^{-4} ºC and a RMS residual of 3.9 x 10^{-4} ºC, which was used to obtain the drift correction for cruise WHOTS-9. When corrected for linear drift to 15 June 2012 (the mid-date of the cruise), the 12 May 2012 calibration gave the smallest deviation in the 0-5 ºC temperature range from the set of all calibrations (also corrected for linear drift to 15 June 2012). A drift correction was obtained using this calibration as a baseline. The resulting drift correction for the cruise was 0.13 m°C, and deemed insignificant. (Table 4-3).

Temperature sensor #2454

This sensor was used during the WHOTS-8 and 9 cruises. The calibrations from September 2008 through May 2012 yielded a sensor drift of 4.22 x 10^{-6} ºC day^{-1} with an intercept of 7.4 x 10^{-4} ºC and a RMS residual of 4.1 x 10^{-4} ºC, and was used to obtain the drift correction for cruise WHOTS-8. When corrected for linear drift to 10 July 2011 (the mid-date when the sensor was used), the 3 August 2011 calibration gave the smallest deviation in the 0-5 ºC temperature range from the set of all calibrations (also corrected for linear drift to 10 July 2011). Drift corrections were obtained using this calibration as a baseline. A drift correction was obtained using this calibration as a baseline. The resulting drift correction for the cruise was -0.11 m°C, and deemed insignificant (Table 4-3).

The calibrations from September 2008 through April 2013 (Table 4-2) yielded a sensor drift of 4.85 x 10^{-6} ºC day^{-1} with an intercept of 2.4 x 10^{-5} ºC and a RMS residual of 5.2 x 10^{-4} ºC, and was used to obtain the drift correction for the WHOTS-9 cruise. When corrected for linear drift to 15 June 2012 (the mid-date when the sensor was used), the 21 December 2012 calibration gave the smallest deviation in the 0-5 ºC temperature range from the set of all calibrations (also corrected for linear drift to 15 June 2012). A drift correction was obtained using this calibration as a baseline. The resulting drift correction for the cruise was -0.92 m°C, and was applied to the data (Table 4-3).

Table 4-3. Temperature (T) and Conductivity (C) sensors used during the WHOTS cruises, including temperature drift correction and the thermal inertia parameter (alpha). Dual temperature and conductivity sensors were used during both cruises. The data reported here are from the sensors marked with (*).

Cruise	T-sensor #	T-correction (m°C)	C-sensor #	alpha
WHOTS-8	1416 (*)	-0.55	2218 (*)	0.028
WHOTS-8	2454	-0.11	3162	0.020
WHOTS-9	1416 (*)	0.13	3162 (*)	0.037
WHOTS-9	2454	-0.92	3984	0.020

Conductivity

Three Sea-Bird SBE 4C conductivity sensors (#2218, #3162, and #3984) were used during the WHOTS cruises. Sensor #3984 is a new sensor acquired in early 2012. Dual sensors were used during all the cruise casts. As mentioned earlier, only the data from the most reliable sensor (and its corresponding temperature sensor pair, as shown in Table 4-3) are reported here.

Sensor #2218 was calibrated at Sea-Bird in October 2010 and February 2012; sensor #3162 was calibrated in October 2010, February 2012, and in April 2013; sensor #3984 was calibrated in January 2012, and in March 2013. The nominal conductivity calibrations were used for data acquisition. Final calibration was determined empirically from salinities of discrete water samples acquired during each cast. Prior to empirical calibration, conductivity was corrected for thermal inertia of the glass conductivity cell using the recursive filter given by Lueck (1990) and Lueck and Picklo (1990). Sensor parameters alpha and beta, which characterize the initial magnitude of the thermal effect and its relaxation time, are needed for this correction. As recommended by Lueck (personal communication, 1990), beta was set to 0.1 s^{-1}, but alpha was calculated for each sensor to close the spread between the down- and up-cast *T-S* curves (Table 4-3).

Salinity samples were collected at selected depths during each cast and measured with a salinometer (Sect. 4.B.1). The nominally calibrated CTD salinity trace was used to identify questionable samples. Salinity samples were later quality controlled and flagged by comparing them against the empirically calibrated CTD salinities.

Calibration of each conductivity sensor was performed empirically by comparing its nominally calibrated output against the calculated conductivity values obtained from the water sample salinities, using the pressure and temperature of the CTD at the time of bottle closure. An initial estimate of bias (*b0*) and slope (*b1*) corrections to the nominal calibration were determined from a linear least squares fit to the ensemble of CTD-bottle conductivity differences as a function of conductivity, from all casts during the sensor use. This calibration was then used to identify suspect water samples. These samples were deleted from the analysis, and the calibration was repeated. Conductivity calibration coefficients for the sensors used during WHOTS cruises are given in Table 4-4.

Table 4-4. CTD Conductivity calibration coefficients obtained from comparison against bottle salinities.

Cruise	Sensor #	b0	b1
WHOTS-8	2218	-0.000137	0.000458
WHOTS-8	3162	-0.000065	0.000229
WHOTS-9	3162	-0.000057	-0.000185
WHOTS-9	3984	0.000203	0.000163

The final step of the calibration was to perform a profile-dependent bias correction, to allow for a drift of the conductivity cell with time during each cruise, or for sudden offsets due to fouling. This offset was determined by taking the median value of CTD-bottle salinity differences for each profile. No offset corrections were necessary for any of the WHOTS cruises casts.

The quality of the conductivity calibration is illustrated by Figure 4-1, which shows the differences between the corrected CTD salinities and the bottle salinities as a function of pressure for the WHOTS-8 and -9 cruises. Table 4-5 gives the mean and standard deviations for the final calibrated CTD minus water sample salinities.

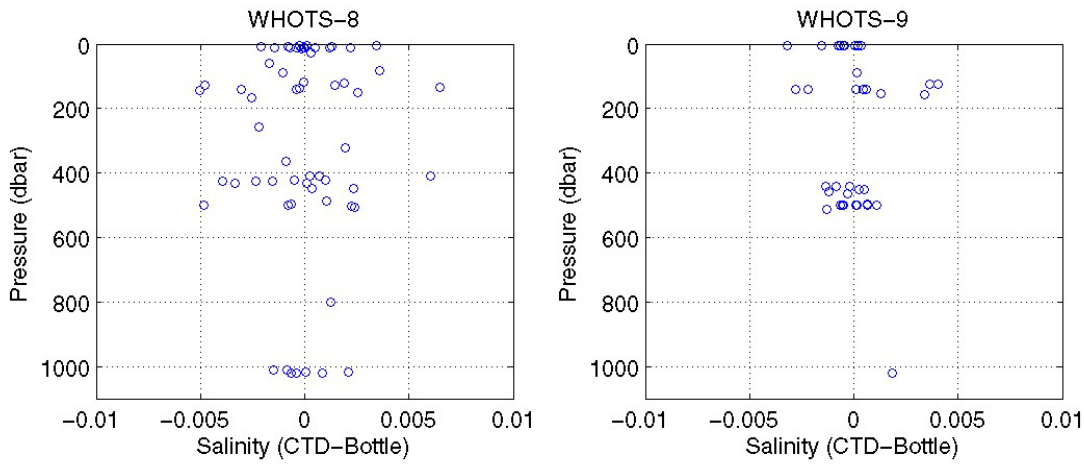

Figure 4-1. Difference between calibrated CTD salinities and bottle salinities for all the casts during WHOTS-8 and –9 deployment cruises.

Table 4-5. CTD-Bottle salinity comparison for each sensor.

		0 to 1200 dbar		500 to 1200 dbar	
Cruise	Sensor #	Mean	Standard Deviation	Mean	Standard Deviation
WHOTS-8	2218	0.0000	0.0022	0.0002	0.0020
WHOTS-8	3162	0.0000	0.0022	0.0005	0.0021
WHOTS-9	3162	0.0000	0.0015	0.0002	0.0012
WHOTS-9	3984	0.0000	0.0014	0.0001	0.0010

Salinity differences between sensor sets were calculated the same way as for the temperature in order to identify problems with any of the sensors. These differences show a behavior similar to the temperature differences in the thermocline region. Maximum absolute salinity differences of about 9×10^{-3} were observed at 100 dbar, decreasing to less than 2×10^{-3} below 200 dbar. This behavior is due to a combination of the residual temperature effect on the temperature sensors described in the previous section, and an additional residual temperature effect on the conductivity sensors (N. Larson personal communication, 1999). The temperature effect on the conductivity sensors is similar to that described for the temperature sensors, and affects the conductivity measurements when the sensor passes through intense temperature gradients.

The largest variability in the salinity difference between sensors was observed in the halocline, with standard deviations of up to 1×10^{-2} between 50 and 100 dbar.

Dissolved Oxygen

Two Sea-Bird SBE-43 oxygen sensors were used during the WHOTS-8 and 9 cruises: #431601 and #43918 (Table 4-6). Sensor #431601 was calibrated at Sea-Bird on 13 July 2010, 18 February 2012, and on 17 April 2013; sensor #43918 was calibrated on 9 November 2010, 11 November 2011, and 1 March 2013. Oxygen data from the WHOTS-8 cruise were further calibrated using empirical calibrations coefficients obtained during the HOT-233 cruise conducted on 18-22 July 2011, one week after WHOTS-8, which used the same oxygen sensors. Similarly, the WHOTS-9 oxygen data were calibrated using calibration coefficients obtained during the HOT-243 cruise conducted on 25-29 June 2012, one week after the WHOTS-9 cruise, which used the same oxygen sensors. The CTD empirical calibration was conducted using oxygen water samples and the procedure from Owens and Millard (1985). See Tupas et al. (1997) for details on these calibrations procedures.

Table 4-6 shows the mean and standard deviation for the calibrated CTD oxygen minus water sample residuals during HOT-233 and HOT-243, whose calibrations were used for the WHOTS-8 and WHOTS-9 cruises respectively. Dual sensors were used during each cruise, and all four sensors performed well, showing small mean (less than 0.06 µmol kg^{-1} in magnitude) and standard deviation (less than 2 µmol kg^{-1}) residual values when compared with the water samples. The data reported here are from the sensors indicated in Table 4-6, and were in the same plumbing line as the temperature and conductivity sensor set whose data are also reported here (see Table 4-3).

Table 4-6. CTD-bottle dissolved oxygen comparison for each sensor during HOT-233 (calibration used for WHOTS-8 data) and HOT-243 (calibration used for WHOTS-9 data). The units are µmol kg^{-1}. The data reported here are from the sensor marked with (*).

		0 to 1200 dbar		500 to 1200 dbar	
Cruise	Sensor #	Mean	Standard Deviation	Mean	Standard Deviation
WHOTS-8/HOT-233	431601 (*)	0.01	0.62	0.01	0.50
WHOTS-8/HOT-233	43918	0.01	0.69	0.03	0.49
WHOTS-9/HOT-243	43918 (*)	0.01	1.30	0.02	1.13
WHOTS-9/HOT-243	431601	0.02	1.37	0.00	1.31

B. Water samples

1. Salinity

Salinity samples were collected during WHOTS-8 and -9. Samples from each cruise were measured after the cruise in the laboratory at the UH using a Guildline Autosal 8400B. IAPSO[1] standard seawater samples were measured to standardize the Autosal, and samples from a large batch of "secondary standard" (substandard) seawater were measured after every 24-48 samples to detect drift in the Autosal. Standard deviations of the secondary standard measurements were less than ± 0.001 for WHOTS-8 and -9 cruises (Table 4-7).

The substandard water was collected during HOT cruises from 1020 m at Station ALOHA and drained into a 50-liter Nalgene plastic carboy. In the laboratory, the water was then thoroughly mixed in a glass carboy for 20 minutes, after which a 2-inch protective layer of white oil was added on top to deter evaporation. The substandard water was allowed to stand for approximately three days before it was used, and was stored in the same temperature controlled room as the Autosal, protecting it from the light with black plastic bags to inhibit biological growth. Substandard seawater batches #50 and #52 were prepared on 5 January 2011, and 22 December 2011, respectively and used for WHOTS-8 and -9 samples respectively. The top of the bottle and the thimble were thoroughly dried before being tightly capped to prevent water from being trapped between the cap or thimble and the bottle's mouth. It has been observed that residual water trapped in this way increases its salinity due to evaporation, and it can leak into the sample when the bottle is opened for measuring.

Salinity samples from the WHOTS-8 cruise were measured prior to the samples from HOT-233. Samples from WHOTS-9 were measured prior to the HOT-243 samples. The substandard statistics in Table 4-7 include the substandard samples measured for the WHOTS-8 samples and the WHOTS-9 samples.

Table 4-7. Precision of salinity measurements using secondary lab standards.

Cruise	Mean Salinity +/- SD	# Samples	Substandard Batch #	IAPSO Batch #
WHOTS-8	34.4655 +/- 0.0003	8	50	P151
WHOTS-9	34.4932 +/- 0.0003	6	52	P153

[1] International Association for Physical Sciences of the Ocean

C. Thermosalinograph data acquisition and processing

1. WHOTS-8 Deployment Cruise

Near-surface temperature and salinity data for the WHOTS-8 cruise were acquired through the use of a thermosalinograph system aboard the NOAA Ship *Hi'ialakai*. The seawater intake was situated approximately 2 m below the sea surface in the bow thruster room. There was no external temperature sensor during the WHOTS-8 cruise. Data were acquired every 60 seconds for the duration of the cruise and salinity samples were taken roughly every 8 hours throughout the cruise for calibration from an outlet in the flowthrough system.

Data from the SBE-21 sensor were only reported to one significant digit; therefore the data were not usable.

2. WHOTS-9 Deployment Cruise

Near-surface temperature and salinity data for the WHOTS-9 cruise were acquired through the use of a thermosalinograph system aboard the Ship *Hi'ialakai*. The seawater intake was situated approximately 2 m below the sea surface in the bow thruster room. There was no external temperature sensor during the WHOTS-9 cruise. Data were acquired every 60 seconds for the duration of the cruise and salinity samples were taken roughly every 8 hours throughout the cruise for calibration from an outlet in the flowthrough system.

Data from the SBE-21 sensor were recorded to only one significant digit; therefore the data were not usable.

D. Shipboard ADCP

3. WHOTS-8 Deployment Cruise

Currents measured by the Ship *Hi'ialaikai's* Ocean Surveyor 75 kHz narrowband/broadband ADCP were processed using the CODAS ADCP processing suite. Horizontal velocity data, latitude and longitude were processed with 15 minute ensemble averages and 10 m depth resolution. The times of the datasets from the OS75 are shown in Table 4-8.

Table 4-8. ADCP record times (UTC) for the Narrowband/Broadband Ocean Surveyor 75 kHz ADCP during the WHOTS-8 cruise.

WHOTS-10	**OS75**
File beginning time	06-Jul-2011 16:24:16
File ending time	13-Jul-2011 16:17:11

4. WHOTS-9 Deployment Cruise

Currents measured by the Ship Hi'ialakai's Ocean Surveyor 75 kHz narrowband and broadband ADCP were processed using the CODAS ADCP processing suite. Horizontal velocity data, latitude and longitude were processed with 15 minute ensemble averages and 10 m depth resolution. The times of the datasets from the OS75 are shown in Table 4-9.

Table 4-9. ADCP record times (UTC) for the Narrow Band 75 kHz ADCP during the WHOTS-10 cruise.

WHOTS-10	**OS75**
File beginning time	13-Jun-2012 03:25:31
File ending time	19-Jun-2012 17:02:58

5. Moored Instrument Observations

A. MicroCAT/SeaCAT data processing procedures

Each moored MicroCAT and SeaCAT temperature, conductivity and pressure (when installed) was calibrated at Sea-Bird prior to their deployment and after their recovery on the dates shown in Table 5-1. The internally-recorded data from each instrument were downloaded on board the ship after the mooring recovery, and the nominally-calibrated data were plotted for a visual assessment of the data quality. The data processing included checking the internal clock data against external event times, pressure sensor drift correction, temperature sensor stability, and conductivity calibration against CTD data from casts conducted near the mooring during HOT and WHOTS cruises. The detailed processing procedures are described in this section.

Table 5-1. WHOTS-8 MicroCAT/SeaCAT temperature sensor calibration dates, and sensor drift during deployments. All sensors had a drift smaller than 1 mili°C during the deployment.

Nominal deployment depth (m)	Sea-Bird Serial number	Pre-deployment calibration	Post-recovery calibration	Total Temperature drift during WHOTS-8 deployment (mili°C)
15	SBE37SM-6893	22-Sep-2010	21-Jul-2012	-0.18
25	SBE37SM-6894	22-Sep-2010	21-Jul-2012	-0.33
35	SBE37SM-6895	22-Sep-2010	21-Jul-2012	-0.38
40	SBE37SM-6896	22-Sep-2010	21-Jul-2012	-0.75
45	SBE37SM-6887	23-Sep-2010	26-Jul-2012	-0.48
50	SBE37SM-6897	30-Sep-2010	21-Jul-2012	-0.18
55	SBE37SM-6898	21-Sep-2010	21-Jul-2012	-0.70
65	SBE37SM-6899	21-Sep-2010	21-Jul-2012	-0.13
75	SBE37SM-3618	22-Sep-2010	26-Jul-2012	0.40
85	SBE37SM-6888	21-Sep-2010	07-Aug-2012	-0.64
95	SBE37SM-3617	21-Sep-2010	27-Jul-2012	-0.86
105	SBE37SM-6889	21-Sep-2010	07-Aug-2012	-0.86
120	SBE37SM-6890	21-Sep-2010	26-Jul-2012	-0.50
135	SBE37SM-3634	22-Sep-2010	24-Jul-2012	-0.32
155	SBE37SM-6891	21-Sep-2010	26-Jul-2012	0.47

1. Internal Clock Check and Missing Samples

Before the WHOTS-8 mooring deployment and after its recovery (before the data logging was stopped), the MicroCATs temperature sensors were placed in contact with an ice pack to create a spike in the data, to check for any problems with their internal clocks, and for possible missing samples (Table 3-2). The cold spike was detected by a sudden decrease in temperature. For all the instruments, the clock time of this event matched correctly the time of the spike (within the sampling interval of each instrument). No missing samples were detected for any of the instruments.

2. Pressure Drift Correction and Pressure Variability

Some of the MicroCATs used in the moorings were outfitted with pressure sensors (Table 3-1). Biases were detected in the pressure sensors by comparing the on-deck pressure readings (which should be zero for standard atmospheric pressure at sea level of 1029 mbar) before deployment and after recovery. Table 5-2 shows the magnitude of the bias for each of the sensors before and after deployment. To correct for this offset, a linear fit between the initial and final on-deck pressure offset as a function of time was obtained, and subtracted from each sensor. Figure 5-1 shows the linearly corrected pressures measured by the MicroCATs during the WHOTS-8 deployment. For most of the sensors, the mean difference from the nominal instrument pressure (based on the deployed depth) was less than 1 dbar. The instrument at 155 m was about 1.4 m deeper than its nominal pressure. The standard deviation of the pressure for the

duration of the record was also less than 1 dbar for all sensors, with the deeper sensors showing a larger standard deviation. The range of variability for all sensors was about ± 3 dbar.

The causes of pressure variability can be several, including density variations in the water column above the instrument; horizontal dynamic pressure (not only due to the currents, but also due to the motion of the mooring); mooring position, etc. (see WHOTS Data Report 1, Santiago-Mandujano et al., 2007).

Table 5-2. Pressure bias of MicroCATs with pressure sensor.

Deployment	**Depth (m)**	**Sea-Bird Serial #**	**Bias before deployment (dbar)**	**Bias after recovery (dbar)**
WHOTS-8	45	37SM31486-6887	0.08	0.01
WHOTS-8	85	37SM31486-6888	0.10	0.08
WHOTS-8	105	37SM31486-6889	0.13	0.05
WHOTS-8	120	37SM31486-6890	0.08	0.04
WHOTS-8	155	37SM31486-6891	0.13	0.10

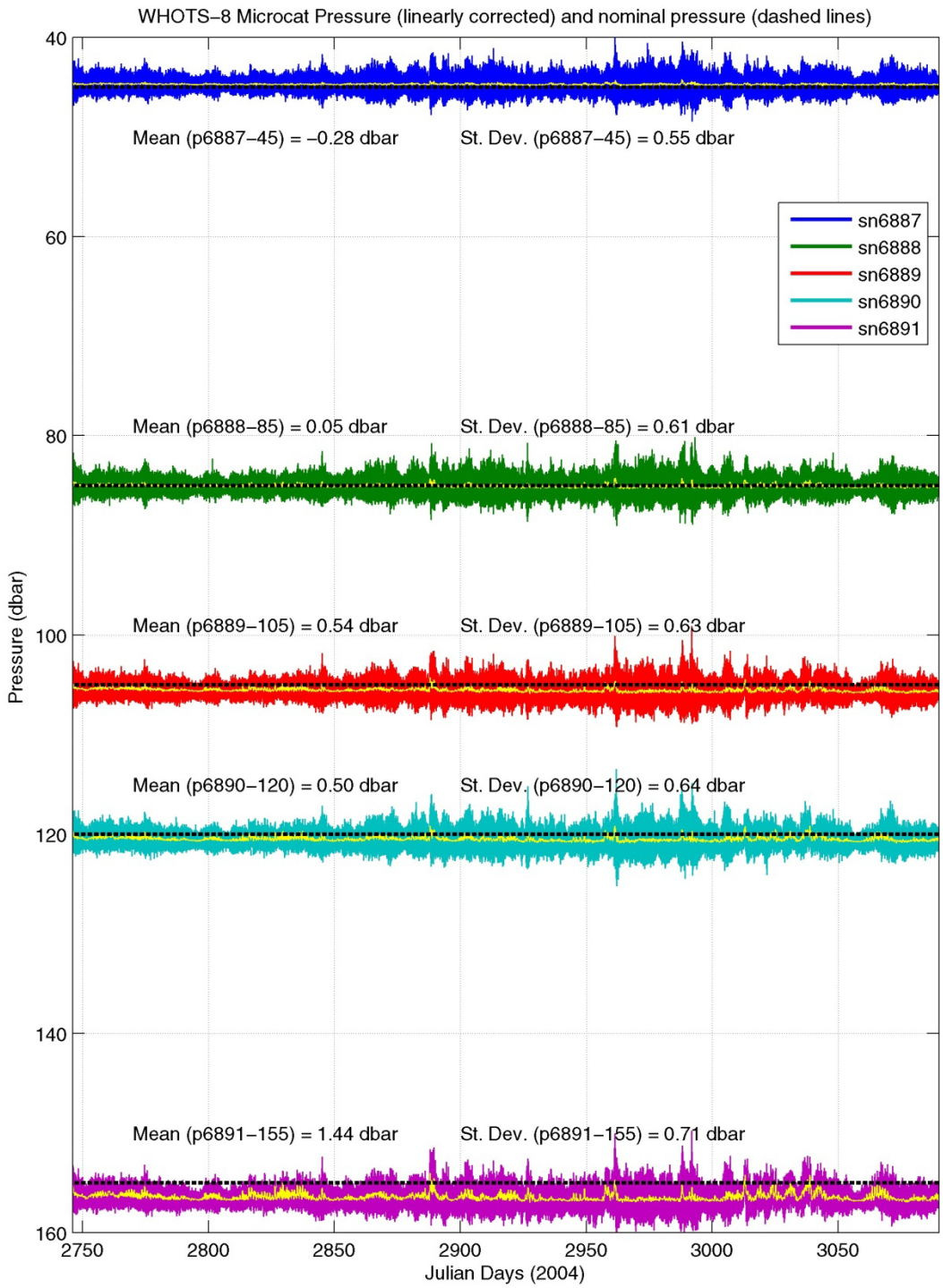

Figure 5-1. Linearly corrected pressures from MicroCATs during WHOTS-8 deployment. The yellow line is a 5-hour running mean. The horizontal dashed line is the sensor's nominal pressure, based on deployed depth.

3. Temperature Sensor Stability

The MicroCAT temperature sensors were calibrated at Sea-Bird before and after each deployment (see Table 5-1). Sea-Bird's evaluation of each sensor's drift was used to calculate the temperature offset for the duration of the deployment (Table 3-1 and Table 3-2). These values turned out to be insignificant (not higher than 1 m °C) for all sensors deployed above 200 m. Comparisons between the MicroCAT and CTD data from casts conducted near the mooring during HOT cruises confirmed that the temperature drift of the moored instruments was insignificant.

A temperature comparison between the two MicroCATs installed underneath the buoy (SN 1835 and SN 1727) show the consistency and inferred stability of the sensors for the duration of the deployment (Figure 5-7, upper panel).

Temperature comparisons between one of the WHOTS-8 near-surface MicroCATs (SN 1835) and the 4 RBR surface temperature sensors in the buoy hull (Table 3-1) are shown in Figure 5-2. All the RBR instruments stopped recording early, instruments #20565 and #20566 lasted 133 and 136 days respectively during the deployment; #20568 has the shortest record of 108 days, and #20567 has the longest with 159 days. None of the instruments show any obvious bias when compared to the MicroCAT measurements.

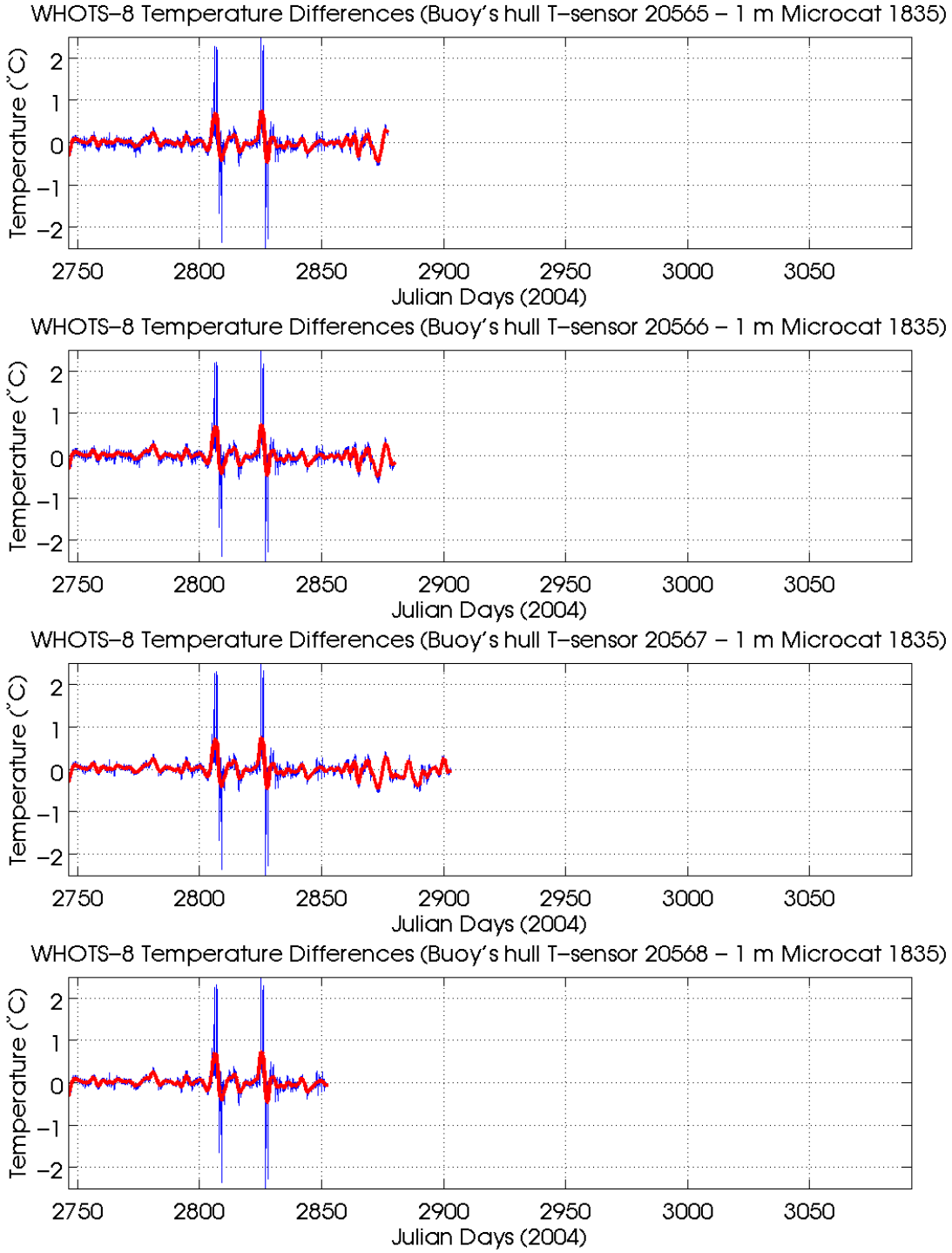

Figure 5-2. Temperature difference between MicroCAT SN 1835 at 1.5 m, and near-surface temperature sensors SN 20565(upper panel), 20566 (second panel), 20567 (third panel), and SN 20568(bottom panel), during WHOTS-8 deployment. The red line is a 24-hour running mean of the differences.

In addition to the temperature sensors in the Sea-Bird and the RBR instruments, there were additional temperature sensors in the VMCMs (at 10 and 30 m), and in the ADCPs (at 47.5 m and 125 m). In order to evaluate the quality of the temperatures from these sensors, comparisons with the temperatures from adjacent MicroCATs were conducted.

Comparisons with VMCM and ADCP temperature sensors

The upper panel of Figure 5-3 shows the difference between the 10-m VMCM and the 15-m MicroCAT temperatures during WHOTS-8, which seem to fluctuate around zero. Also shown for comparison in the lower panel of the figure are the differences between MicroCAT temperatures at 15 and 25 m. The temperature fluctuations in the differences between the 15 and 25-m MicroCATs seem to be around zero.

Temperature differences between the 30-m VMCM and the temperatures from adjacent MicroCATs at 25 and 35-m during WHOTS-8 are shown in Figure 5-4. For comparison, the differences between the MicroCATs temperatures are also shown. These plots indicate that there was no offset in the 30-m VMCM with respect to the adjacent MicroCATs (top and middle plots).

Temperature differences between the 47.5-m ADCP and the temperatures from adjacent MicroCATs at 45 and 50-m during WHOTS-8 are shown in Figure 5-5. For comparison, the differences between the MicroCATs temperatures are also shown. These plots indicate that there was no offset in the 47.5-m ADCP with respect to the adjacent MicroCATs (top and middle plots).

Temperature differences between the 125-m ADCP and the temperatures from adjacent MicroCATs at 120 and 135-m during WHOTS-8 are shown in Figure 5-6. For comparison, the differences between the MicroCATs temperatures are also shown. It is difficult to assess the quality of the ADCP temperature from these comparisons, as these sensors were located at the top of the thermocline, where we expect to find large temperature differences between adjacent sensors.

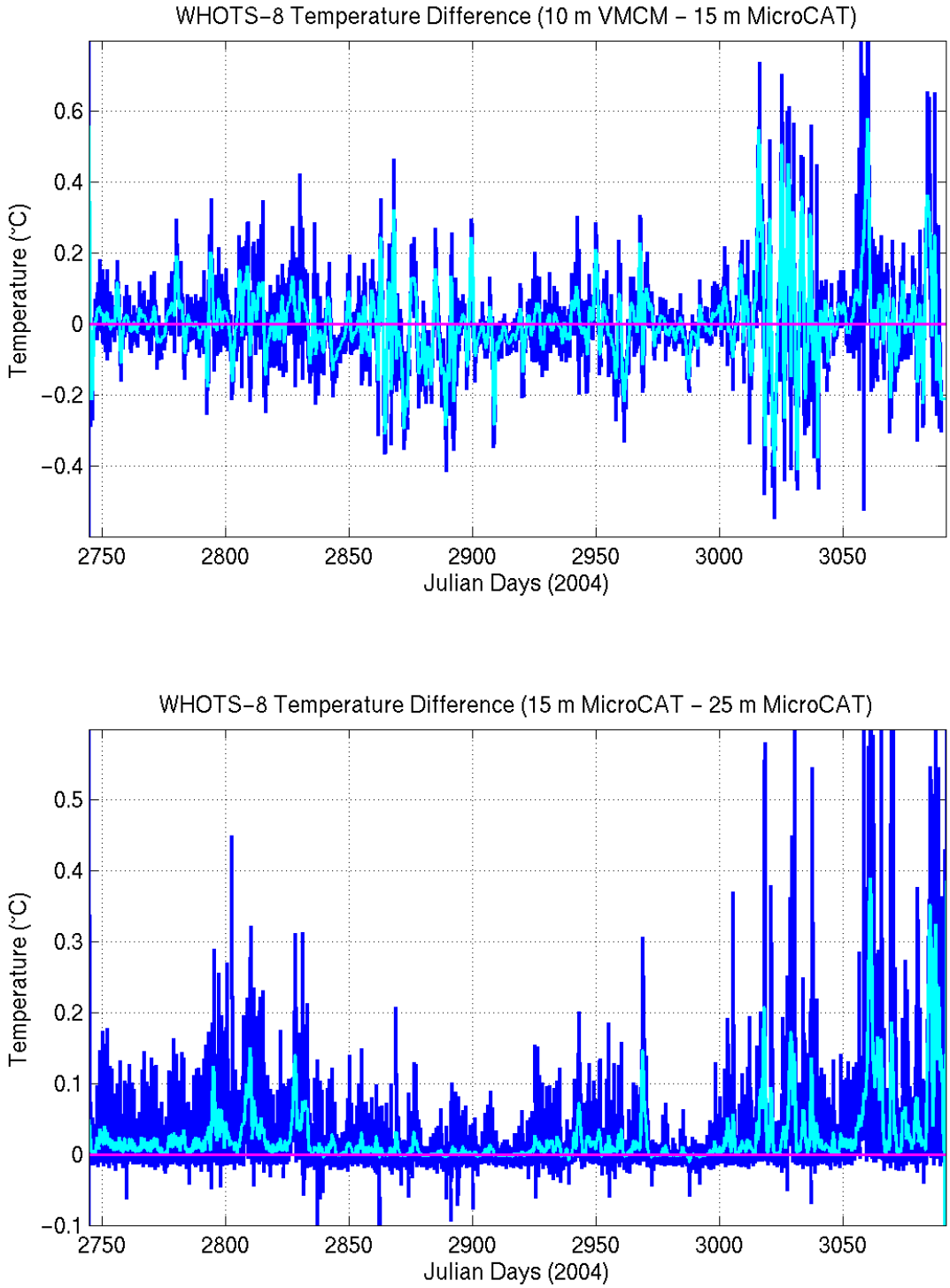

Figure 5-3. Temperature differences between the 10-m VMCM and the 15-m MicroCAT (upper panel), and between the 15-m MicroCAT and the 25-m MicroCAT (lower panel) during the WHOTS-8 deployment. The light blue line is a 24-hour running mean of the differences.

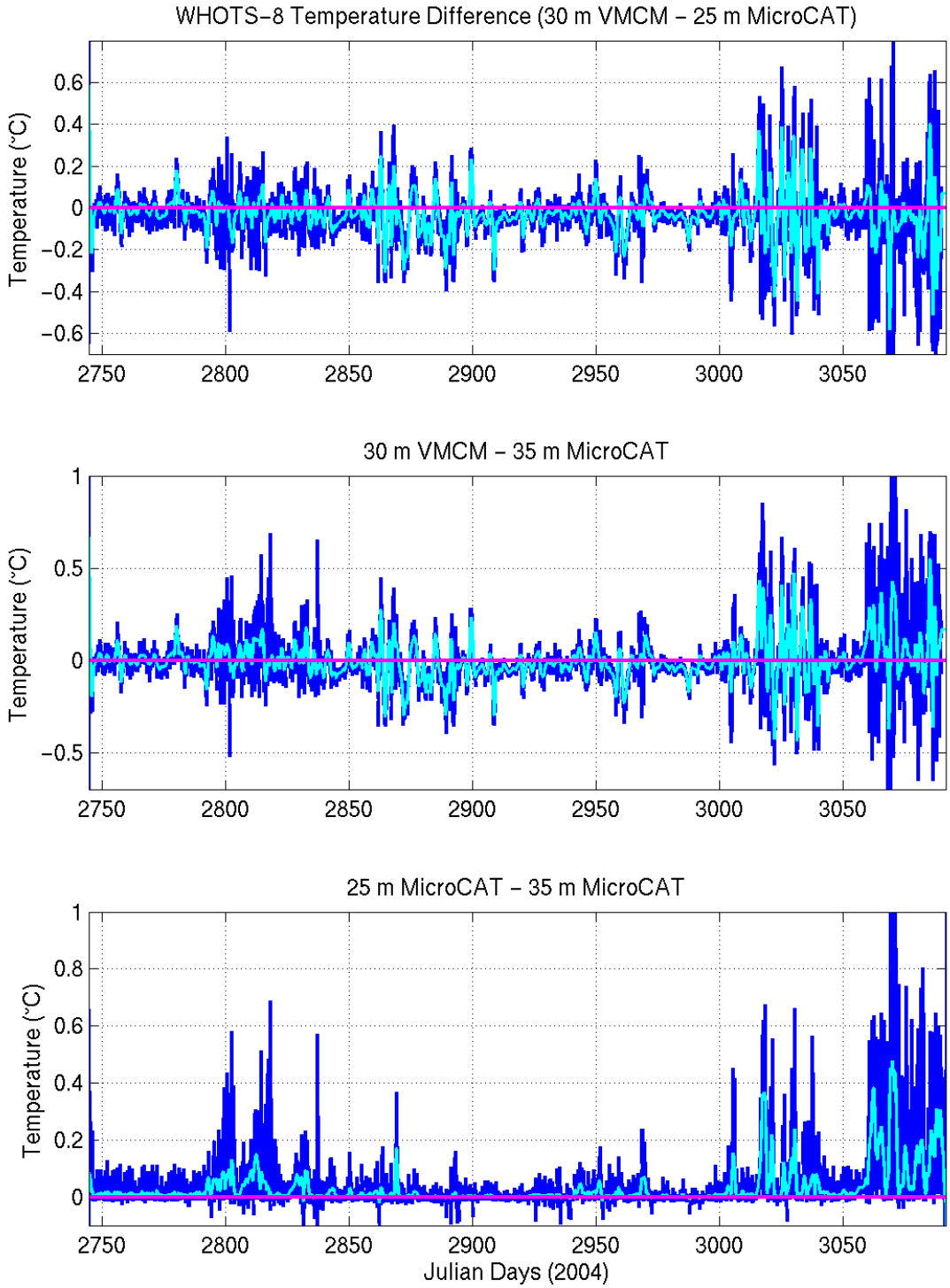

Figure 5-4. Temperature difference between the 30-m VMCM and the 25-m MicroCAT (upper panel); between the 30-m VMCM and the 35-m MicroCAT (middle panel); and between the 25-m and the 35-m MicroCATs (lower panel) during the WHOTS-8 deployment. The light blue line is a 24-hour running mean of the differences.

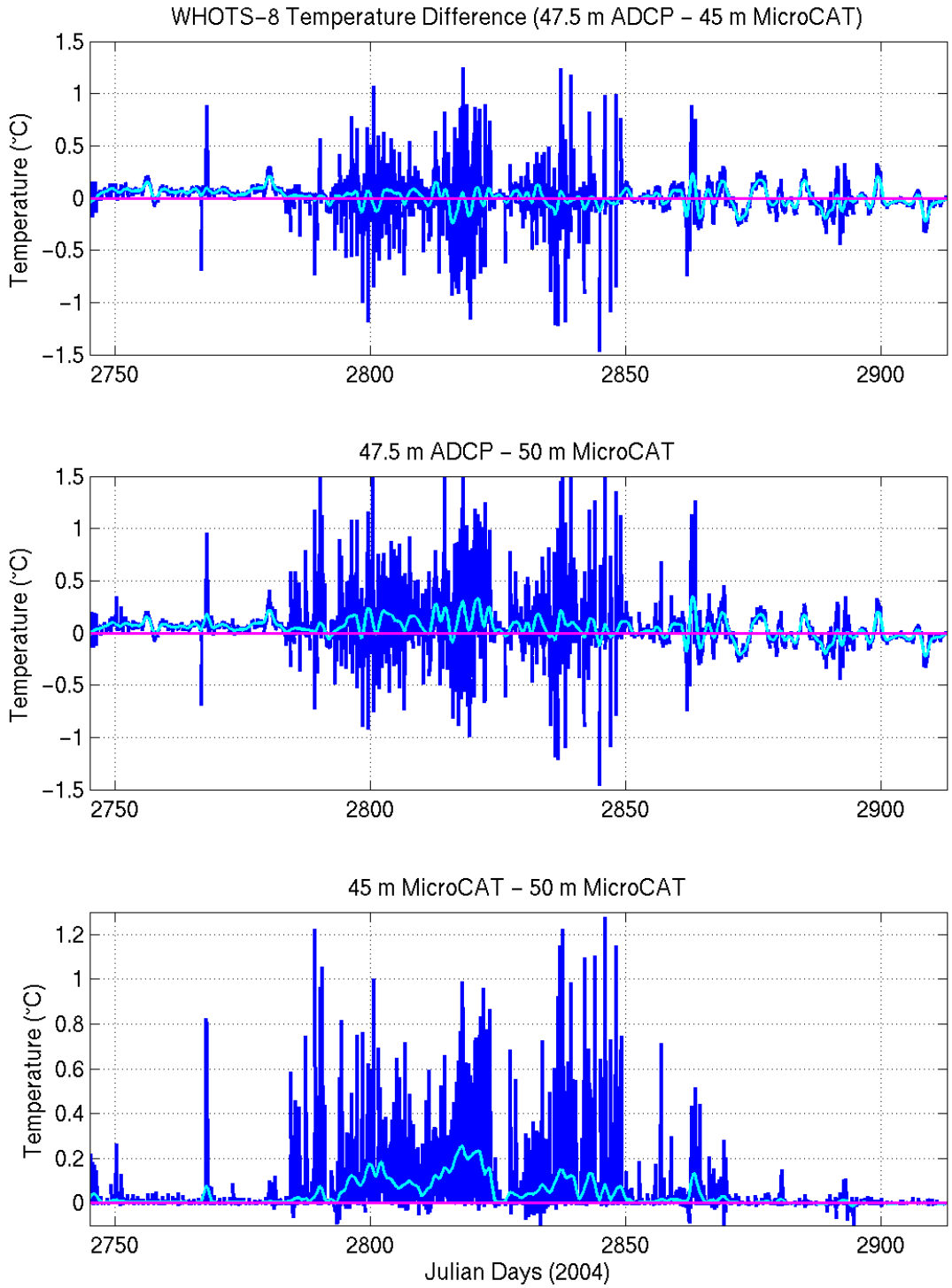

Figure 5-5. Temperature differences between the 47.5-m ADCP and the 45-m MicroCAT (upper panel); between the 47.5-m ADCP and the 50-m MicroCAT (middle panel); and between the 45-m and the 50-m MicroCATs (lower panel) during the WHOTS-8 deployment. The light blue line is a 24-hour running mean of the differences.

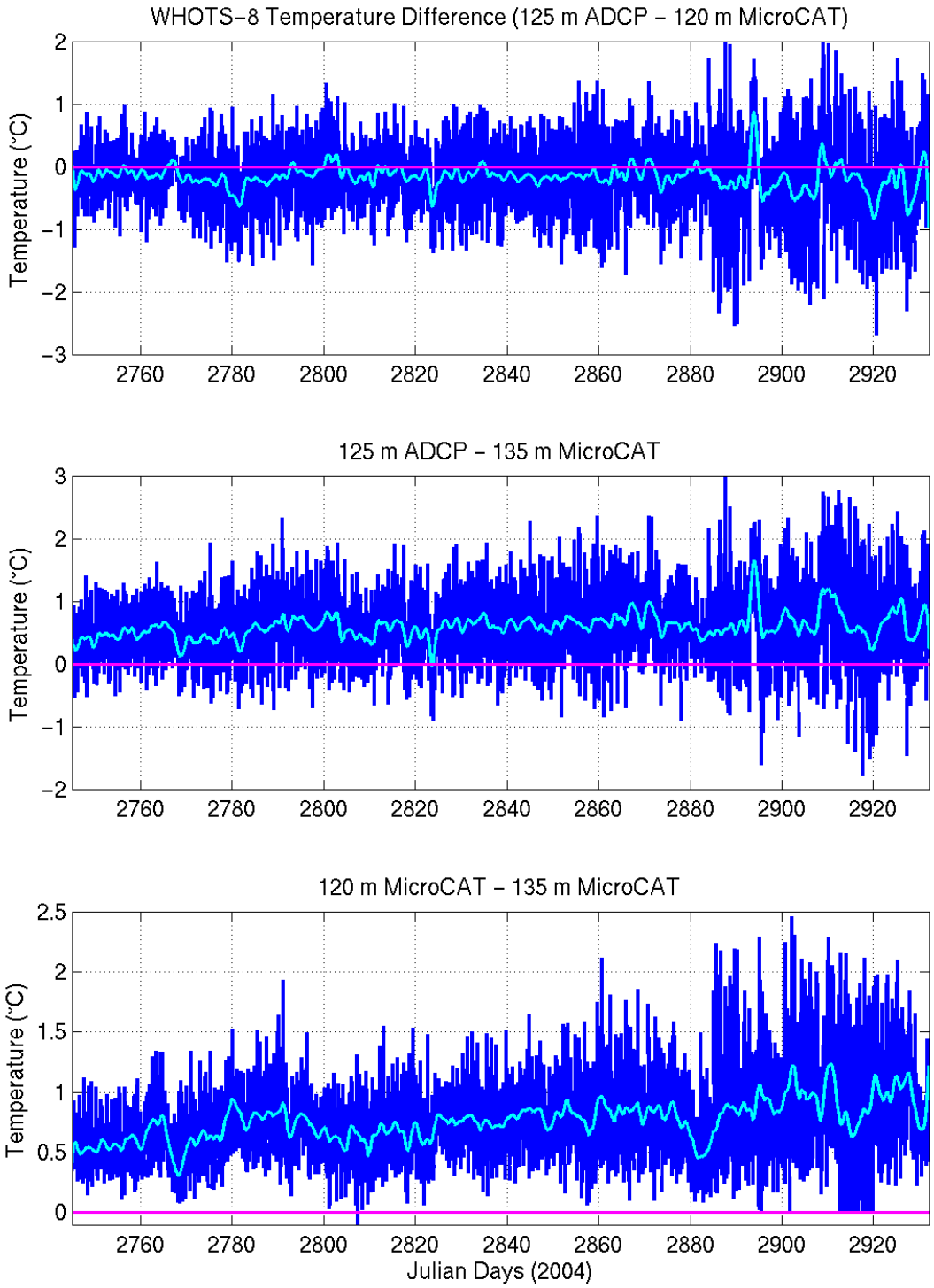

Figure 5-6. Temperature differences between the 125-m ADCP and the 120-m MicroCAT (upper panel); between the 125-m ADCP and the 135-m MicroCAT (middle panel); and between the 120-m and the 135-m MicroCATs (lower panel) during the WHOTS-8 deployment. The light blue line is a 24-hour running mean of the differences.

4. Conductivity Calibration

The results of the Sea-Bird post-recovery conductivity calibrations indicated that some of the MicroCAT conductivity sensors experienced relatively large offsets from their pre-deployment calibration. These were qualitatively confirmed by comparing the mooring data against CTD data from casts conducted between 200 m and 5 km from the mooring during HOT cruises. The causes of the conductivity offsets are not clear, and there may have been multiple causes (see Freitag et. al, (1999) for a similar experience with conductivity cells during COARE). For some instruments the offset was negative, caused perhaps by biofouling of the conductivity cell while for others the offset was positive, caused possibly by scouring of the inside of the conductivity cell (possibly by the continuous up and down motion of the instrument in an abundant field of diatoms). A visual inspection of the instruments after recovery did not show any obvious signs of biofouling, and there were no cell scourings reported in the post-recovery inspections at Sea-Bird.

Corrections of the MicroCATs conductivity data were conducted by comparing them against CTD data from profiles and yo-yo casts conducted near the mooring during HOT cruises, and during deployment/recovery cruises. Casts conducted between 200 and 1000 m from the mooring were given extra weight in the correction, as compared to those conducted between 1 and 5 km away. Casts more than 5 km away from the mooring were not used. Given that the CTD casts are conducted at least 200 m from the mooring, the alignment between CTD and MicroCAT data was done in density rather than in depth. For cases in which the alignment in density was not possible due to large conductivity offsets (causing unrealistic mooring density values), alignment in temperature space was done. A cubic least-squares fit (LSF) to the CTD-MicroCAT/SeaCAT differences against time was applied as a first approximation, and the corresponding correction was applied.

Some of the sensors had large offsets and/or obvious variability that could not be explained by a cubic LSF (see below). A characteristic of the offsets is that their development is not always linear in time, and their behavior can be highly variable (see WHOTS Data Report 1, Santiago-Mandujano et al., 2007). For these sensors, a stepwise correction was applied matching the data to the available CTD cast data, and then using the differences between consecutive sensors to determine when the sensor started to drift. For instance, during periods of weak stratification the conductivity difference between neighboring sensors A, B, and C could reach near-zero values, in particular for instruments near the surface, which are the ones most prone to suffer conductivity offsets. A sudden conductivity offset observed during this period between sensors A and B, but not between sensors A and C could indicate the beginning of an offset for sensor B.

Given that the deepest instruments on the mooring are less likely to be affected by biofouling and consequent sudden conductivity drift, the deep instruments served as a good reference to find any possible malfunction in the shallower ones. Therefore the deepest instruments' conductivity was corrected first, and the correction was continued sequentially upwards toward the shallower ones.

As a quality control to the conductivity corrections, the buoyancy frequency between neighboring instruments was calculated using finite differences. Over- or under-corrected conductivities yielded instabilities in the water column (negative buoyancy frequency) that were easy to detect and were obviously not real when lasting for several days. Based on this, the conductivity correction of the corresponding sensors was revised.

The corrections applied to each of the conductivity sensors during WHOTS-8 can be seen in Figure 5-8. Most of the instruments had a drift of less than 0.015 Siemens/m for the duration of the deployment, which was corrected with a step-wise linear or a cubic least-squares fit.

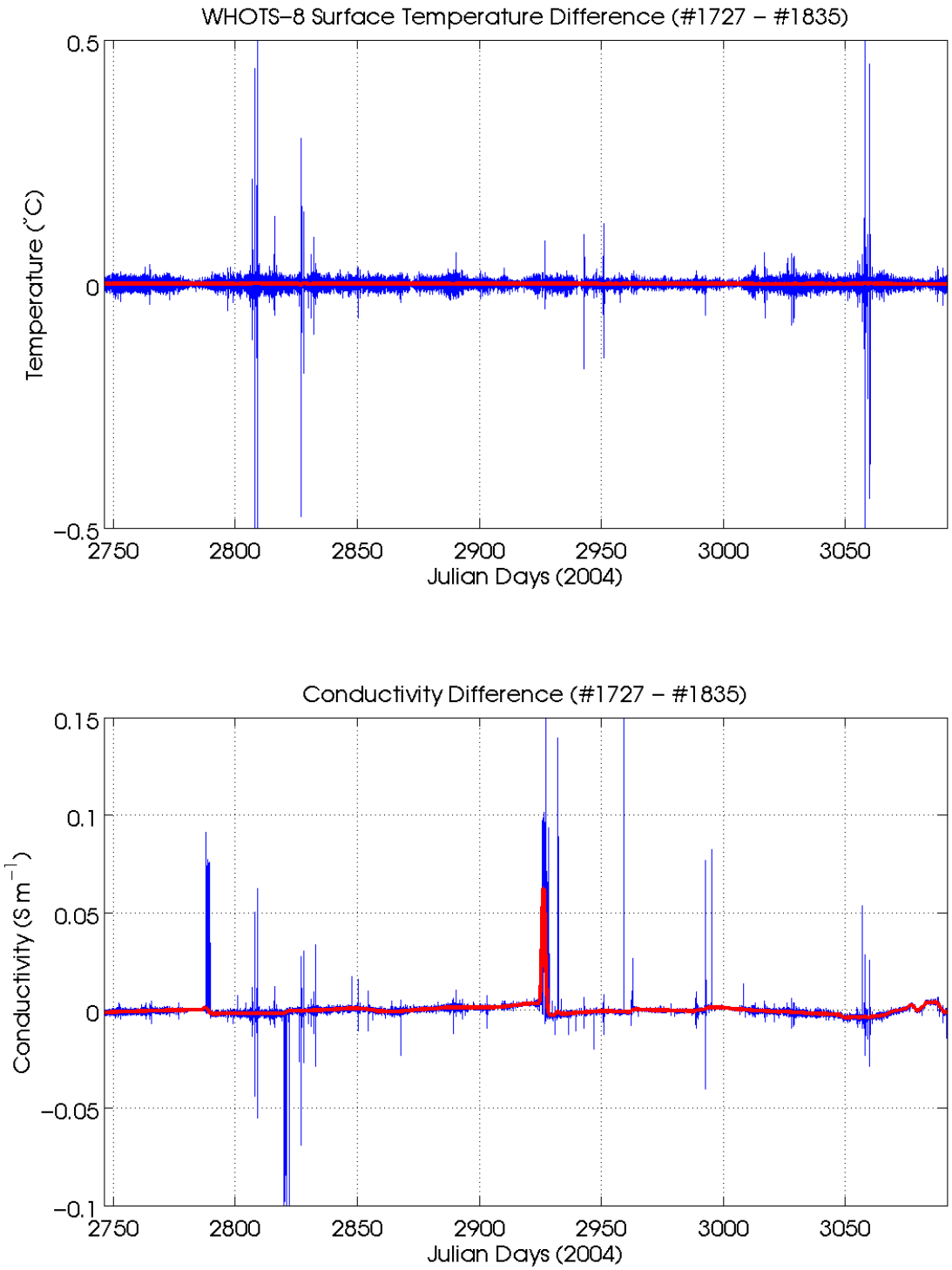

Figure 5-7. Temperature difference (top panel), and conductivity difference between near-surface MicroCATs #1727 and #1835 during WHOTS-8 (lower panel). The red line is a 24-hr running mean.

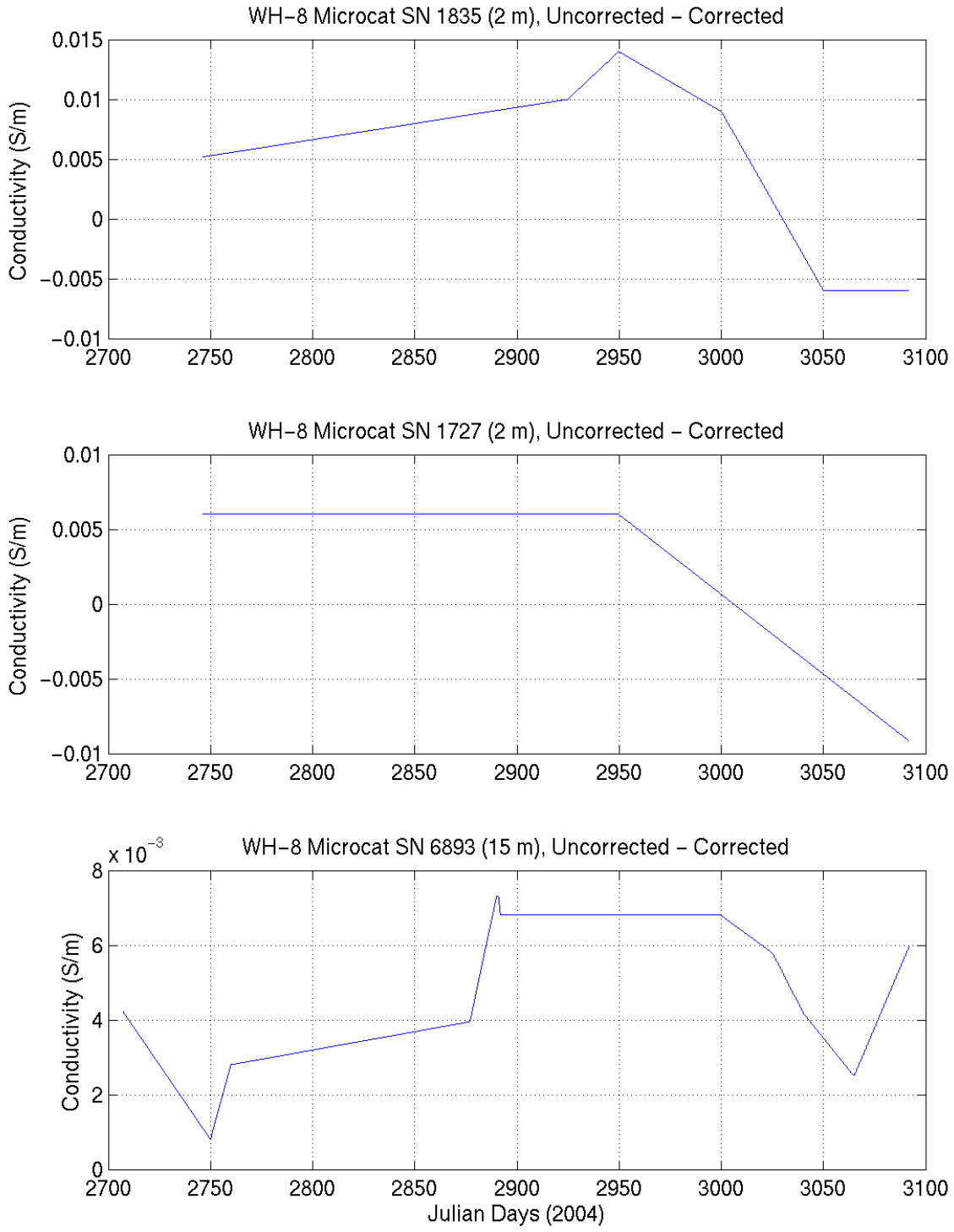

Figure 5-8. Conductivity sensor corrections for MicroCATs and SeaCATs during WHOTS-8

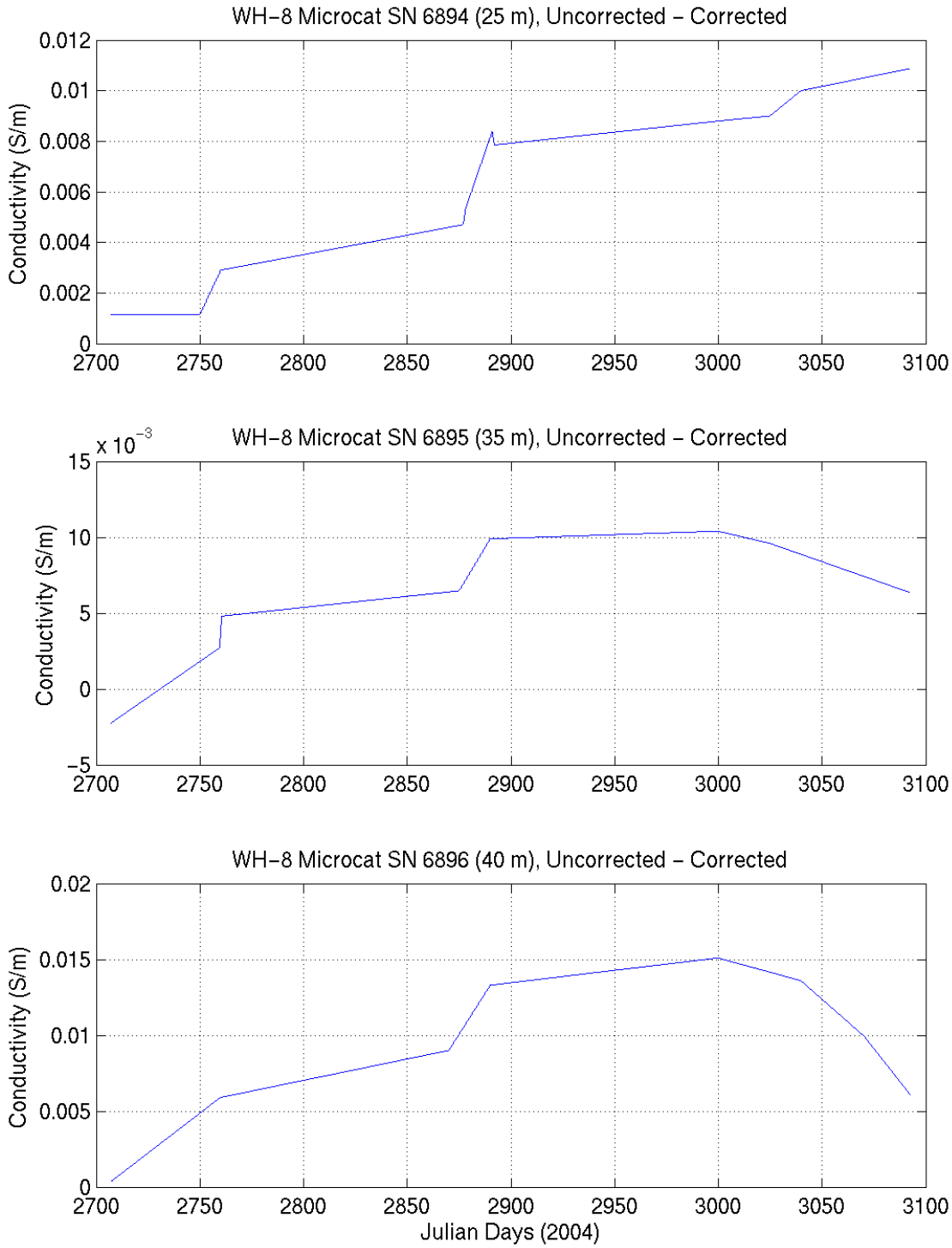

Figure 5-8. (Contd.)

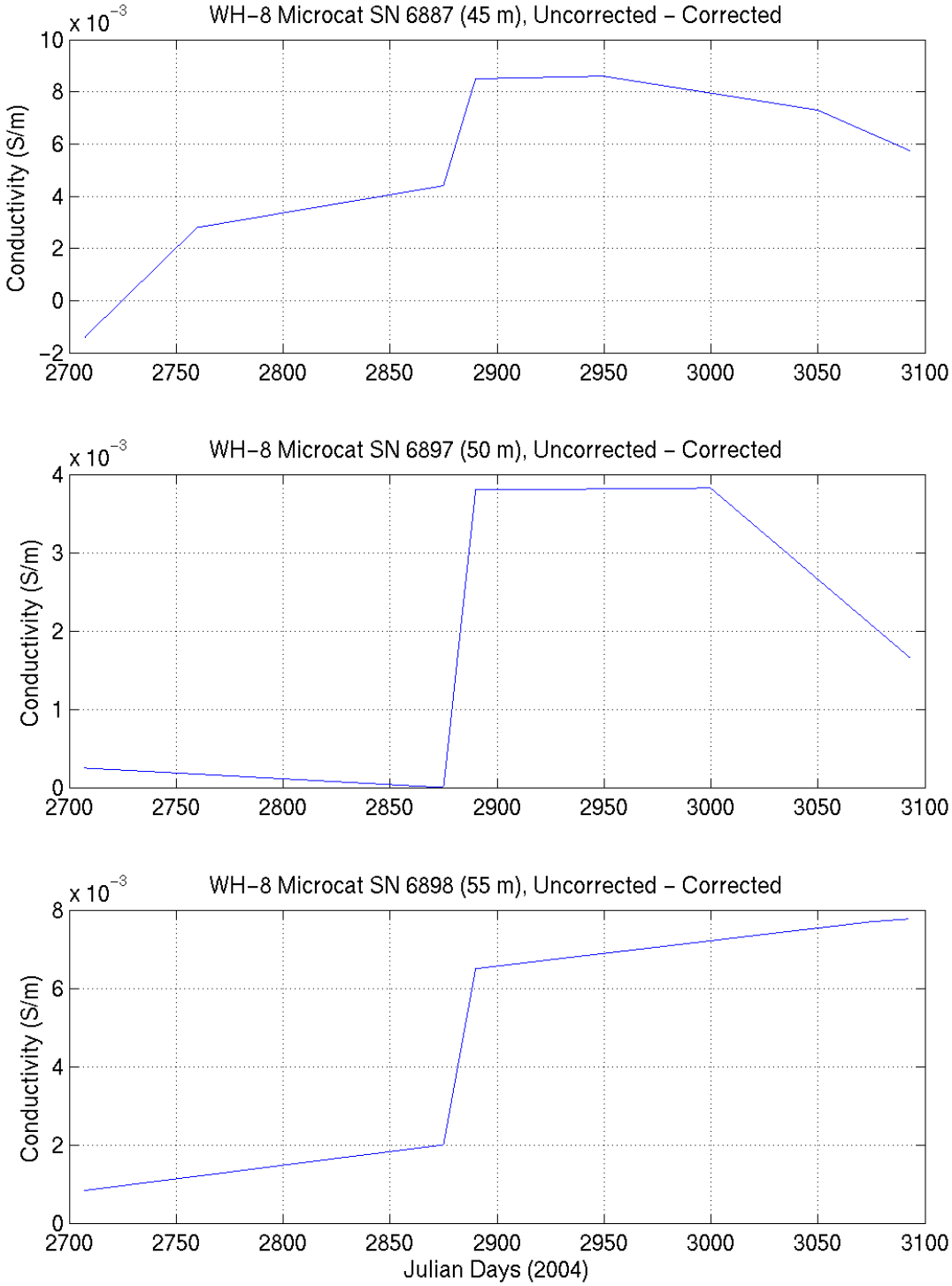

Figure 5-8. (Contd.)

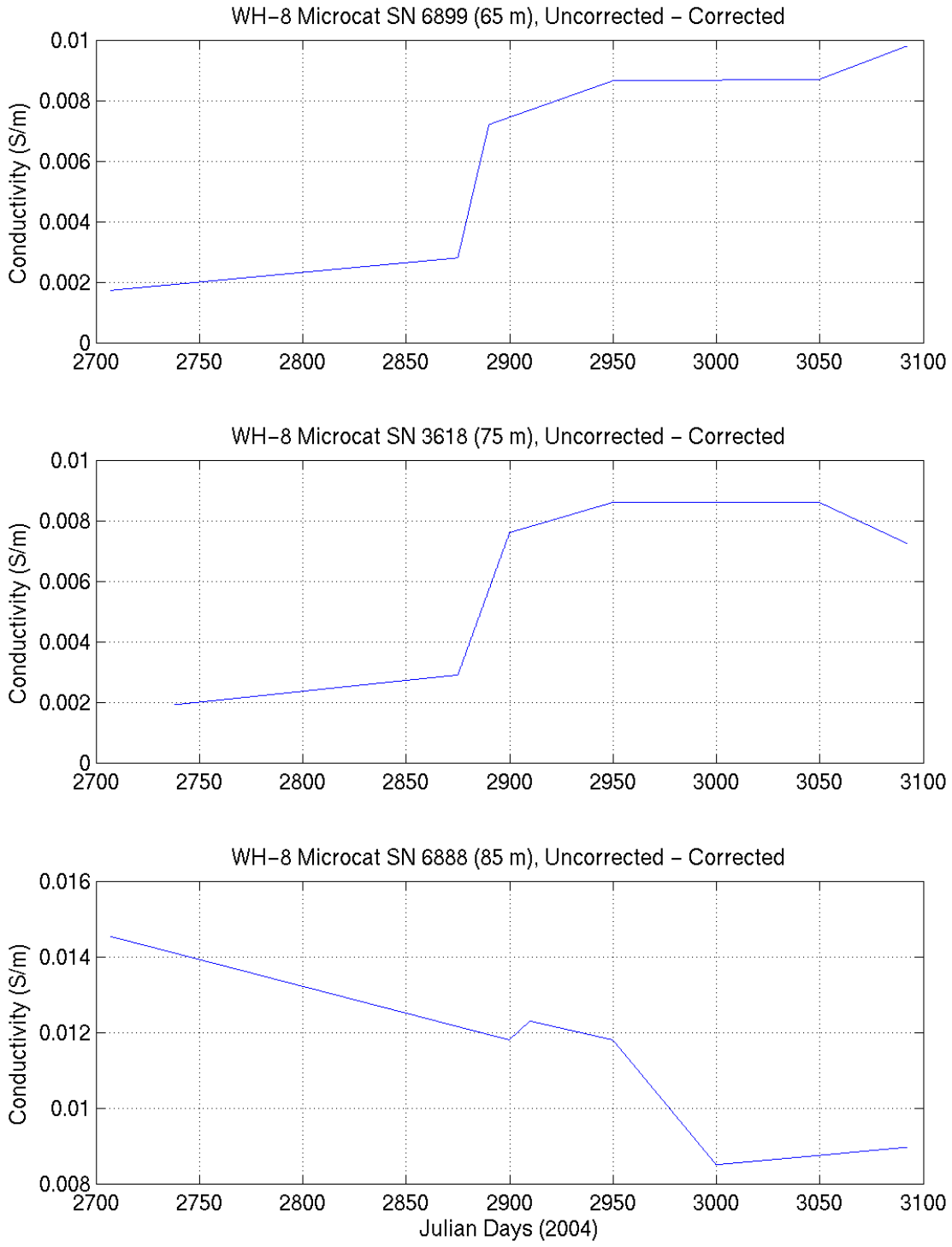

Figure 5-8. (Contd.)

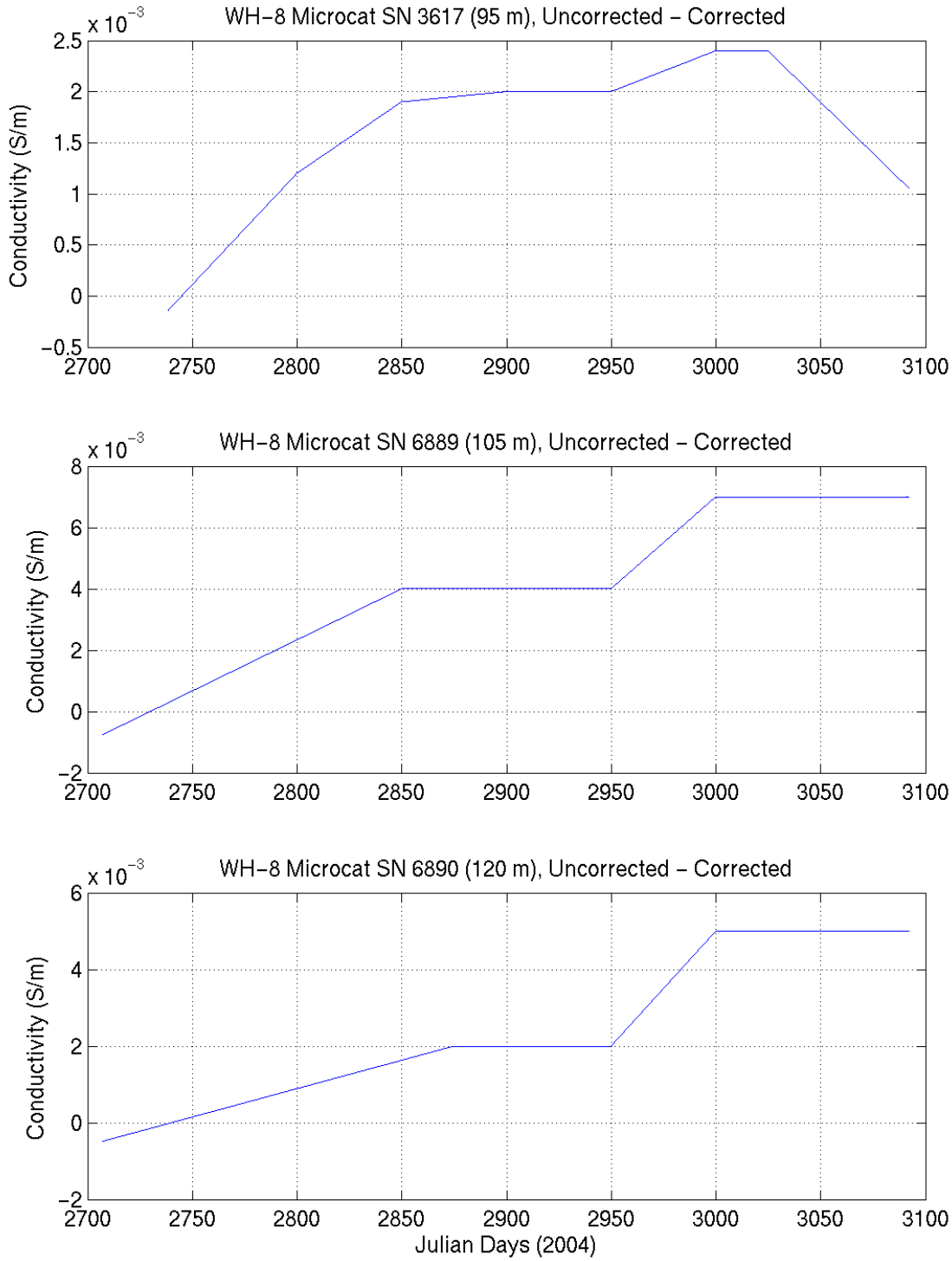

Figure 5-8. (Contd.)

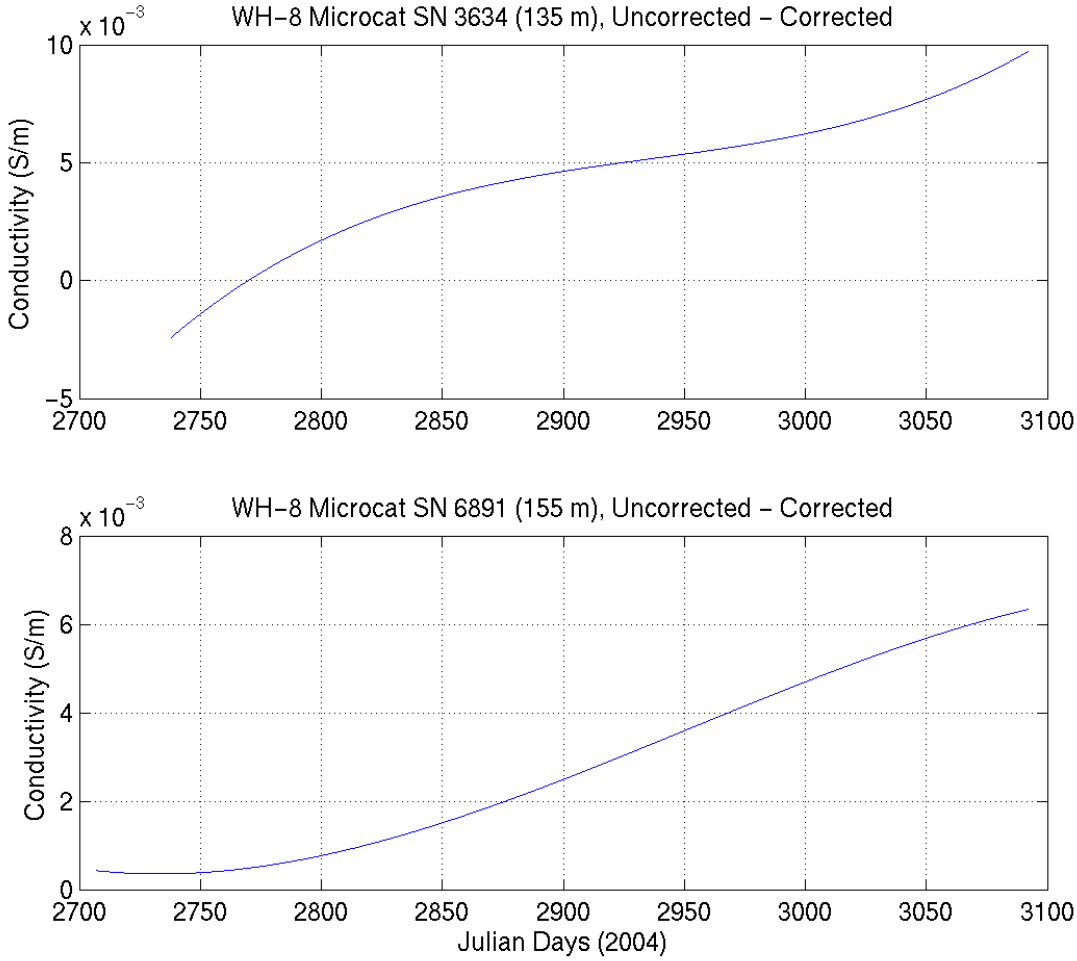

Figure 5-8. (Contd.)

B. Acoustic Doppler Current Profiler

Two Teledyne/RD Instruments broadband Workhorse Sentinel ADCP's were deployed on the WHOTS-8 mooring. A 600 kHz ADCP was deployed at 47.5 m depth in the upward-looking configuration, and a 300 kHz ADCP was deployed at 125 m, also in the upward-looking configuration. The instruments were installed in aluminum frames along with an external battery module to provide sufficient power for the intended period of deployment. The four ADCP beams were angled at 20° from the vertical line of the instrument. The 300 kHz ADCP was set to profile across 30 range cells of 4 m with the first bin centered 2.76 m from the transducer. The maximum range of the instrument was just short of 119 m. The 600 kHz ADCP was set to profile across 25 range cells of 2 m. The shallowest bin with any data was centered at 0.38 m while the first bin was centered at 44.38 m. The specifications of the instruments are shown in Table 5-3.

Table 5-3. Specifications of the ADCP's used for the WHOTS-8 mooring.

Instrument	Description
ADCP	*RDI Workhorse Sentinel, 300KHz* Model: WHS300-I-UG86; Serial Number: 4891 *RDI Workhorse Sentinel, 600KHz* Model: WHS600; Serial Number: 1825
Battery module	*300 kHz* Model: 717-3001-00; Serial Number: 3169 *600 kHz* Model: WH-EXT-BCL; Serial Number: 182

1. Compass Calibrations

Pre-Deployment

Prior to the WHOTS-8 deployment a field calibration of the internal ADCP compass was performed at the football field of the University of Hawai'i at Manoa on 23 June 2011 for both the 300 kHz and the 600 kHz instruments. Each instrument was mounted in the deployment cage along with the external battery module and was located away from potential sources of magnetic field disturbances. The ADCP was mounted to a turntable, which was aligned with magnetic north using a surveyor's compass. Using the built-in RDI calibration procedure, the instrument was tilted in one direction between 10 and 20 degrees and then rotated through 360 degrees at less than 5 ° /sec. The ADCP was then tilted in a different direction and a second rotation made. Based on the results from the first two rotations, calibration parameters are temporarily loaded and the instrument, tilted in a third direction is rotated once more to check the calibration. Results from each pre-deployment field calibration are shown in Table 5-4 (Figure 5-9 and Figure 5-9).

Table 5-4. Results from the WHOTS-8 pre-deployment ADCP compass field calibration procedure.

300 kHz (SN 7637)	Single Cycle Error (°)	Double Cycle Error (°)	Largest Double + Single Cycle Error (°)	RMS of 3rd Order and Higher + Random Error (°)	**Over all Error** (°)	Pitch Mean and Standard Deviation (°)	Roll Mean and Standard Deviation (°)
Before Calibration	1.96	0.16	2.11	0.09	**1.97**	0.34 ± 0.52	0.35 ± 0.34
	1.80	0.12	1.92	0.15	**1.82**	15.14 ± 0.46	0.22 ± 0.48
After Calibration	2.56	0.45	3.01	0.23	**2.61**	-0.12 ± 0.49	13.32 ± 0.43

600 kHz (SN 1825)	Single Cycle Error (°)	Double Cycle Error (°)	Largest Double + Single Cycle Error (°)	RMS of 3rd Order and Higher + Random Error (°)	**Over all Error** (°)	Pitch Mean and Standard Deviation (°)	Roll Mean and Standard Deviation (°)
Before Calibration	1.27	0.44	1.71	0.11	**1.48**	-1.81 ± 0.38	0.12 ± 0.37
	0.42	0.19	0.61	0.19	**0.48**	13.10 ± 0.59	0.45 ± 0.52
After Calibration	1.50	0.54	2.03	0.09	**1.69**	-0.32 ± 0.39	12.80 ± 0.41

Post-Deployment

After the WHOTS-8 mooring was recovered, the performance of the ADCP compass was tested at the football field of the University of Hawai'i at Manoa on 12 August 2012 with an identical compass calibration procedure as during the pre-deployment calibration. Results from the WHOTS-8 post-deployment ADCP compass field calibration procedure are listed in Table 5-5 (Figure 5-10).

Table 5-5. Results from the WHOTS-8 post-deployment ADCP compass field calibration procedure

300 kHz	Single Cycle Error (°)	Double Cycle Error (°)	Largest Double + Single Cycle Error (°)	RMS of 3rd Order and Higher + Random Error (°)	**Over all Error** (°)	Pitch Mean and Standard Deviation (°)	Roll Mean and Standard Deviation (°)
After Calibration	1.71	0.48	2.20	0.18	**1.75**	0.78 ± 1.04	0.46 ± 0.88

600 kHz	Single Cycle Error (°)	Double Cycle Error (°)	Largest Double + Single Cycle Error (°)	RMS of 3rd Order and Higher + Random Error (°)	**Over all Error** (°)	Pitch Mean and Standard Deviation (°)	Roll Mean and Standard Deviation (°)
After Calibration	1.13	0.19	1.33	0.14	**1.15**	-1.21 ± 0.95	0.57 ± 0.79

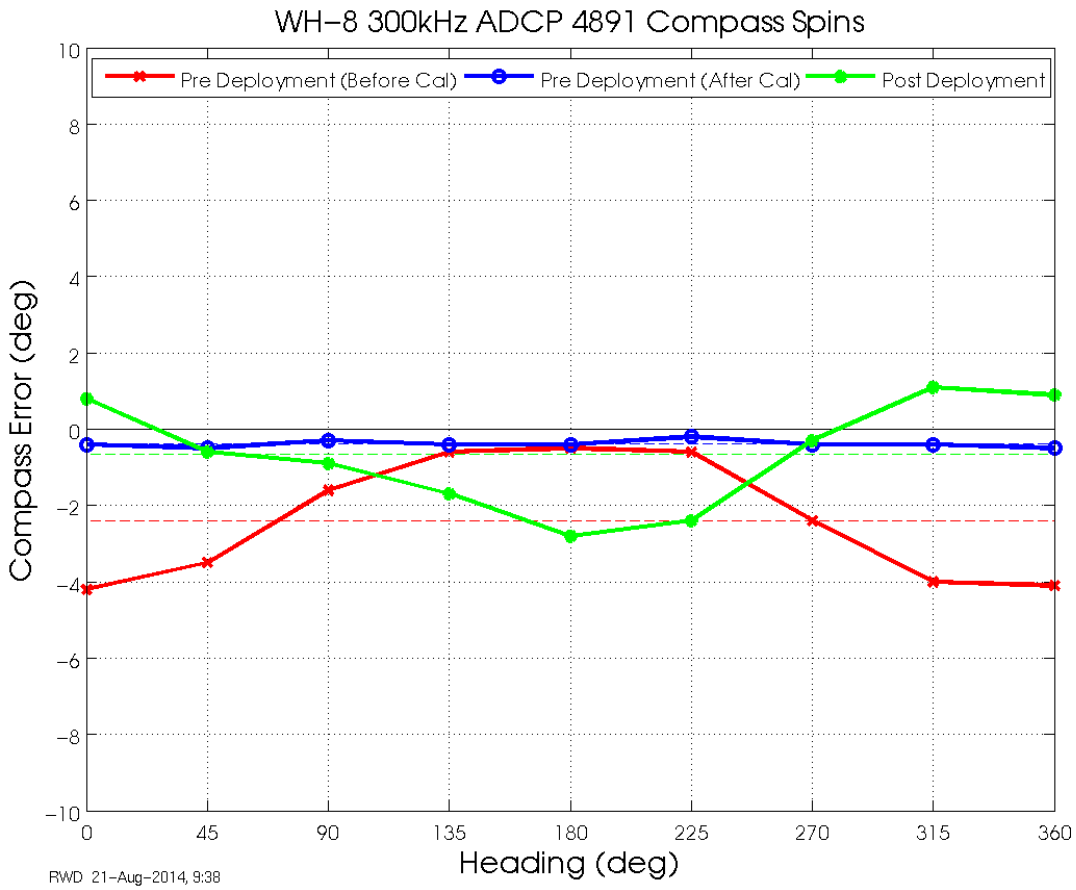

Figure 5-9. Results of the post-cruise compass calibration, conducted 12 August 2012 on ADCP SN4891 at the University of Hawai'i at Manoa.

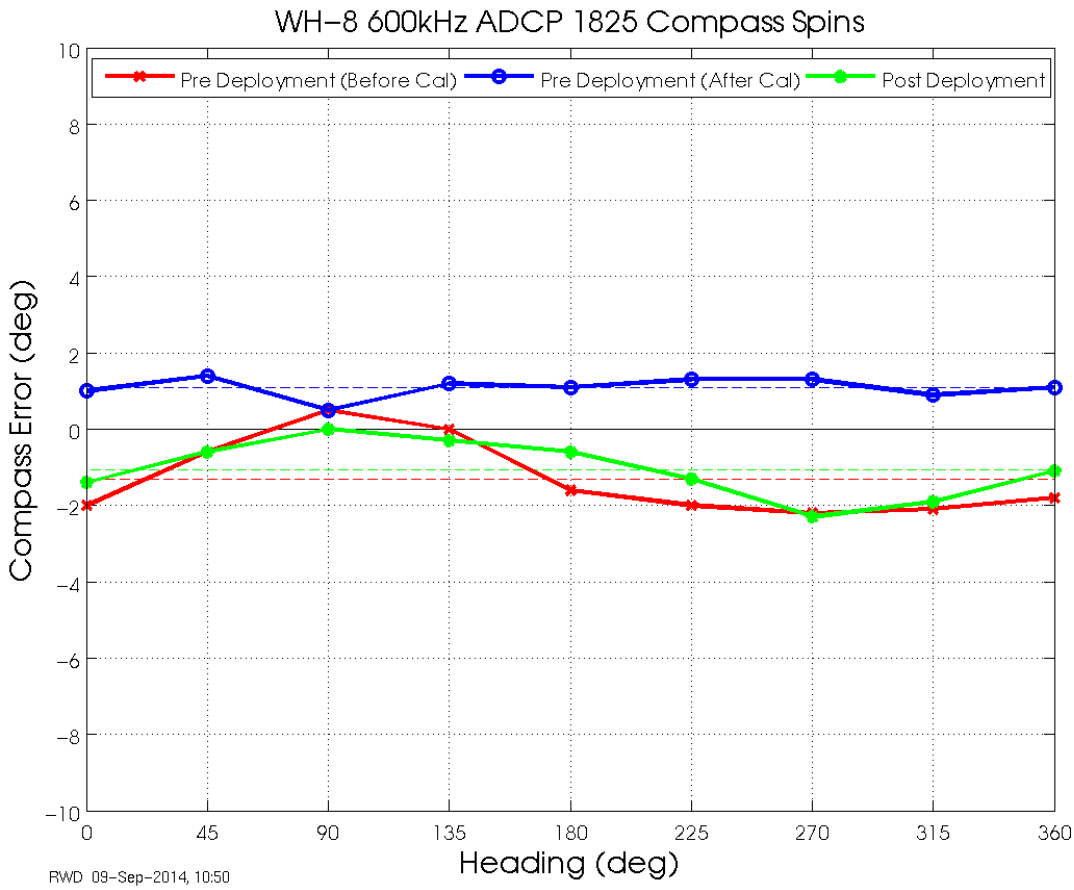

Figure 5-10. Results of the post-cruise compass calibration, conducted 12 August 2012, on ADCP SN1825 at the University of Hawai'i at Manoa.

2. ADCP Configurations

Individual configurations for the two ADCP's on the WHOTS-8 mooring are detailed in Appendices 1 and 2. The salient differences for each of the ADCP's are summarized below.

300 kHz (125m)

The ADCP, set to a beam frequency of 300 kHz, was configured in a burst sampling mode consisting of 40 pings per ensemble in order to resolve low-frequency wave orbital motions. The interval between each ping was 4 seconds so the ensemble length was 160 seconds. The interval between ensembles was 10 minutes. Data were recorded in earth coordinates with a heading bias of 9.92° E used. This heading bias was corrected in post-deployment processing to a heading bias of 9.88° E. False targets, usually fish, were screened by setting the threshold maximum to 70 counts. Velocity data were rejected if the difference in echo intensity among the four beams exceeded this threshold.

600 kHz (47.5m)

The ADCP, set to a beam frequency of 600 kHz, was configured in a burst sampling mode consisting of 80 pings per ensemble. The interval between each ping was 2 seconds so the ensemble length was also 160 seconds. The interval between ensembles was 10 minutes. Data were recorded in earth coordinates with a heading bias of 9.92° E used. This heading bias was corrected in post-deployment processing to a heading bias of 9.88° E. The threshold maximum was also set to 70 counts. Velocity data were rejected if the difference in echo intensity among the four beams exceeded this threshold.

3. ADCP data processing procedures

Binary files output from the ADCP were read and converted to MATLAB™ binary files using scripts developed by Eric Firing's ADCP lab (http://current.soest.hawaii.edu). The beginning of the raw data files were truncated to a time after the mooring anchor was released in order to allow time for the anchor to reach the seabed and for the mooring motions that follow the impact of the anchor on the sea floor to dissipate. The pitch, roll, and ADCP temperature were examined in order to pick reasonable times that ensured good data quality but without unnecessarily discarding too much data (see Figure 5-11 and Figure 5-12). Truncation at the end of the data files were chosen to be the ensemble prior to the time that the acoustic release signal was sent to avoid contamination due to the ascent of the instrument. The times of the first ensemble from the raw data, deployment and recovery time, along with the times of the truncated records of both deployments are shown in Table 5-6.

Table 5-6. ADCP record times (UTC) during WHOTS-8 deployment.

	300 kHz	600 kHz
Raw file beginning and end times	06-Jul-2011 00:00:00 11-Jan-2012 01:59:59	06-Jul-2011 00:00:00 22-Dec-2011 23:00:00
Deployment and recovery times	06-Jul-2011 19:17 in water 07-Jul-2011 01:08 anchor over 16-Jun-2012 17:47 release triggered 17-Jun-2012 03:31 on deck	06-Jul-2011 19:50 in water 07-Jul-2011 01:08 anchor over 16-Jun-2012 17:47 release triggered 17-Jun-2012 03:04 on deck
Processed data beginning and end times	07-Jul-2011 02:10:00 11-Jan-2012 01:59:59	07-Jul-2011 02:10:00 22-Dec-2011 23:00:00

ADCP Clock Drift

During past deployments, upon recovery the ADCP clocks were compared with the ship's time server and the difference between the two was recorded. Any discrepancies between the clocks would lead to adjustments in the ADCP data. Due to both ADCP's failing around January 2012, clock drift could not be determined for the WHOTS-8 moored ADCPs.

Heading Bias

As mentioned in the ADCP configuration section, the data were recorded in earth coordinates. A heading bias, the angle between magnetic north and true north, can be included in the setup to obtain output data in true earth coordinates. Magnetic variation was obtained from the National Geophysical Data Center 'Geomag' calculator (http://www.ngdc.noaa.gov/seg/geomag). For a yearlong deployment a constant value is acceptable because the change in declination is small, approximately -0.02° year^{-1} at the WHOTS location. A heading bias of 9.92° was entered in the setup of the WHOTS-8 ADCP's, but was corrected to 9.88° during post-deployment processing.

Speed of sound

Due to the constant of proportionality between the Doppler shift and water speed, the speed of sound needs only be measured at the transducer head (Firing, 1991). The sound speed used by the ADCP is calculated using a constant value of salinity (35) and the temperature recorded by the transducer temperature sensor of the ADCP. Using CTD profiles close to the mooring during HOT cruises, HOT-233 to HOT-242, and from the WHOTS deployment/recovery cruises, the mean salinity at 125 dbar was 35.27 while the mean salinity at 47.5 dbar was 35.09. Mean ADCP temperature at 125 dbar was 22.94 °C and 24.53 °C at 47.5 dbar (Figure 5-13). The maximum associated mean sound velocity difference is less than 0.4 m s^{-1} which represents a change of less than 0.03%, so no correction was made.

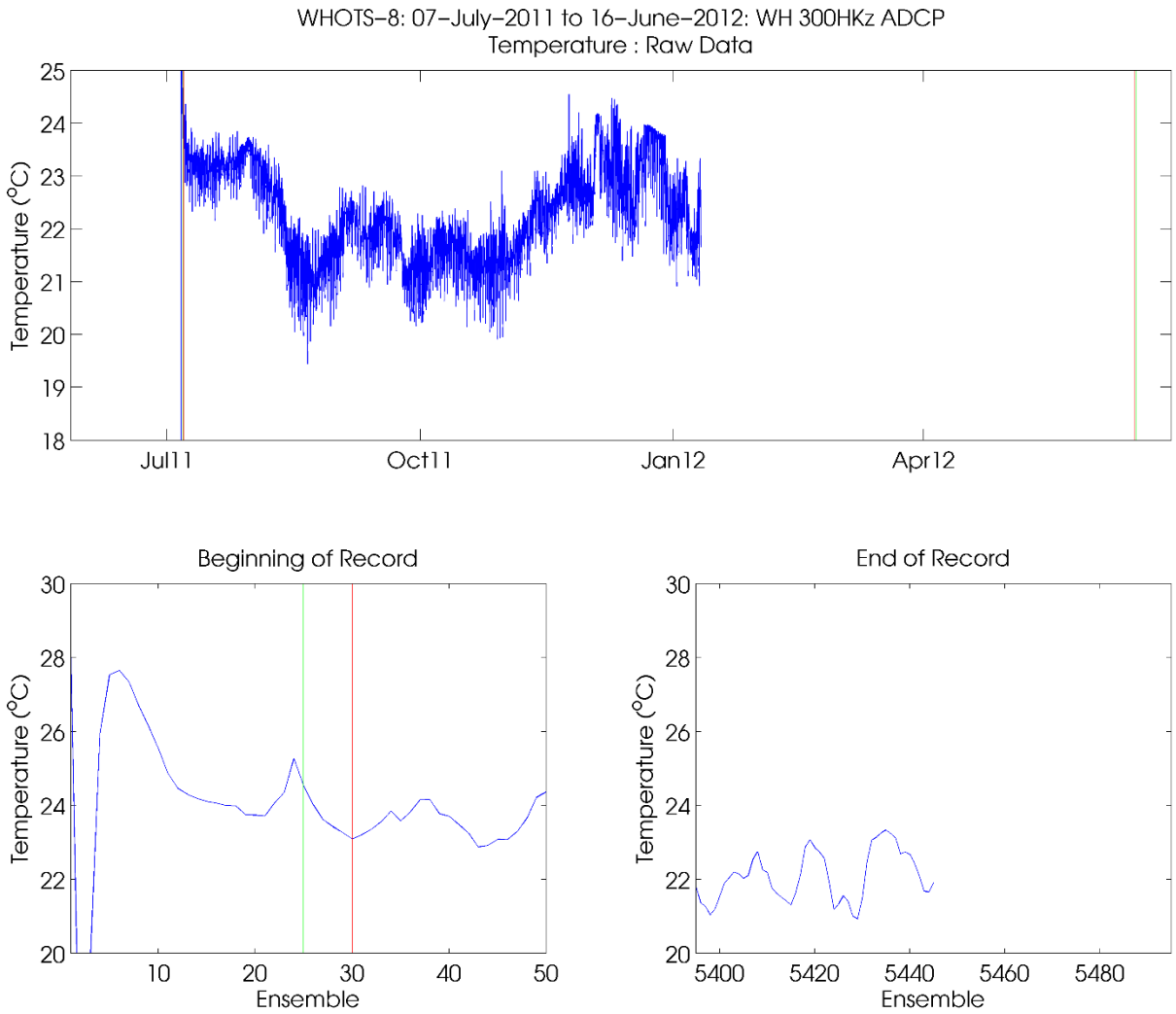

Figure 5-11. Temperature record from the 300 kHz ADCP during WHOTS-8 mooring (top panel). The bottom panel shows the beginning and end of the record with the green vertical line representing the in-water time during deployment and out-of-water time for recovery. The red line represents the anchor release and acoustic release trigger for deployment and recovery respectively.

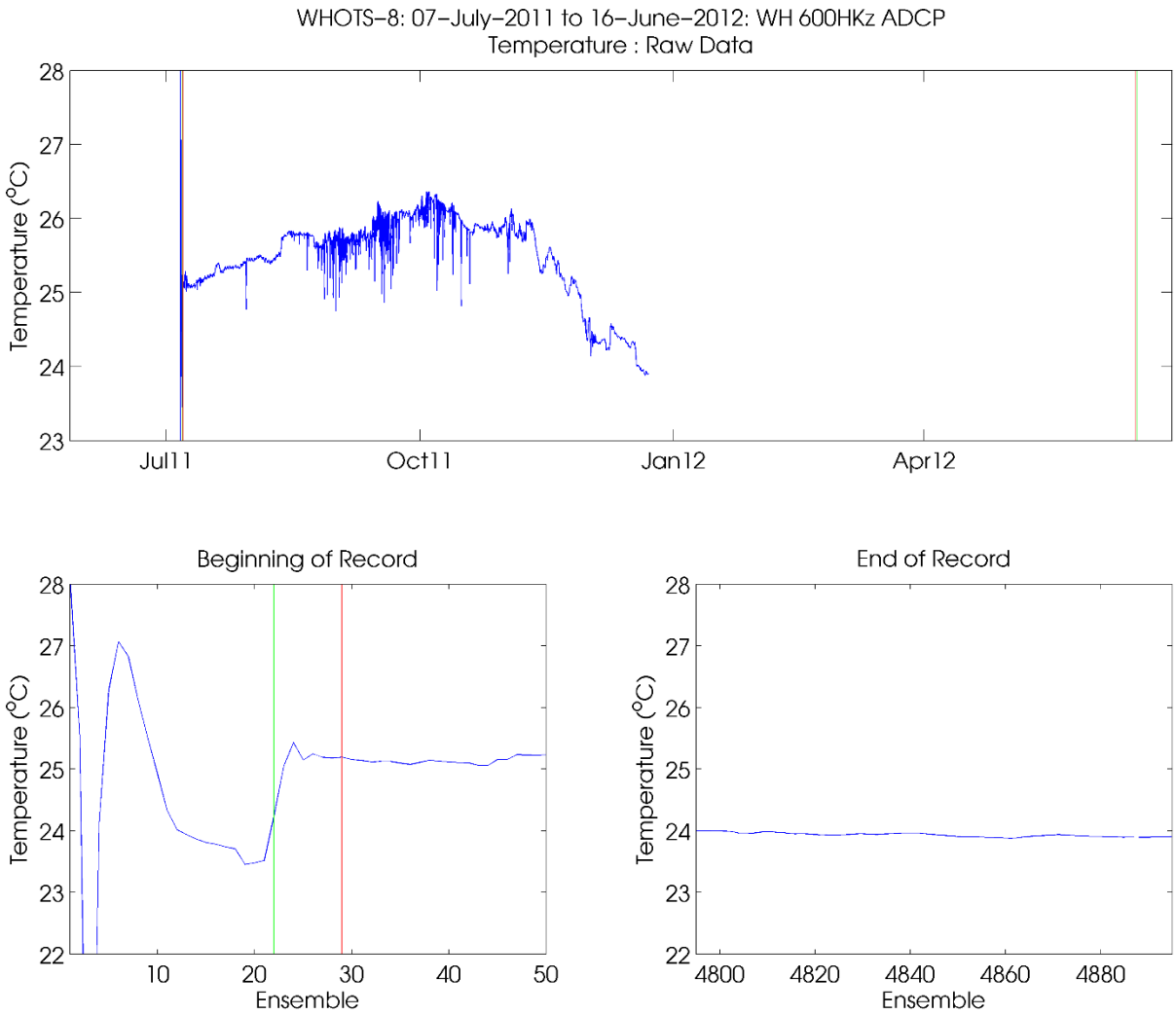

Figure 5-12. Same as Figure 5-11, but for the 600 kHz ADCP.

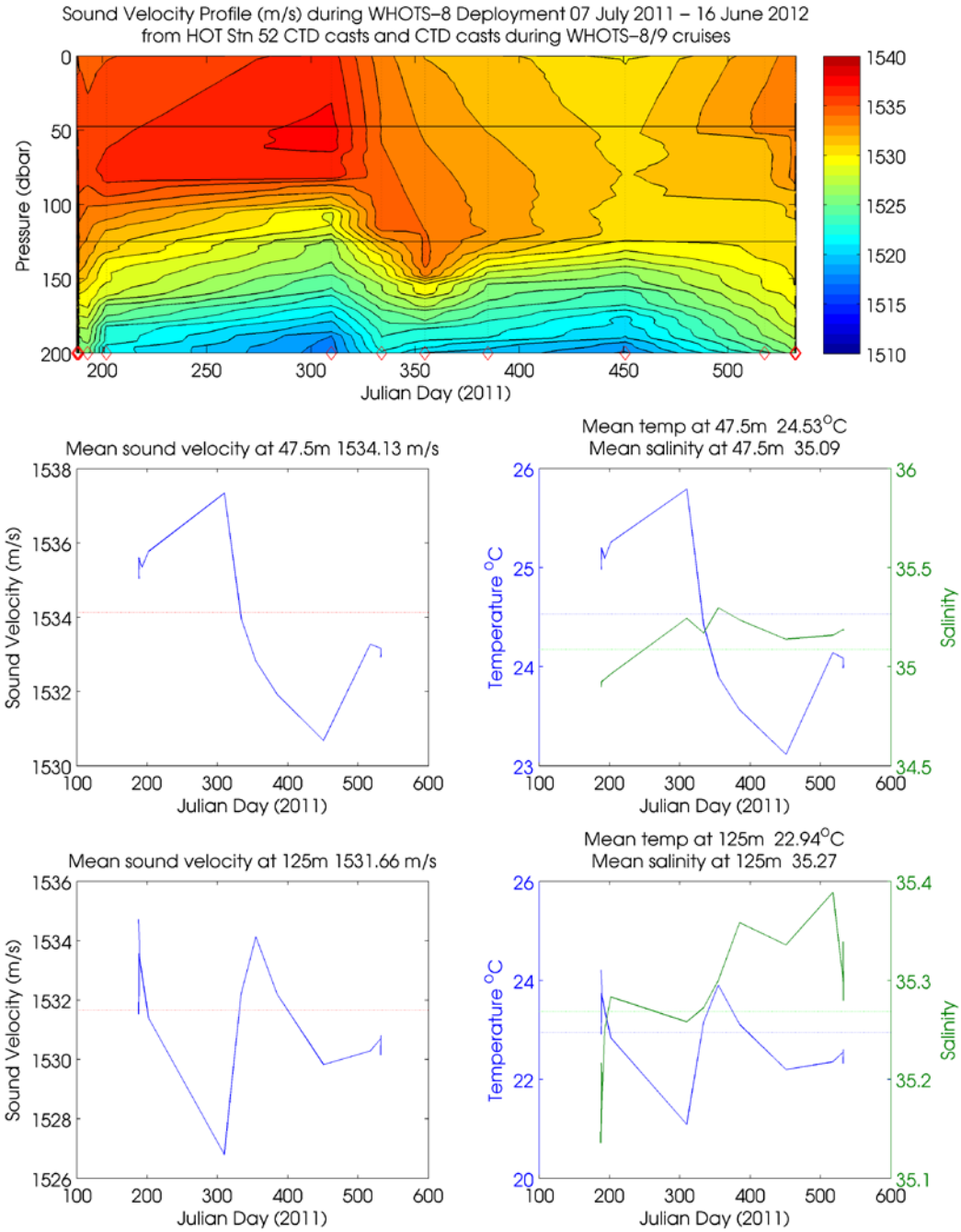

Figure 5-13. Sound speed profile (top panel) during the deployment of the WHOTS-8 mooring from 2 dbar CTD data taken during regular HOT cruises and CTD profiles taken during the WHOTS-9 recovery/deployment cruise (individual casts marked with a red diamond). The bottom left panels show the sound velocity at the depth of the ADCP's (47.5 m and 125 m), with the mean sound velocity indicated with a red line. The lower right panels show the temperature and salinity at each ADCP depth for the time series with the mean temperatures indicated with blue lines and mean salinity indicated with green lines.

Quality Control

Quality control of the ADCP data involved the thorough examination of the velocity, instrument orientation and diagnostic fields to develop the basis of the QC flagging procedures. Details of the methods used can be found in the WHOTS Data Report 1 (Santiago-Mandujano et al., 2007). The following QC procedures were applied to the WHOTS-8 deployment ADCP data.

1) The first bin (closest to the transducer) is sometimes corrupted due to what is known as ringing. A period of time is needed for the sound energy produced during a transmit pulse at the transducer to dissipate before the ADCP is able to properly receive the returned echoes. The blanking interval is used to prevent useless data from being recorded. If it is too short, signal returns can be contaminated from the lingering noise from the transducer. The default value for the blanking interval, (expressed as a distance) of 1.76 m was used for the 300 kHz ADCP, whereas an interval of 0.88 m was used for the 600 kHz ADCP. Thus bin 1 was flagged and replaced with Not a Number (NaN) in the quality controlled dataset (Figure 5-14).

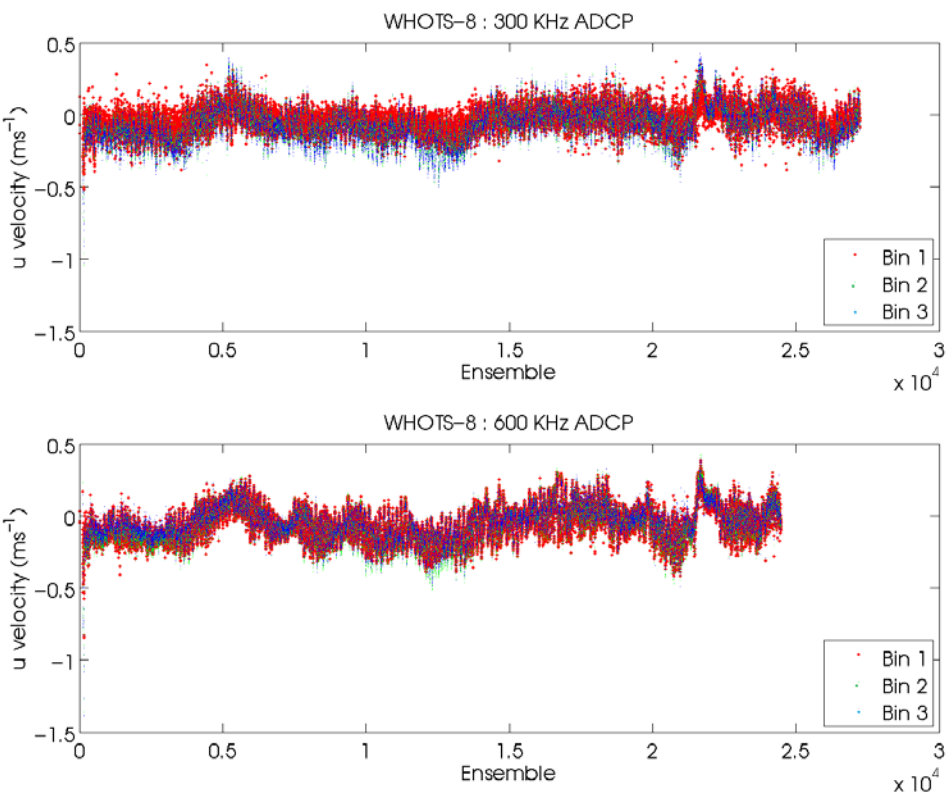

Figure 5-14. Eastward velocity component for the 300 kHz (top panel) and the 600 kHz (bottom panel) ADCPs showing the incoherence between depth 1 (red) and bins 2 (green) and 3 (blue).

2) For an upward-looking ADCP with a beam angle of 20° within range of the sea surface, the upper 6% of the depth range is contaminated with sidelobe interference (RDI, 1996). This is a result of stronger signal reflection from the sea surface (than from scatterers)

overwhelming the sidelobe suppression of the transducer. Data are flagged using echo intensity (a measure of the strength of the return signal) from each beam to determine when the signal is contaminated with reflection from the sea surface.

3) The use of four beams (along with instrument orientation) to resolve currents into their component earth-referenced velocities provides us with a second estimate of the vertical velocity. The scaled difference between these estimates is defined as the error velocity and it is useful for assessing data quality. Error velocities with an absolute magnitude greater than 0.15 m s^{-1} (a value comparable to the standard deviation of observed horizontal velocities) were flagged and removed.

4) An indication of data quality for each ensemble is given by the "percent good" data indicator which accompanies each individual beam for each individual bin. The use of the percent good indicator is determined by the coordinate transformation mode used during the data collection. With profiles transformed into earth coordinates (as in the case of the WHOTS-8 deployment) the percent good fields show the percentage of data that was made using 4 and 3 beam solutions in each depth cell within an ensemble, and the percentage that was rejected as a result of failing one of the criteria set during the instrument setup (see Appendix 1: WHOTS-8 300 kHz ADCP Configuration). Data were flagged when data in each depth cell within an ensemble made from 3 or 4 beam solutions was 20% or less.

5) Data were rejected using correlation magnitude, which is the pulse-to-pulse correlation (in ping returns) for each depth cell. If anyone beam had a correlation magnitude of 20 counts or less, that data point was flagged.

6) Histograms of raw vertical velocity data and partially cleaned data from the ADCP [see Figure 5-15 and the WHOTS Data Report 1 (Santiago-Mandujano et al., 2007)] showed vertical velocities larger than expected, some exceeding 1 m s^{-1}. Recall that the instruments' burst sampling (4-second intervals for the 300 kHz and 2-second intervals for the 600 kHz, for 160 seconds every 10 minutes) was designed to minimize aliasing by occasional large ocean swell orbital motions (Section 3), and therefore are not the source of these large speeds in the data. These large vertical speeds are possibly fish swimming in the beams based on the histograms of the partially cleaned data; depth cells with an absolute value of vertical velocity greater than 0.3 m s^{-1} were flagged.

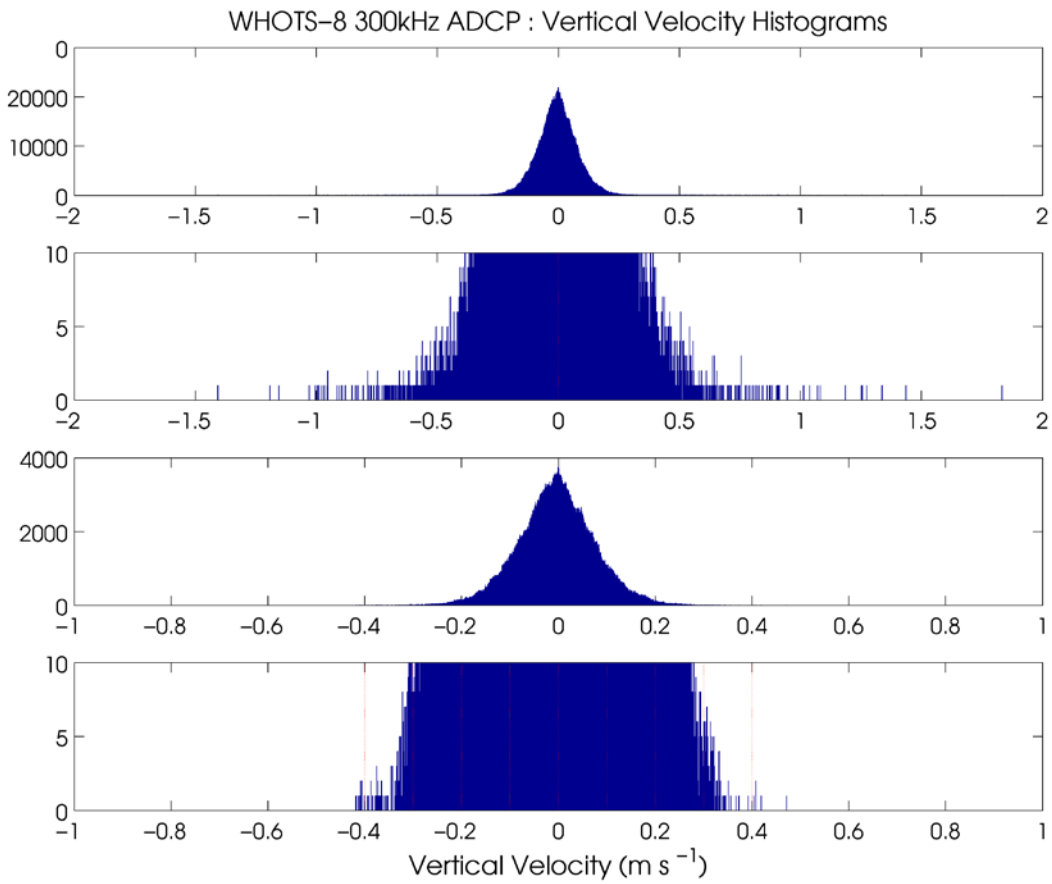

Figure 5-15. Histogram of vertical velocity of the 300 kHz ADCP for raw data (top panel) and enlarged for clarity (upper middle panel), and for partial quality controlled data (lower middle panel) and enlarged for clarity (bottom).

7) A quality control routine known as 'edgers' identifies outliers in surface bins using a five point median differencing method. The median velocity from surface bins was calculated for each ensemble, and then a five point running median of the surface bin median was calculated. This was then compared to individual velocity observations in the surface bins, and those differing by greater than 0.48 m/s were flagged.

8) A 5-pole low pass Butterworth filter with a cutoff frequency of 1/4 cycles/hour was used upon the length of the time-series to isolate low frequency flow for each bin independently. The low frequency flow is then subtracted giving a time series of high frequency velocity component fluctuations for each bin. Data points were considered outliers when their values exceeded four standard deviations from the mean (for each bin) and were removed.

9) A median residual filter used a 7-point (70 minute) median differencing method to define velocity fluctuations. A 7-point running median is calculated for each bin independently and the result is subtracted out giving time series of fluctuations relative

to the running median. Outliers greater than four standard deviations from the mean of the 7 points are flagged and removed for each bin.

10) Meticulous verification of all the quality control routines was performed through visual inspections of the quality controlled velocity data. Two methods were utilized; time-series of u and v components for multiple bins were evaluated as well as individual vertical profiles. The time-series methodology involved inspecting u and v components separately, five bins at a time, over 600 ensembles (100 hours). Any instance showing one bin behaving erratically from the other four bins was investigated further. If it seemed that there could be no reasonable rationale for the erratic points from the identified bin, the points were flagged [see Figure 5-16 and Figure 5-17 and the WHOTS Data Report 1 (Santiago-Mandujano et al., 2007)]. The intent of the vertical inspection of vertical profiles of the u and v components was to find entire profiles that were not aligned with neighboring profiles. Thirty u and v profiles were stacked at a time and were visually inspected for any anomalous data.

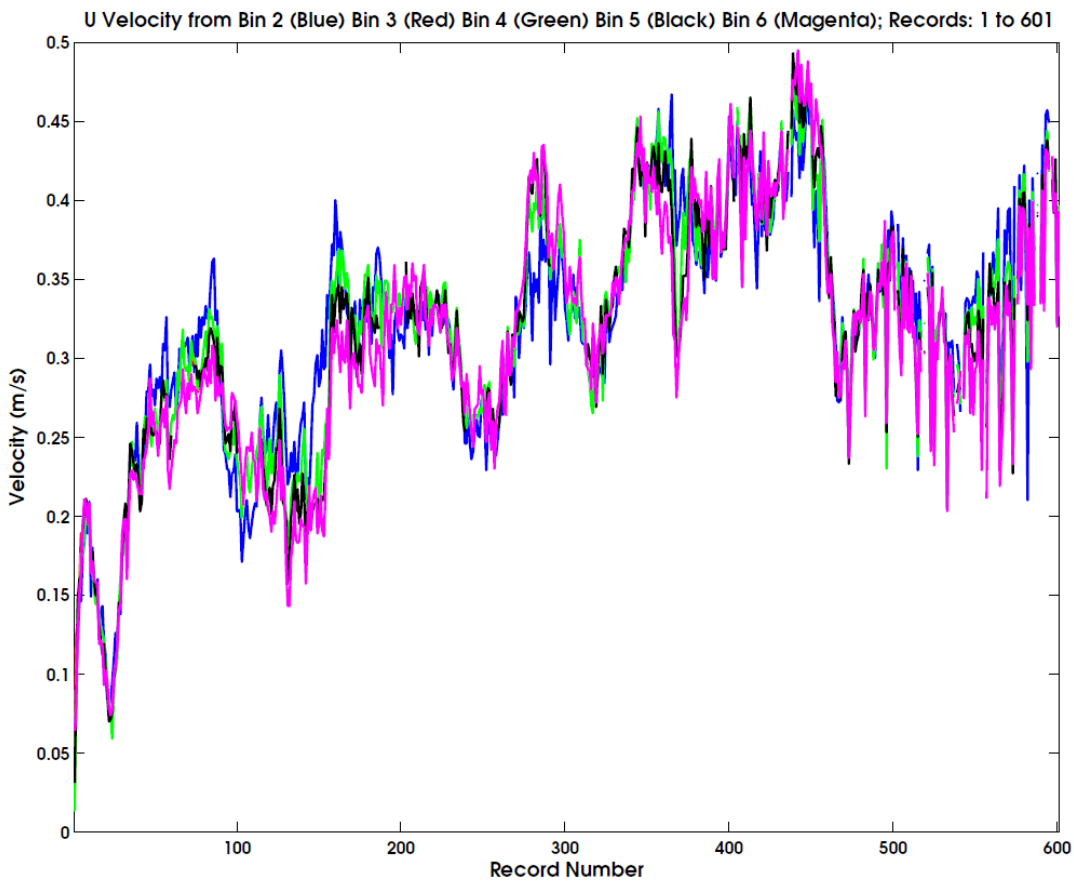

Figure 5-16. A sample of the horizontal inspection during WHOTS ADCP quality control

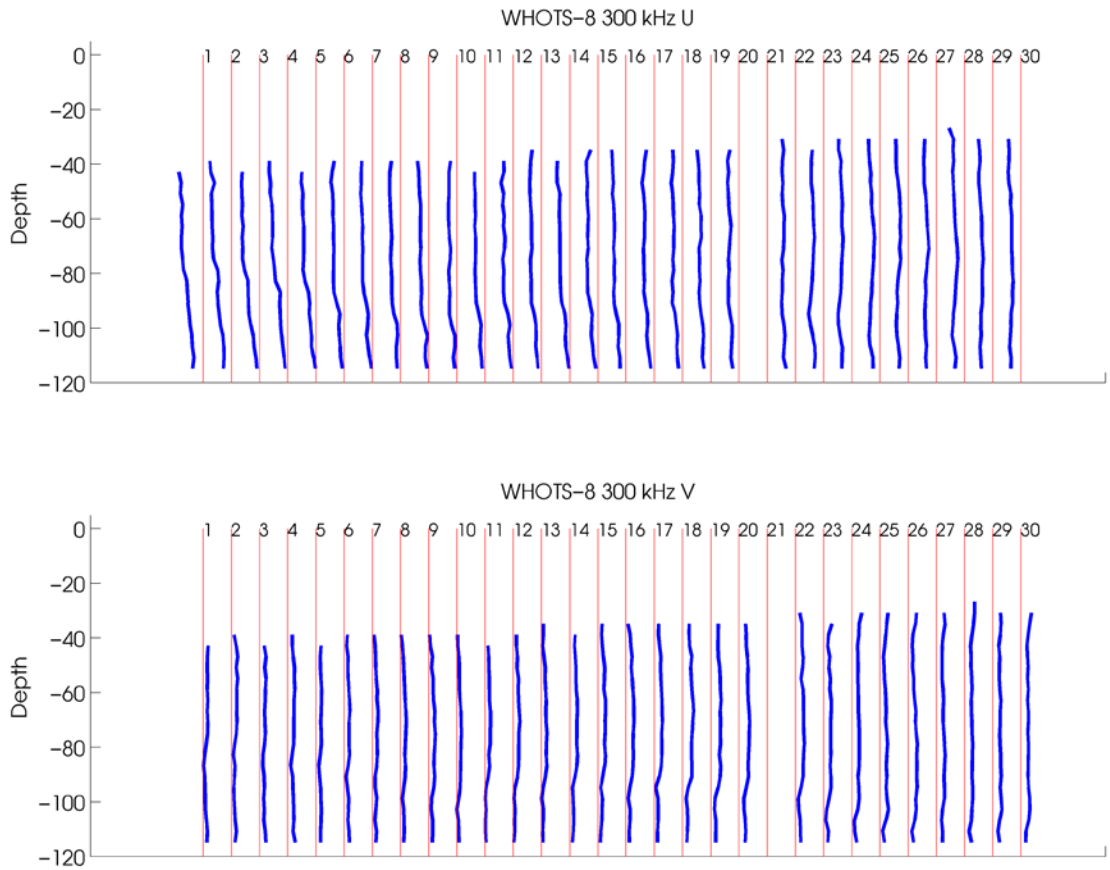

Figure 5-17. A sample of the profile consistency inspection from the WHOTS-8 ADCP quality control.

C. Vector Measuring Current Meter (VMCM)

Vector measuring current meters (VMCM) were deployed on the WHOTS-8 mooring at depths of 10 m and 30 m. VMCM data were processed by the WHOI/UOP group. A copy of the processing report is in Appendix 3 in Section 8.C. VMCM record times are shown in Table 5-7.

Table 5-7. Record times (UTC) for the VMCMs at 10 m and 30 m during the WHOTS-8 deployment

	WHOTS-8	
	VMCM016	VMCM019
Deployment and recovery times	05-Jul-2011 20:00:15 16-Jun-2012 17:46:15	05-Jul-2011 20:00:45 16-Jun-2012 17:46:45
Processed file beginning and end times	07-Jul-2011 03:00:00 16-Jun-2012 17:46:00	07-Jul-2011 03:00:00 16-Jun-2012 17:46:00

Daily (24 hour) moving averages of quality controlled 600 kHz ADCP data are compared to VMCM data interpolated to the ADCP ensemble times in the top panels of Figure 5-18 through Figure 5-21, and the difference is shown in the middle panels (ADCP data records ended in late 2011, early 2012, section 5-B-3). Velocities are not compared if greater than 80% of the ADCP data within a 24 hour average was flagged. The absolute value of mean differences for all deployments and both velocity components varied between 3 and 4 cm/s, with standard deviations between 2.5 and 5 cm/s. The VMCM data does not appear to degrade over time for any deployment. Propeller fouling would dampen measured VMCM velocity magnitudes, but a decrease in VMCM velocity magnitude compared to ADCP velocity magnitude with time is not observed.

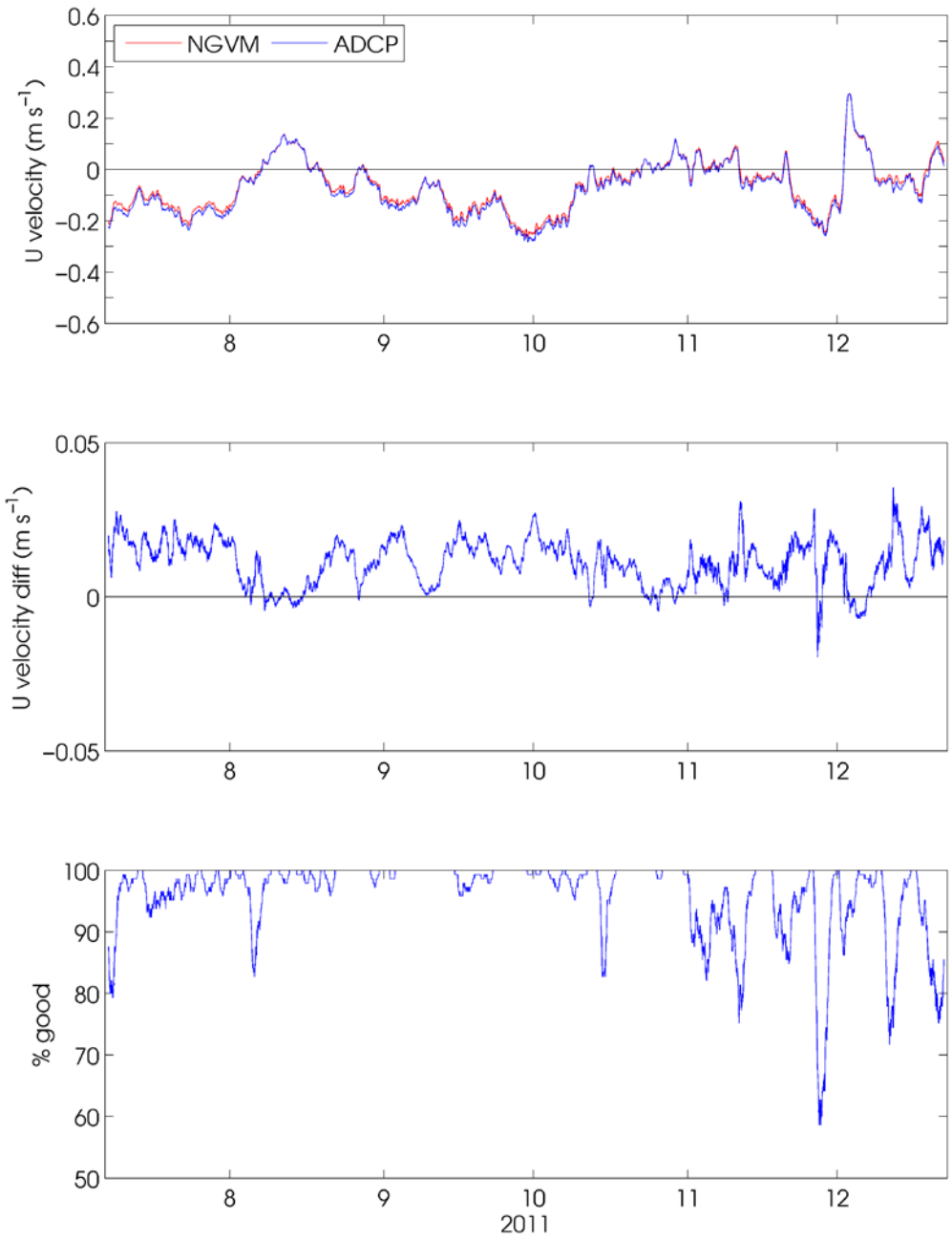

Figure 5-18. A comparison of 30 m VMCM and ADCP U velocity for WHOTS-8. The top panel shows 24 hour moving averages of VMCM zonal (U) velocity at 30 m depth (red) and ADCP U velocity from the nearest depth bin to 30 m (30.22 m). The middle panel shows the U velocity difference, and the bottom panel shows the percentage of ADCP data within the moving average not flagged by quality control methods.

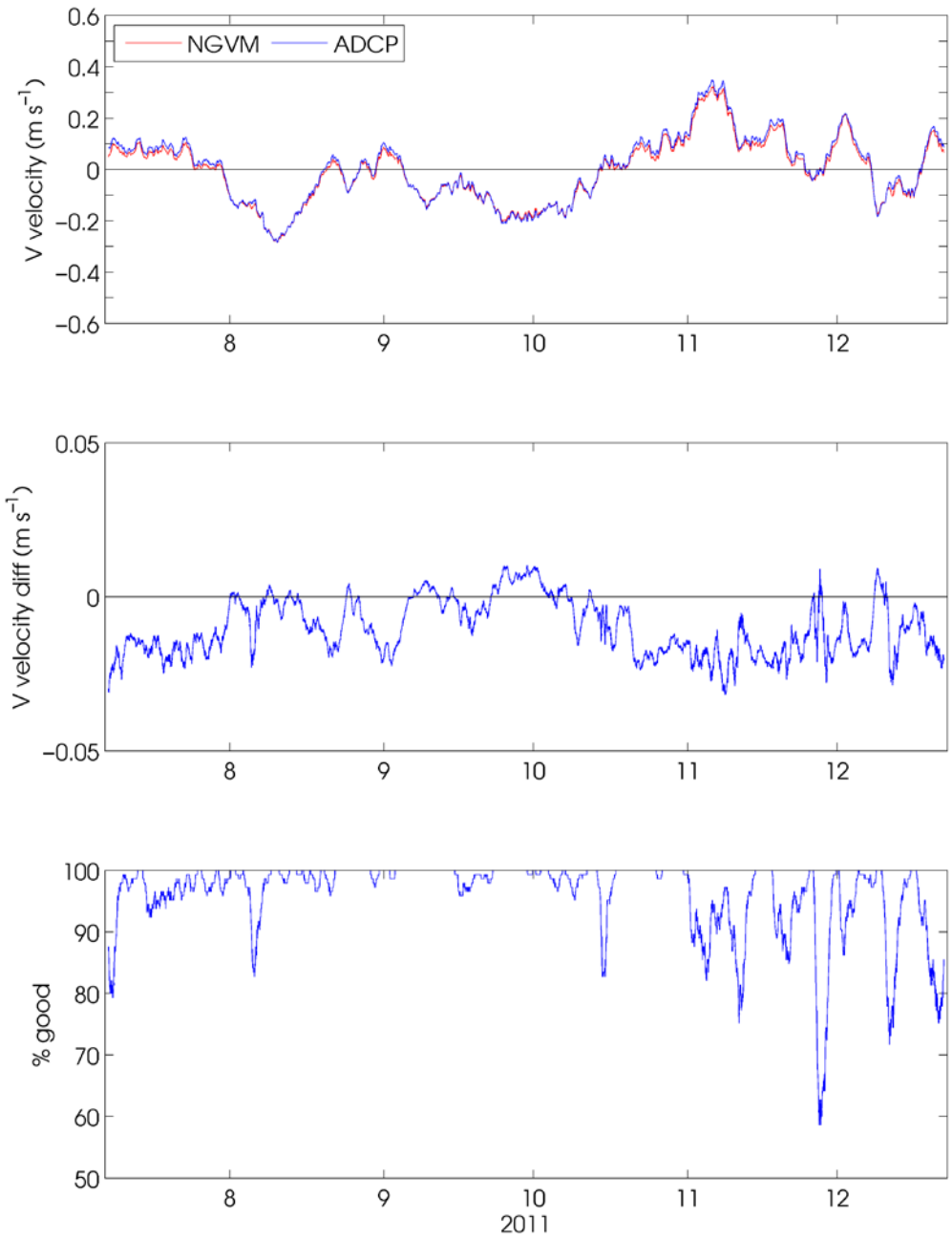

Figure 5-19. Same as in Figure 5-18 but for the meridional (V) velocity component.

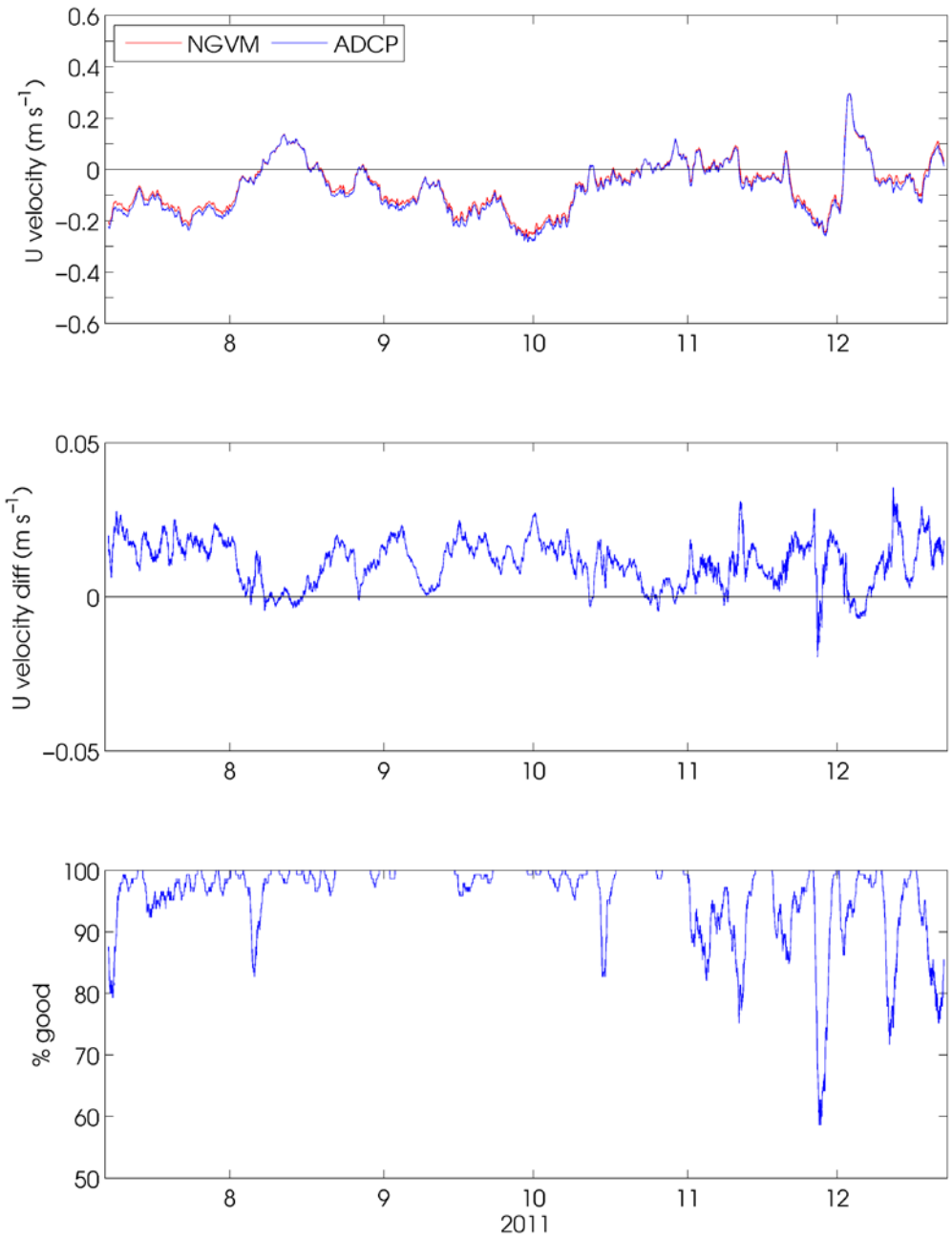

Figure 5-20. Same as in Figure 5-18 but for the 10 m VMCM.

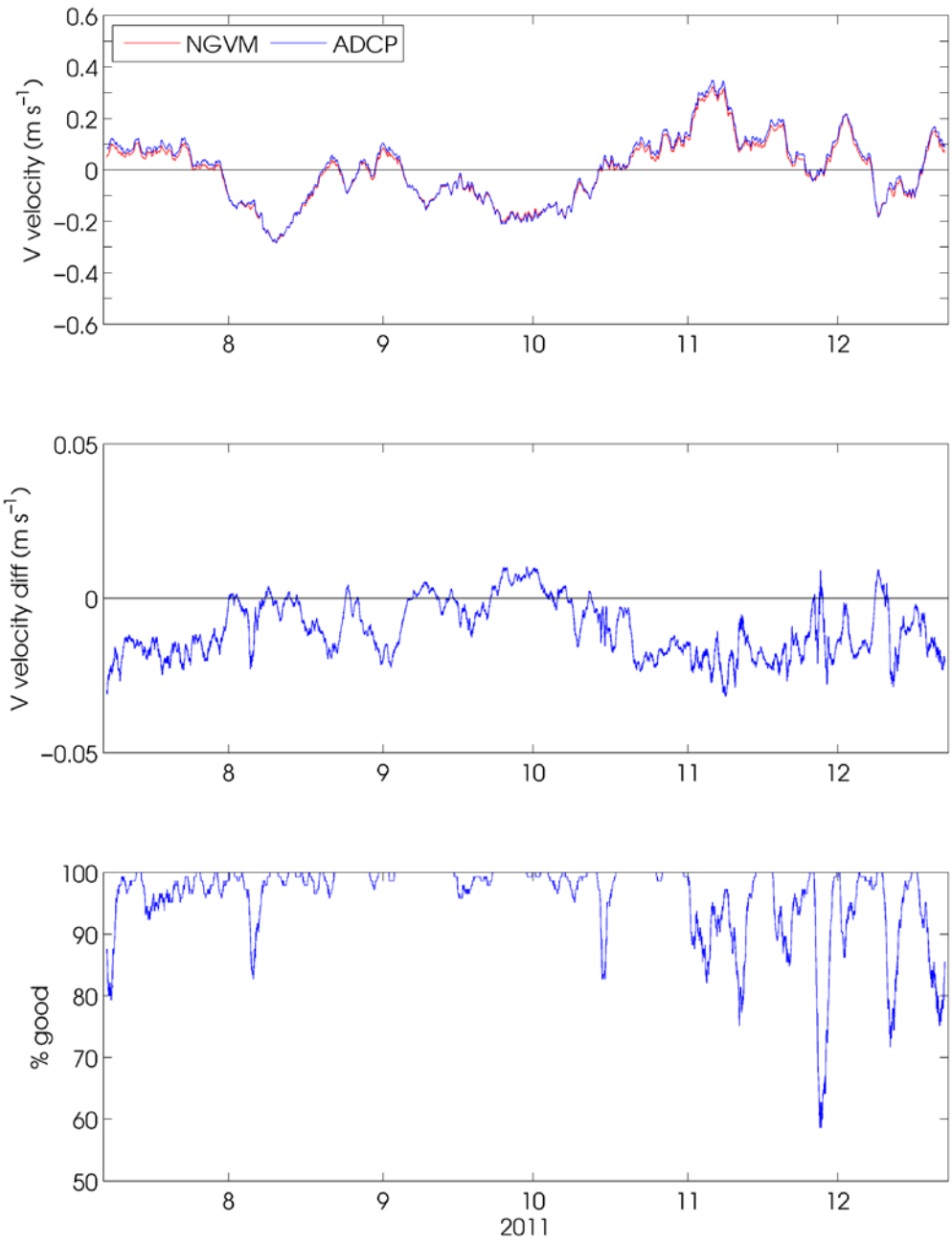

Figure 5-21. Same as in Figure 5-18 but for the V velocity component.

Velocity differences between the 10m VMCM and the 600 kHz ADCP were smaller in comparison to the 30m VMCM. A seasonal pattern in the "percent good" field is observed for both VMCM's. ADCP and VMCM velocities tend to agree most from summer to early winter, and larger differences often occur in late winter and spring.

D. Global Positioning System Receiver and ARGOS Positions

Xeos MELO (IMEI 30003401261150) and Xeos Sable (300034012194230) Global Positioning System receivers were attached to the tower top of the buoy and the bottom of the buoy hull (respectively) during the WHOTS-8 deployment. Additional ARGOS satellite data transmission systems were mounted to the buoy towers (SN# 14637 and SN# 12790). Data returns from the ARGOS receivers were high, but MELO GPS data ended on 21 May 2012 (Table 5-8). The instrument memory wasn't cleared before the cruise, resulting in insufficient memory for a complete deployment.

Table 5-8. GPS and ARGOS record times (UTC) during WHOTS-8

WHOTS-8	Xeos MELO GPS	ARGOS
Raw file beginning and end times	07-Jul-2011 01:20:23 21-May-2012 12:20:11	07-Jul-2011 02:40:00 18-Jun-2012 07:48:00

ARGOS positions were available during the WHOTS-8 deployment and they provided additional information on the buoy's motion. ARGOS data were recorded at 10 minutes intervals, although there are some small gaps at repeated times present in the records. Samples taken before mooring deployment were eliminated. Data were screened for points that were greater than 2.5 nautical miles from the surveyed anchor positions for each deployment which was considered to be the buoy watch circle radius. The velocity magnitude was calculated and positions that resulted in speeds greater than 1 m s^{-1} were removed. Data were interpolated onto a regular time grid in order to compute spectra.

For comparison, Figure 5-22 shows the ARGOS buoy's positions together with the GPS positions during the WHOTS-8 deployment. The standard deviation of the difference between these two records is about 420 m.

The ARGOS positions of the WHOTS-8 buoy for the duration of the deployment are in Figure 5-23, and shows the color-coded positions according to their data quality. The data quality is determined by its distance from the satellite track. Data of a better quality have a higher flag number: 3 is for a distance less than 150 m, 2 is for a distance between 150 and 350 m, and 1 is for a distance between 350 and 1000 m. For the duration of the deployment, the buoy had a mean position of about 3 km from the anchor, with a standard deviation of about 600 m.

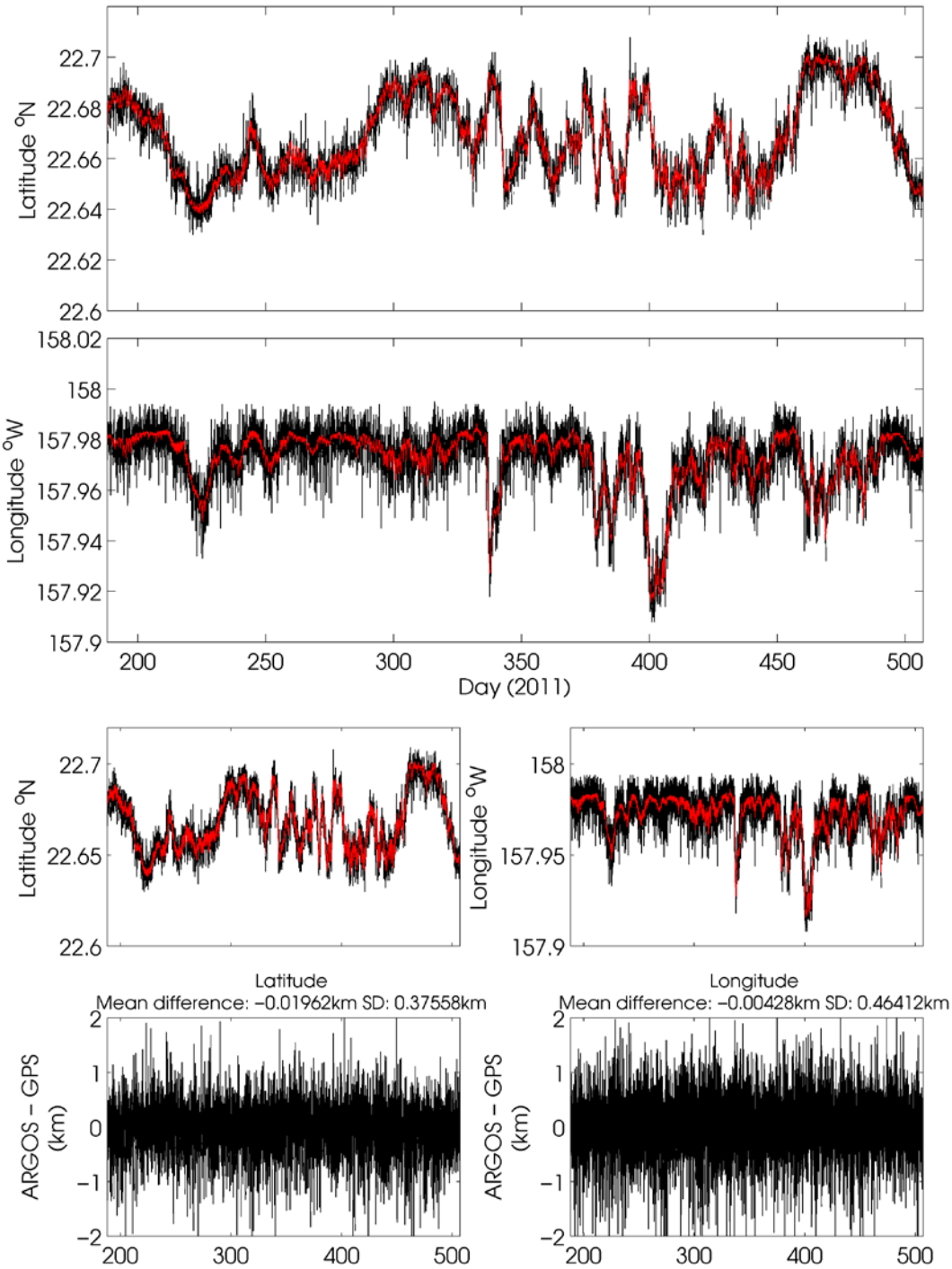

Figure 5-22. WHOTS-8 buoy position from ARGOS data (black line), and from GPS data (red line). The top and two middle panels show the latitude and longitude of the buoy. The bottom panel shows the difference between the GPS positions and the ARGOS positions interpolated to the GPS times.

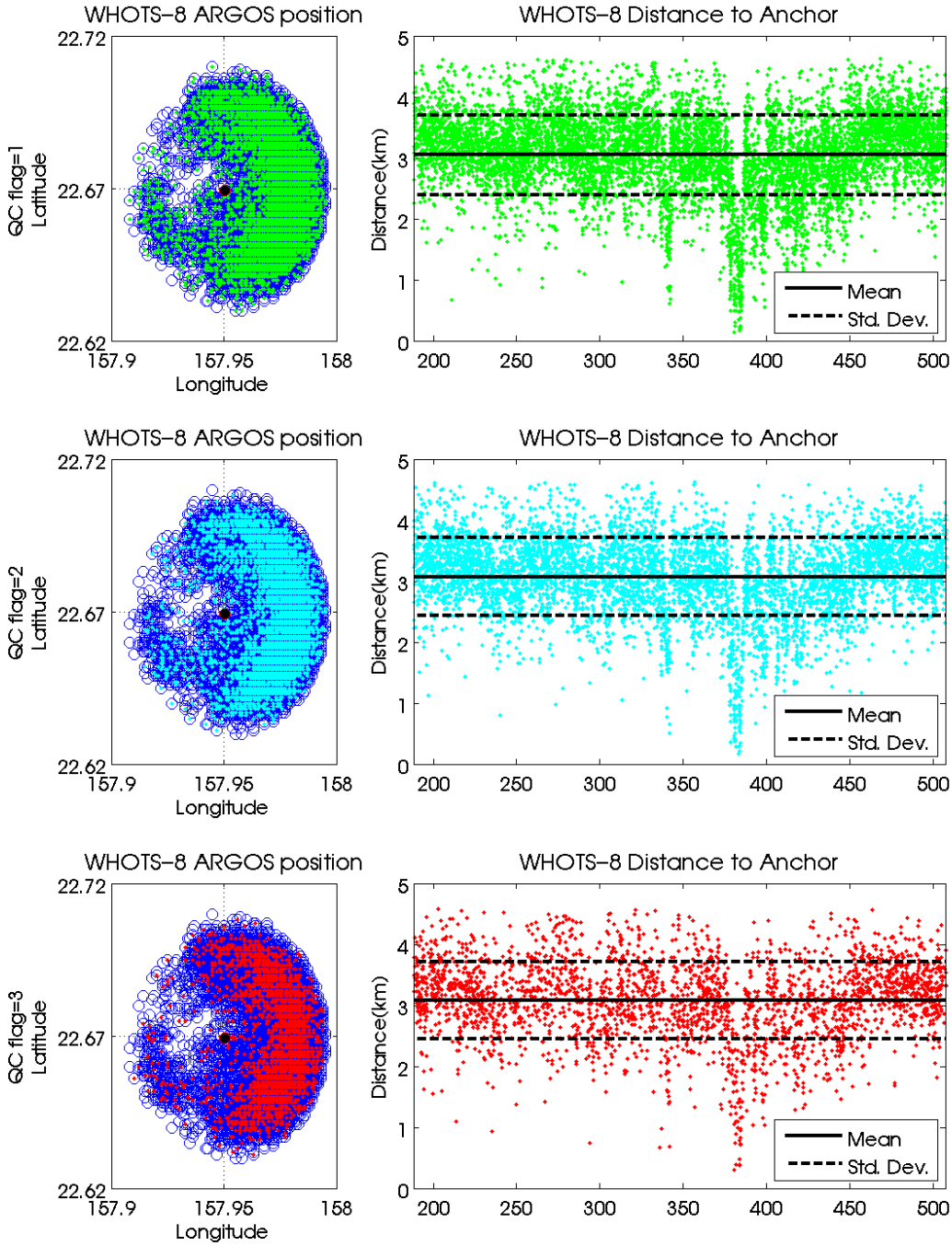

Figure 5-23. WHOTS-8 buoy ARGOS positions (circles, left panels), and distance from its anchor (dots, right panels). The data are colored according to their quality control flag, 1: green, 2: light blue, 3: red. The black circle in the center of the left side panels is the location of the mooring's anchor. The black line in the right panel plots is the mean distance between the buoy and its anchor, and the dashed line is the mean plus minus one standard deviation.

E. MAVS Acoustic Velocity Sensor

A Nobska MAVS acoustic velocity sensor (SN 10260) was deployed at 20 m on the WHOTS-8 mooring. Data return from the sensor was degraded due to failure of transducer ‘C’ soon after deployment, yielding unreasonably high current speeds (Figure 5-24, Figure 5-25).

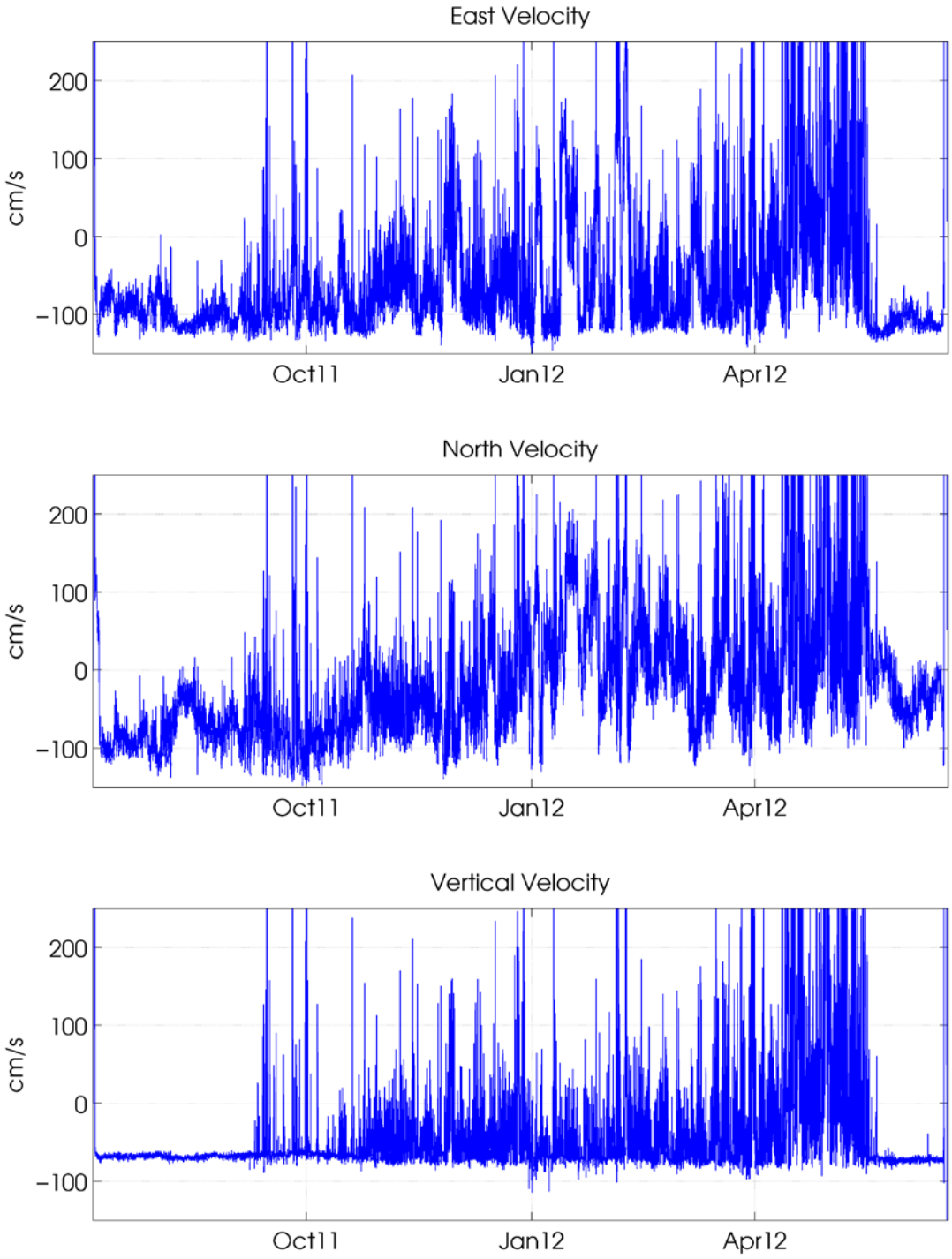

Figure 5-24. Eastward (upper panel), northward (middle panel), and upward velocity data (lower panel) as a function of time from the MAVS acoustic velocity sensor deployed at 20 m. Units are cm s^{-1}

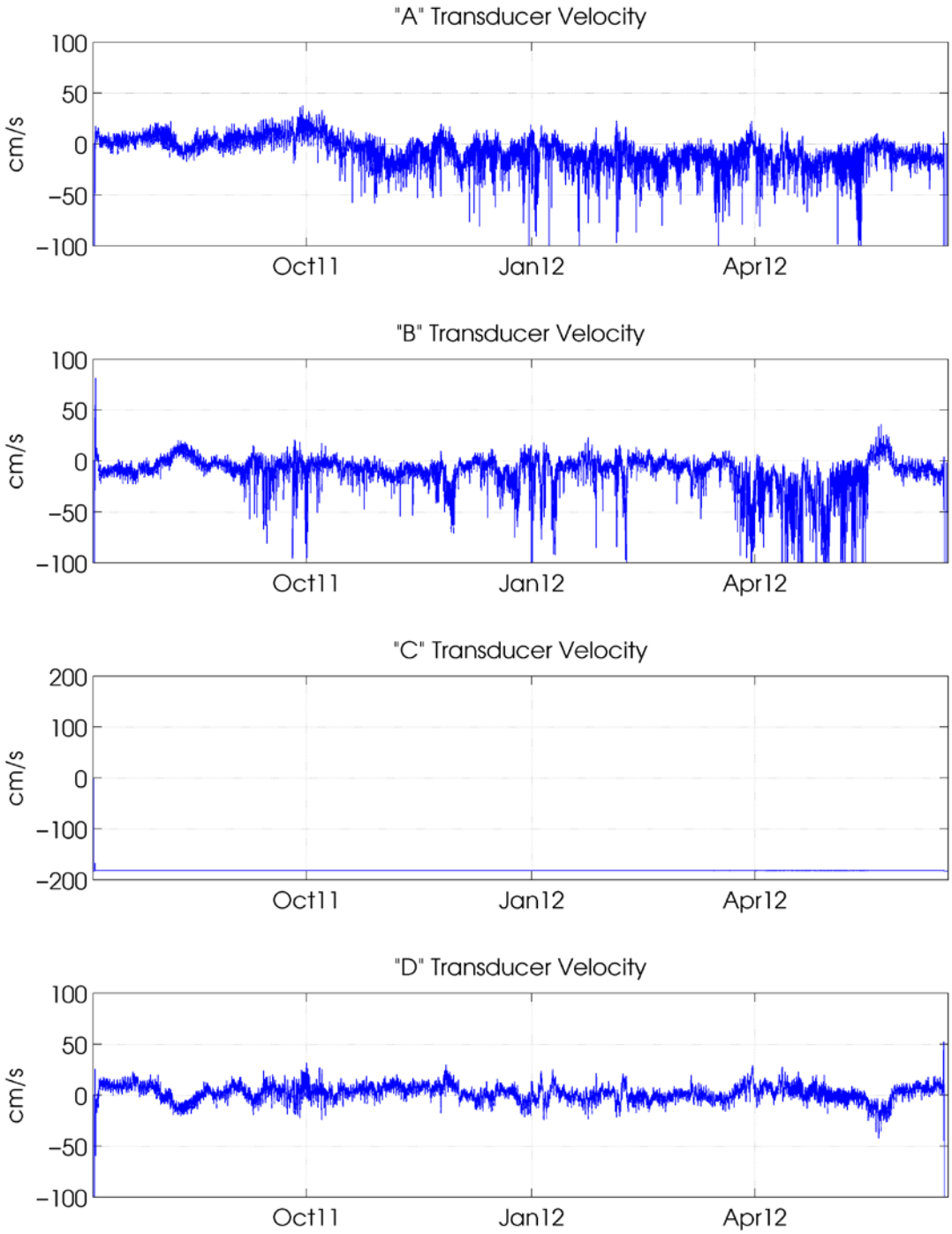

Figure 5-25. Time series of the raw acoustic velocity measured by each of the A, B, C and D transducers in cm s^{-1} from the MAVS deployed at 20 m.

6. Results

During the WHOTS-8 cruise (WHOTS-8 mooring deployment), Station ALOHA was under the influence of the eastern North Pacific high pressure system, and subject to moderate east-northeasterly trade winds. Winds were light (10-15 kts) during July 5-6th, 2011 strengthening July 7th – 9th, with greater vertical development of the boundary layer and shower activity. Winds moderated on the 10th through 11th, picking up again on the 12th. The real-time shipboard ADCP system was not available at the beginning of the cruise, but was online the 2nd day. The 88 m currents at Station ALOHA were mainly northwestward along the southwest flank of a nearly stationary anticyclonic eddy to the east of ALOHA. The currents were also influenced by M2 internal tides (strongest in the upper 100 m) and by inertial waves. Surface currents on the transit back from Station ALOHA to Oahu was marked by modest westward flow.

The upper ocean flow during the majority of the WHOTS-9 cruise (WHOTS-8 mooring recovery, WHOTS-9 mooring deployment) was unusual. An anticyclonic feature developed to the east of ALOHA, and northward currents were seen early in the cruise (June 12th, 2012), with southeasterly light winds (~12 kt) during the deployment of the WHOTS-9 mooring. CTD casts conducted near the mooring site (Station 50) after the deployment (Figure 6-6 through Figure 6-9) displayed a subsurface salinity maximum at 150 dbar, and stratification reaching near the surface, with a shallow mixed layer during June 14-15. The winds turned northeasterly and increased steadily to more than 20 kt starting on June 16th, and the currents turned to northwestward during the recovery of the WHOTS-8 mooring. CTD casts conducted before recovering this mooring (Station 52, Figure 6-1 through Figure 6-5) showed an increasing mixed layer reaching nearly 50 m. The currents in the upper 200 m turned eastward at more than 0.5 m/s by June 18th.

The temperature MicroCAT records during the WHOTS-8 deployment (Figure 6-11 to Figure 6-14) show obvious seasonal variability in the upper 100 m. The salinity records (Figure 6-15 to Figure 6-18) do not show an obvious seasonal cycle.

Figure 6-23 and Figure 6-24 show contours of the WHOTS-8 MicroCAT data in context with data from the previous 7 deployments. The seasonal cycle is obvious in the temperature record, with record temperatures (higher than 26 °C) in the summer of 2004, and to a minor extent in the summer of 2005. Salinities in the subsurface salinity maximum were relatively low during the first 6 years of the record, only to increase drastically after 2008, with some episodes of lower salinity in mid-2011 and early 2012. The salinity maximum extended to near the surface during some instances in early 2010, 2011, and late 2012. When plotted in σ_θ coordinates (Figure 6-24), the salinity maximum seems to be centered roughly between 24 and 24.5 σ_θ.

Figure 6-28 through Figure 6-30 show time series of the zonal, meridional, and vertical currents recorded with the moored ADCPs during the WHOTS-8 deployment, and Figure 6-39 shows the currents at 10 and 30 m collected by the VMCMs. Figure 6-25 through Figure 6-27 show contours of the ADCP current components in context with data from the previous deployments. In spite of the gaps in the data, an obvious variability is seen in the zonal and meridional currents, apparently caused by passing eddies. On top of this variability there have been periods of intermittent positive or negative zonal currents, for instance during 2007-2008.

The contours of vertical current component (Figure 6-27) show a transition in the magnitude of the contours near 47 m, indicating that the 300 kHz ADCP located at 126 m moves more vertically than the 600 kHz ADCP located at 47.5 m.

A comparison between the moored ADCP data and the shipboard ADCP data obtained during the WHOTS-8 cruise is shown in Figure 6-31 and Figure 6-32. Some of the differences seen especially in the zonal component may be due to the mooring motion, which was not removed from the data. Comparisons between the shipboard ADCP from HOT cruises and the mooring data are compiled in Table 6-1, and shown in Figure 6-33 through Figure 6-38. Data existed for HOT-233, HOT-236, and HOT-238 only; both ADCPs failed after HOT-238 and shipboard ADCP profiles near the mooring weren't available for HOT-234, HOT-235, and HOT-237. The correlation coefficients from the remaining comparisons were poor, most likely due to the small amount of recorded ensemble samples from the moored ADCPs during inter-comparison periods.

The motion of the WHOTS-8 buoy was registered by the Xeos-GPS receiver, and its positions are plotted in Figure 6-40. The buoy was located west of the anchor for the majority of the deployment, except during February 2012 when it was east of it. Power spectrum of these data (Figure 6-41) shows extra energy at the inertial period (~31 hr). Combining the buoy motion with the tilt (a combination of pitch and roll) from the ADCP data (Figure 6-42) showed that the tilt increased as the buoy distance from the anchor increased. This was expected since the inclination of the cable increases as the buoy moves away from the anchor.

A. CTD Profiling Data

Profiles of temperature, salinity and potential density (σ_θ) from the casts obtained during the WHOTS-8 deployment cruise are presented in Figure 6-1 through Figure 6-5, together with the results of bottle determination of salinity. Figure 6-6 through Figure 6-10 are the results of the CTD profiles during the WHOTS-9 cruise.

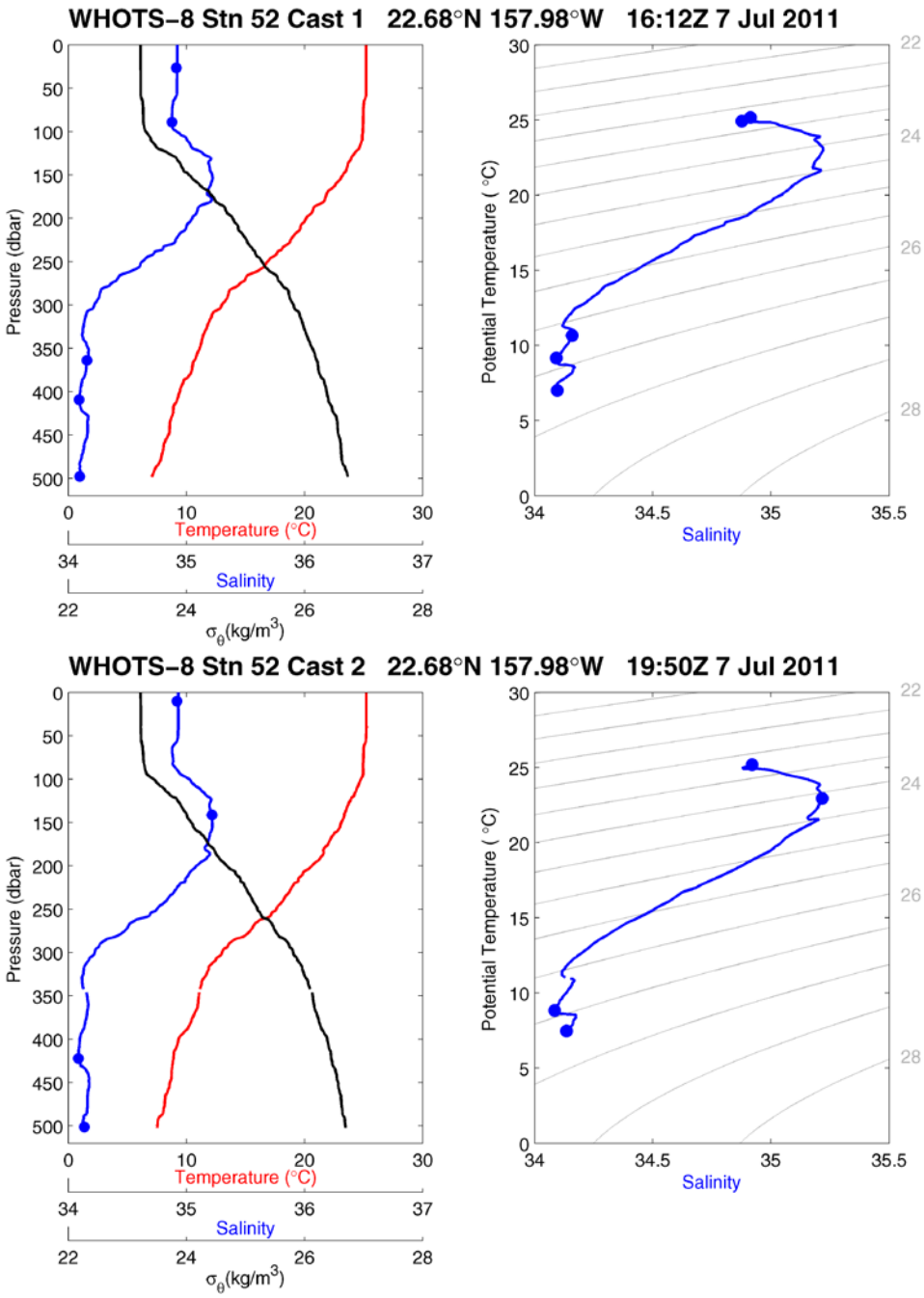

Figure 6-1. [Upper left panel] Profiles of CTD temperature, salinity, and potential density (σ_θ) as a function of pressure, including discrete bottle salinity samples (when available) for station 52 cast 1 during the WHOTS-8 cruise. [Upper right panel] Profiles of CTD salinity as a function of potential temperature, including discrete bottle salinity samples (when available) for station 52 cast 1 during the WHOTS-8 cruise. [Lower left panel] Same as in the upper left panel, but for station 52 cast 2. [Lower right panel] Same as in the upper right panel, but for station 52 cast 2.

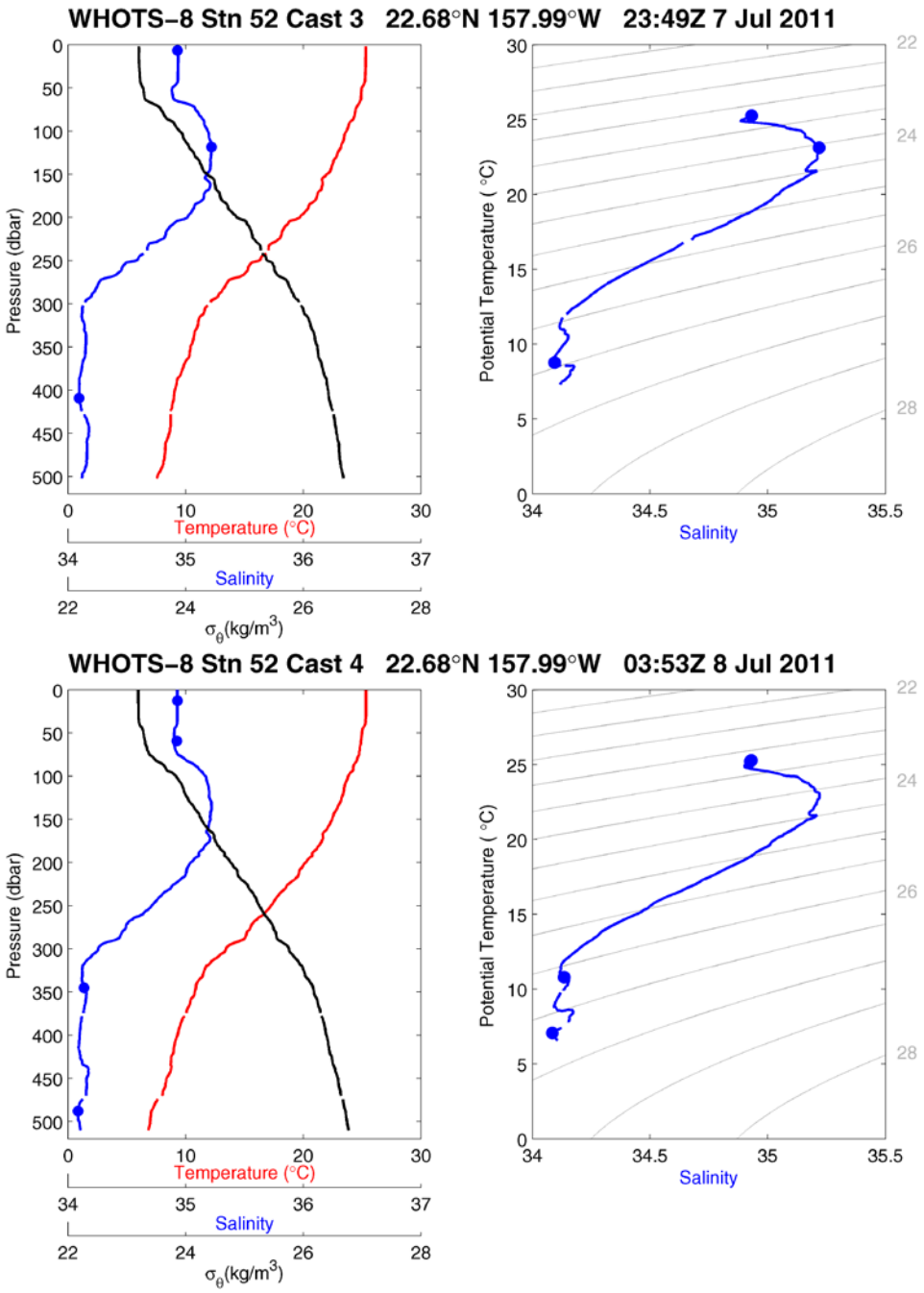

Figure 6-2. [Upper panels] Same as in Figure 6-1, but for station 52, cast 3. [Lower panels] Same as in Figure 6-1, but for station 52, cast 4.

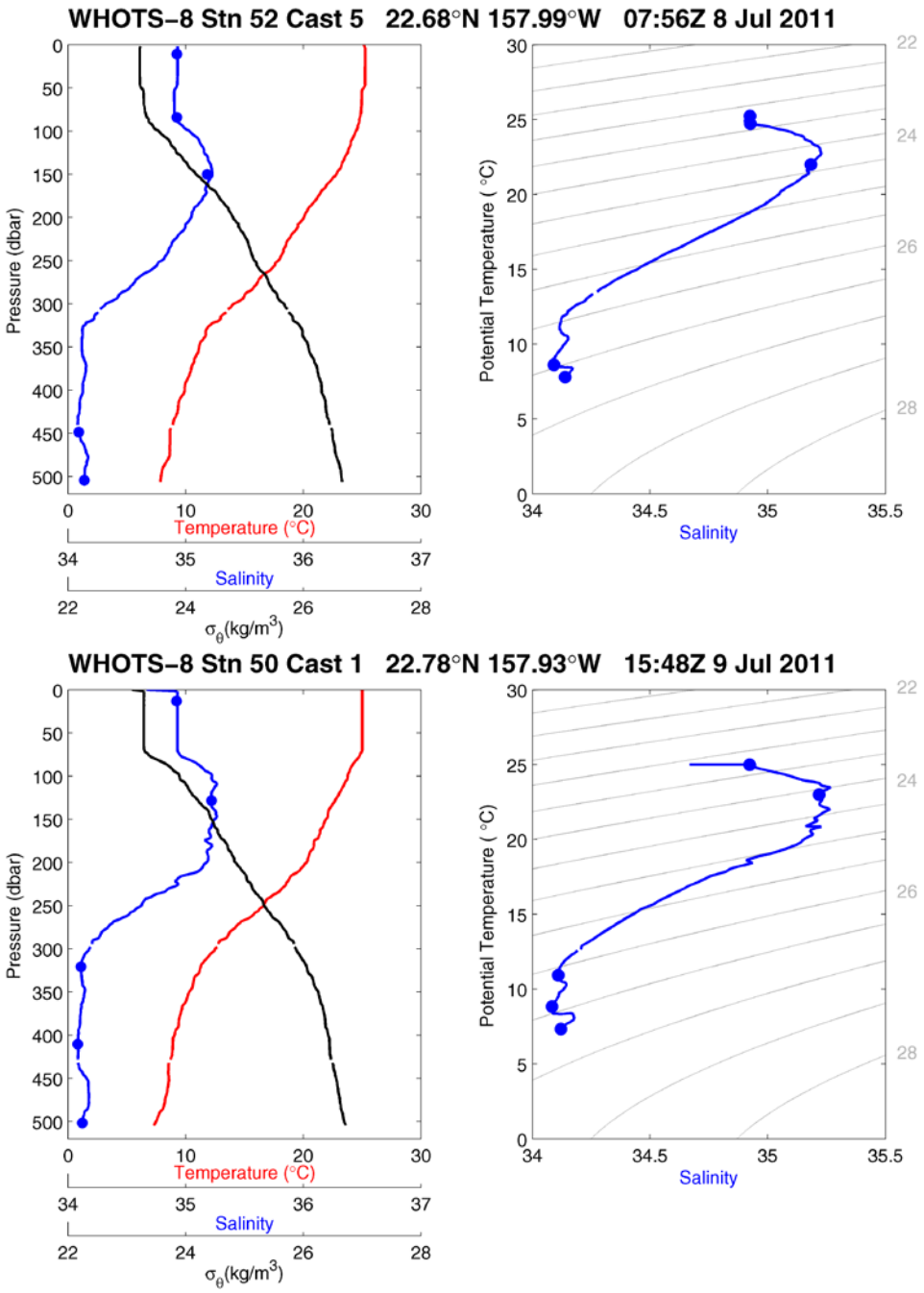

Figure 6-3. [Upper panels] Same as in Figure 6-1, but for station 52, cast 5. [Lower panels] Same as in Figure 6-1, but for station 50, cast 1.

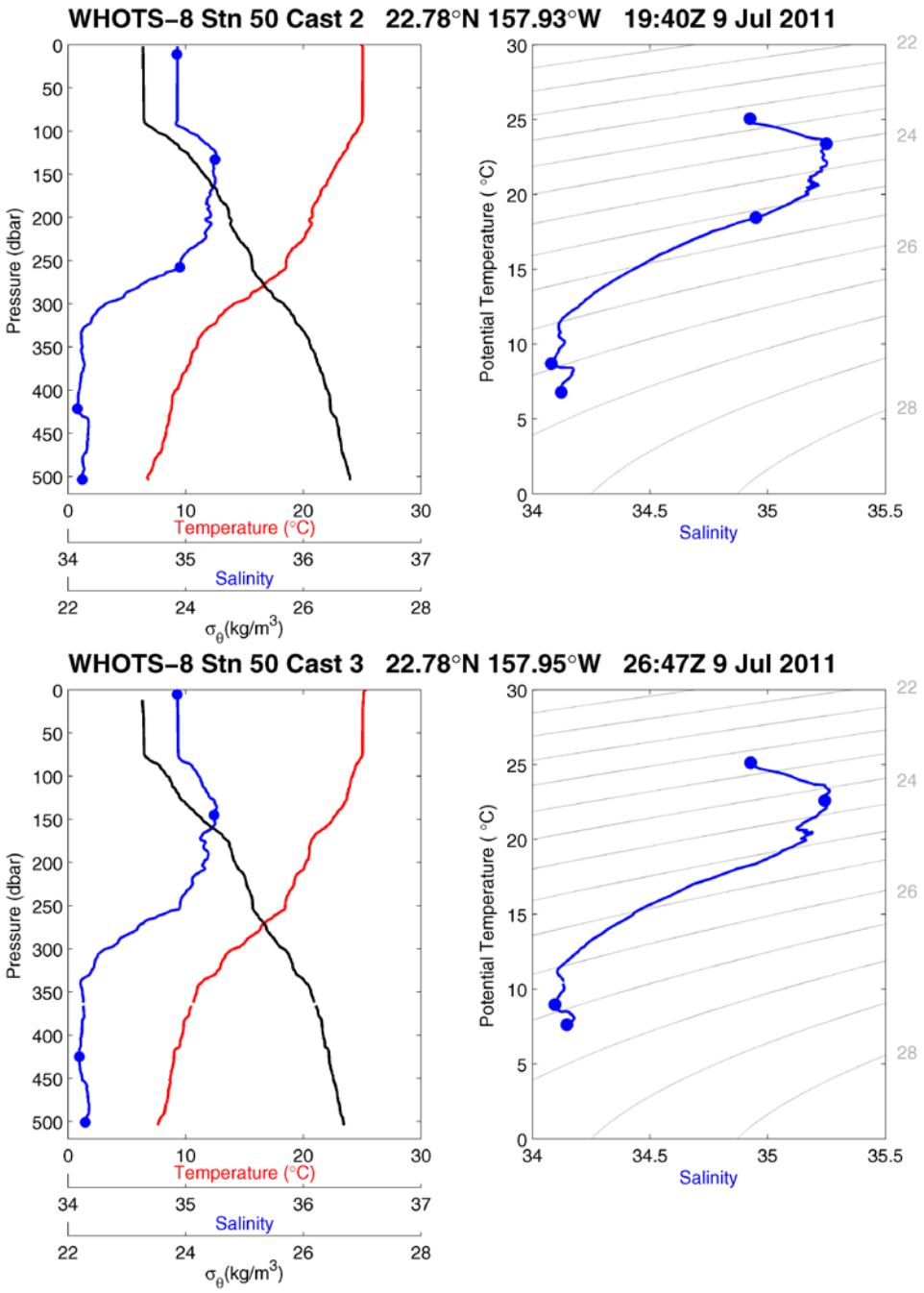

Figure 6-4. [Upper panels] Same as in Figure 6-1, but for station 50, cast 2. [Lower panels] Same as in Figure 6-1, but for station 50, cast 3.

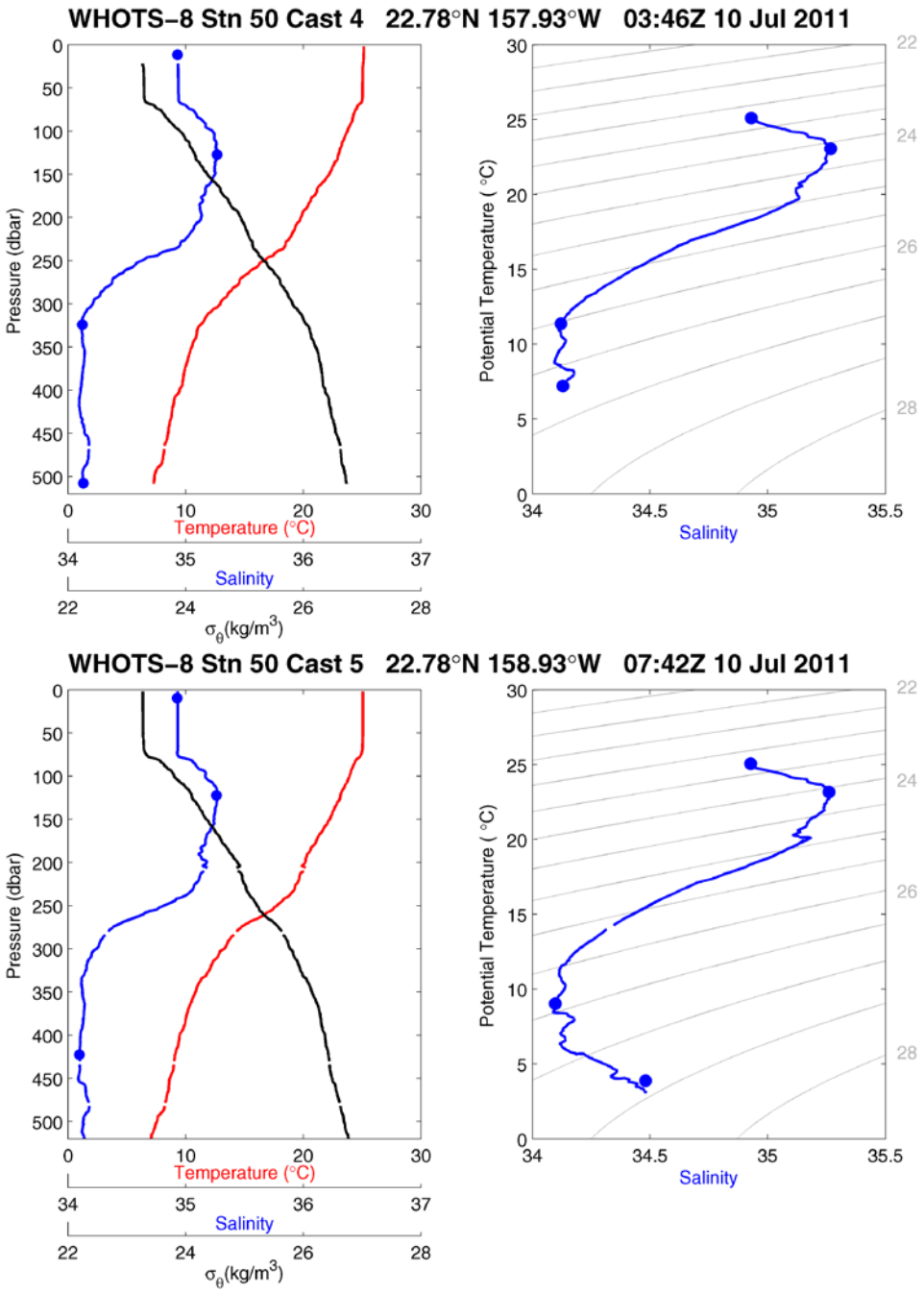

Figure 6-5. [Upper panels] Same as in Figure 6-1, but for station 50, cast 4. [Lower panels] Same as in Figure 6-1, but for station 50, cast 5.

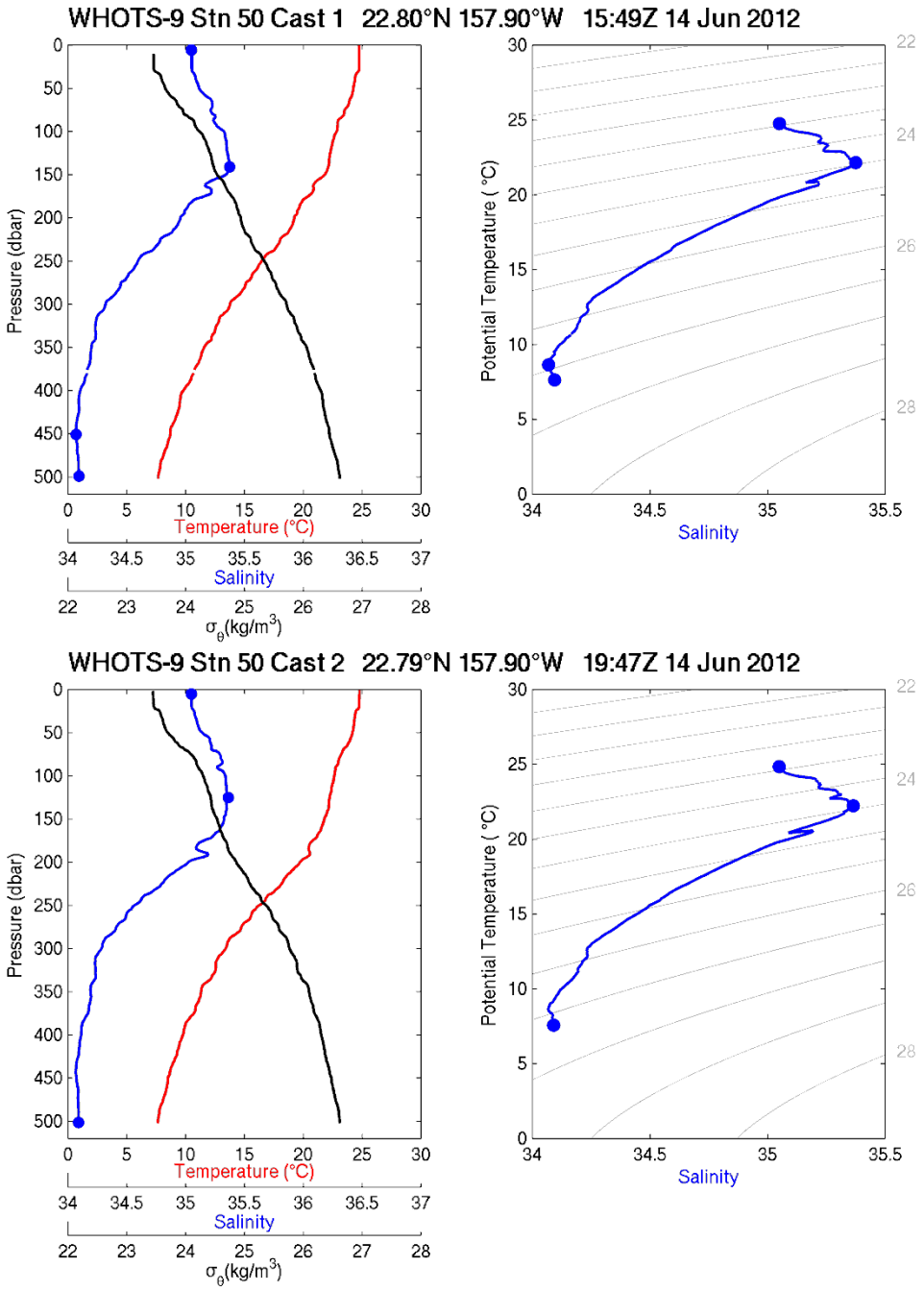

Figure 6-6. [Upper left panel] Profiles of CTD temperature, salinity, and potential density (σθ) as a function of pressure, including discrete bottle salinity samples (when available) for station 50 cast 1 during the WHOTS-9 cruise. [Upper right panel] Profiles of CTD salinity as a function of potential temperature, including discrete bottle salinity samples (when available) for station 50 cast 1 during the WHOTS-9 cruise. [Lower left panel] Same as in the upper left panel, but for station 50 cast 2. [Lower right panel] Same as in the upper right panel, but for station 50 cast 2.

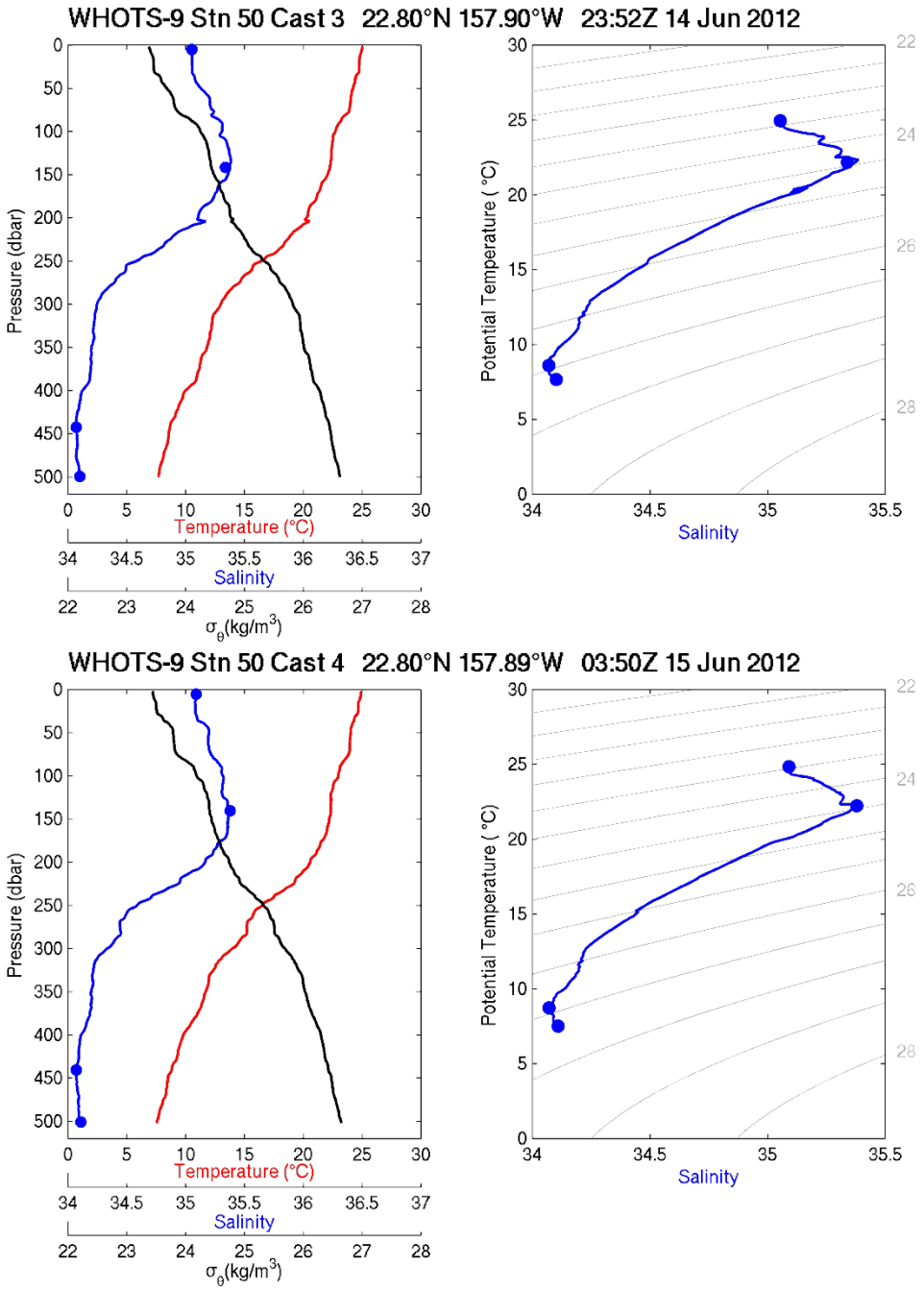

Figure 6-7. [Upper panels] Same as in Figure 6-6, but for station 50, cast 3. [Lower panels] Same as in Figure 6-6, but for station 50, cast 4.

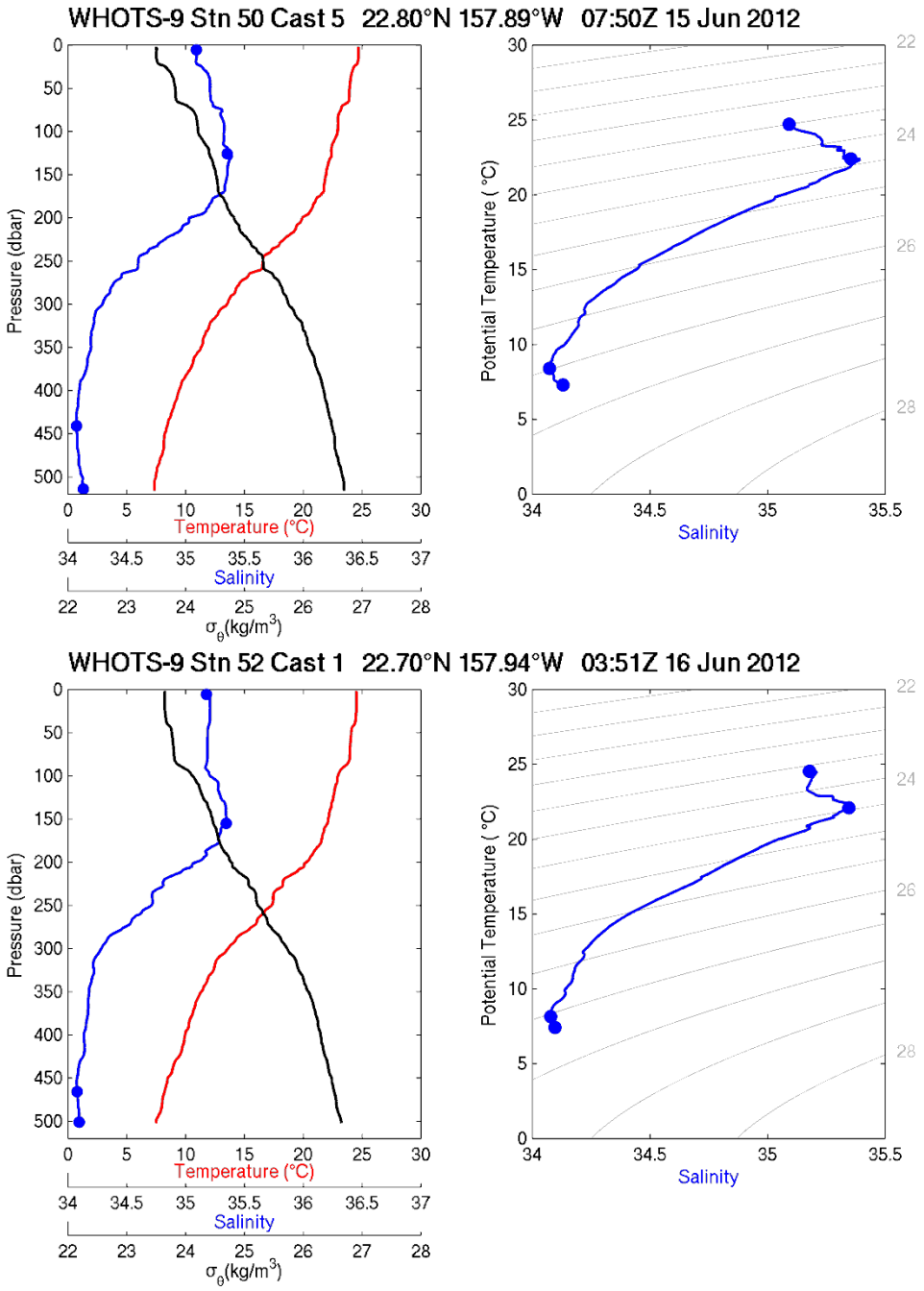

Figure 6-8. [Upper panels] Same as in Figure 6-6 but for station 50, cast 5. [Lower panels] Same as in Figure 6-6, but for station 52, cast 1.

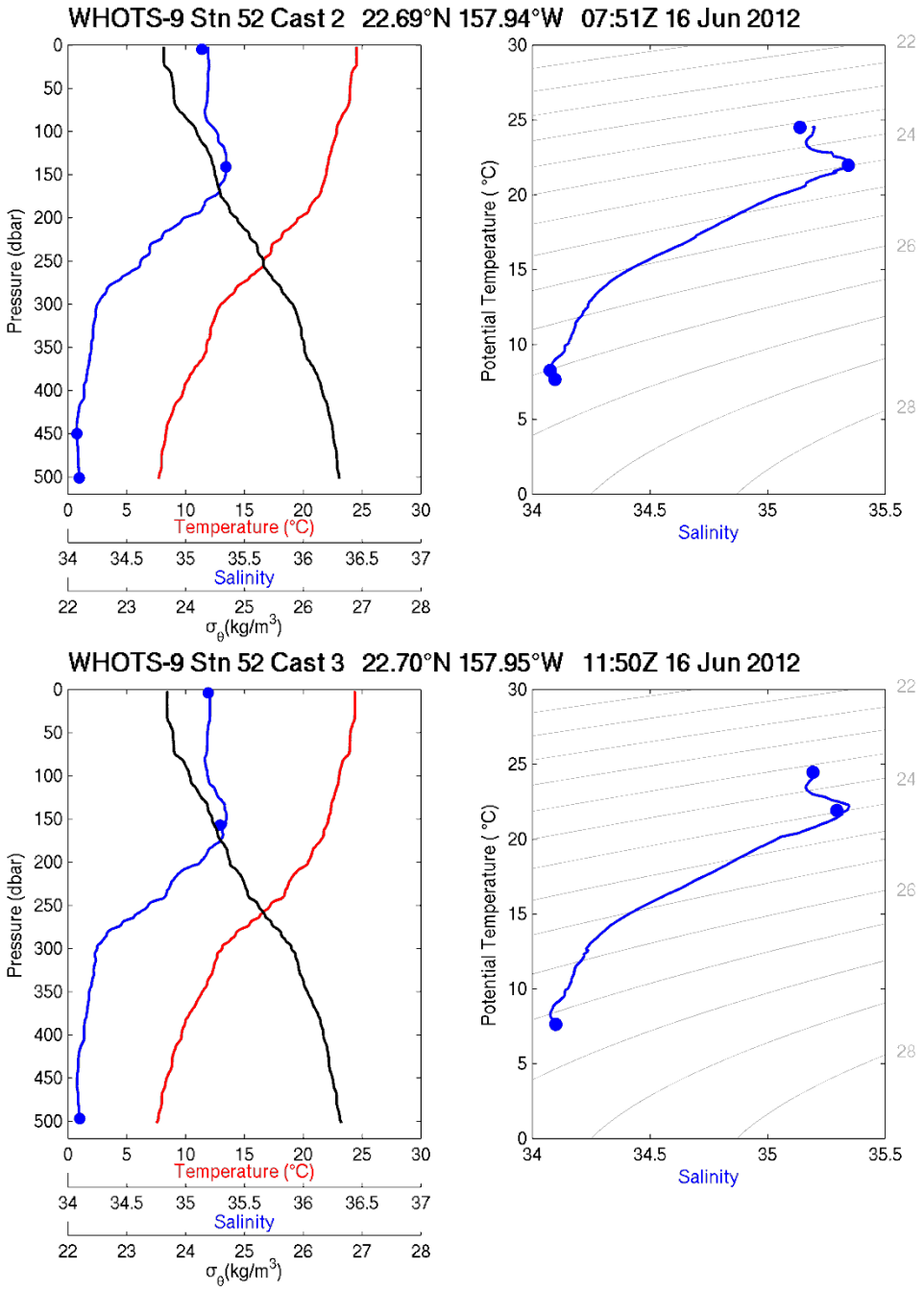

Figure 6-9. [Upper panels] Same as in Figure 6-6, but for station 52, cast 2. [Lower panels] Same as in Figure 6-6, but for station 52, cast 3.

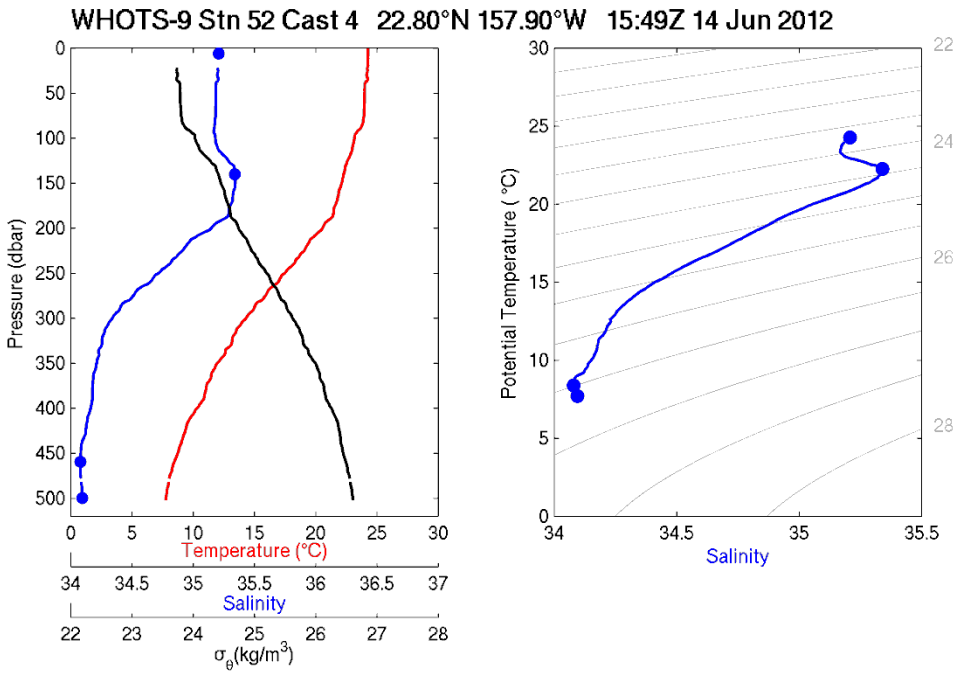

Figure 6-10. [Upper panels] Same as in Figure 6-6, but for station 52, cast 4.

B. Thermosalinograph data

Due to a lack of external temperature data and poor resolution in the record of internal conductivity sensor, underway measurements of near surface temperature and near surface salinity from thermosalinograph for the WHOTS-8 and WHOTS-9 cruises weren't evaluated. There were no plots generated.

C. MicroCAT data

The temperature and salinity measured by MicroCATs during the mooring deployment are presented in Figure 6-11 to Figure 6-18 for each of the depths where the instruments were located. The potential density (σ_θ) is also plotted in Figure 6-19 to Figure 6-22.

Contoured plots of temperature and salinity as a function of depth are presented in Figure 6-23 and contoured plots of potential density (σ_θ) as a function of depth, and of salinity as a function of σ_θ are in Figure 6-24.

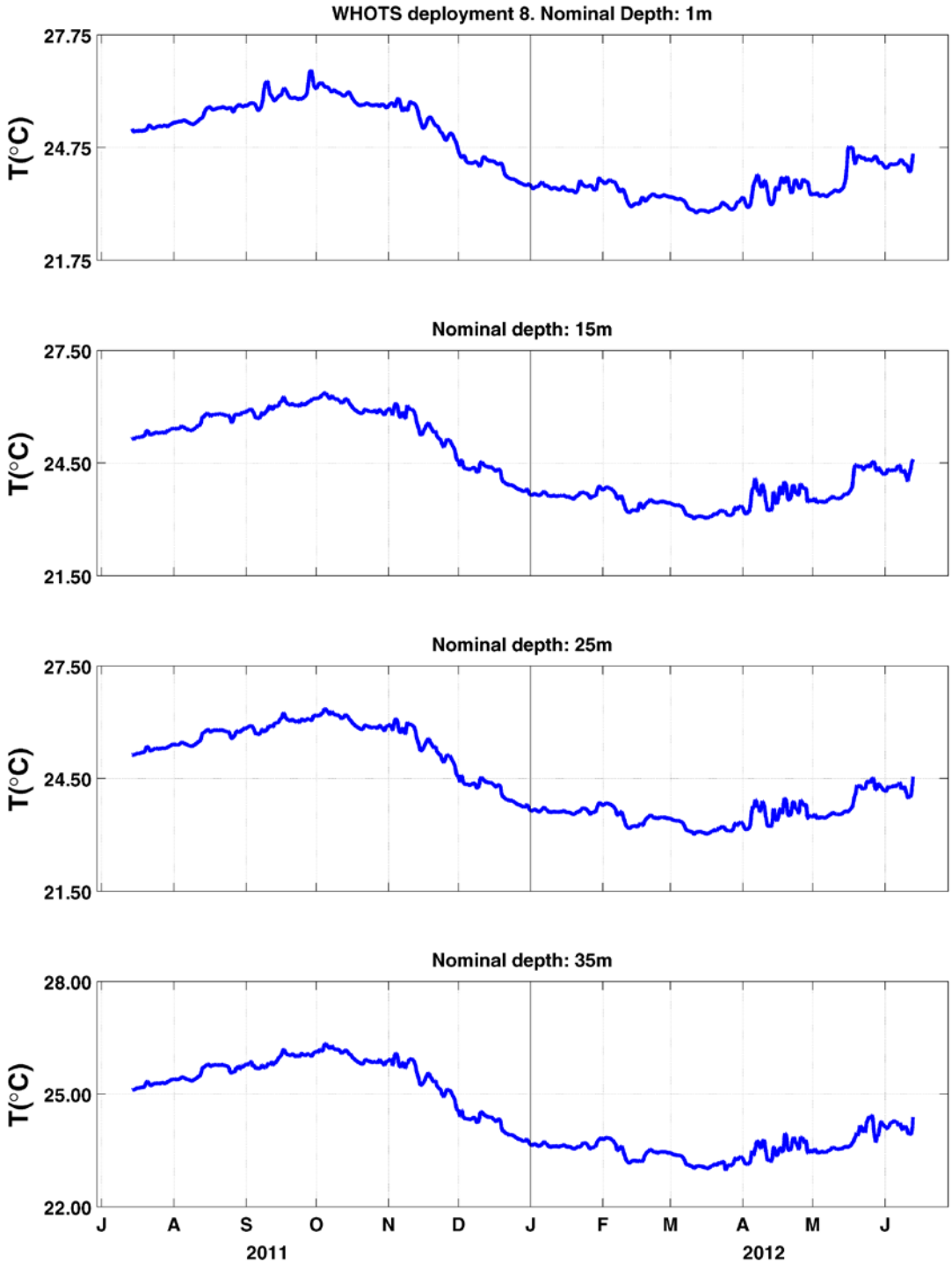

Figure 6-11. Temperatures from MicroCATs during WHOTS-8 deployment at 1, 15, 25, and 35 m.

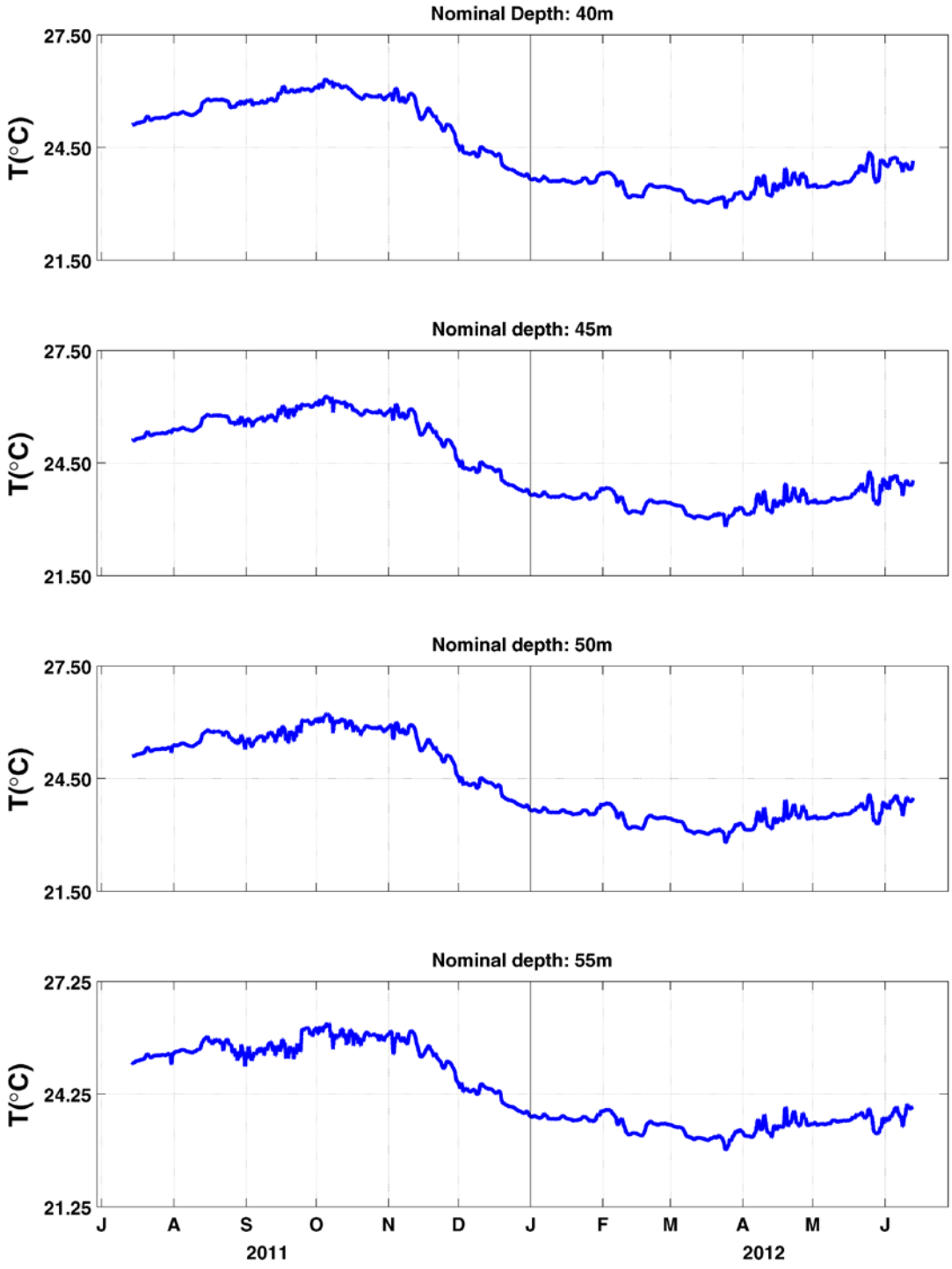

Figure 6-12. Same as in Figure 6-11, but at 40, 45, 50, and 55 m.

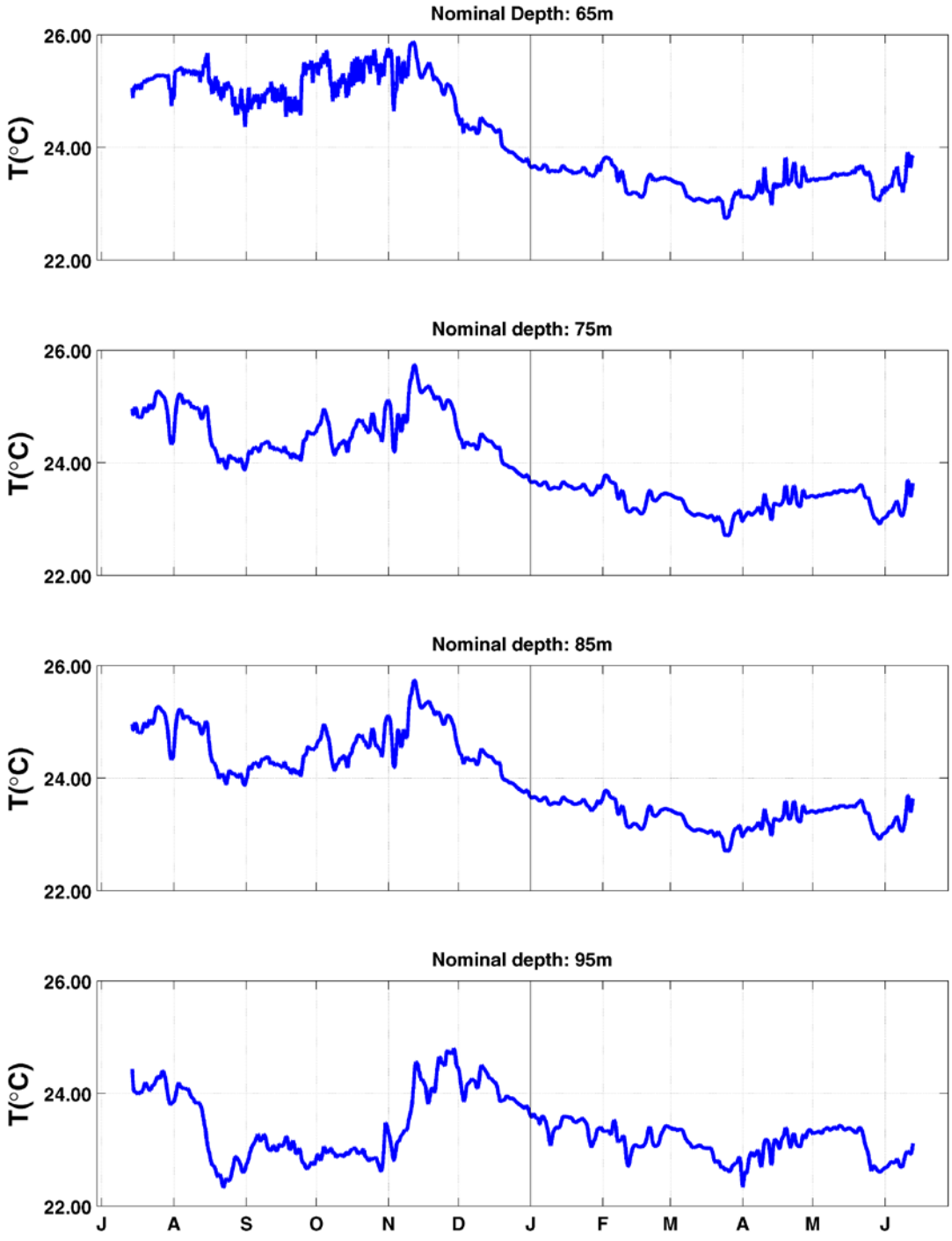

Figure 6-13. Same as in Figure 6-11, but at 65, 75, 85, and 95 m.

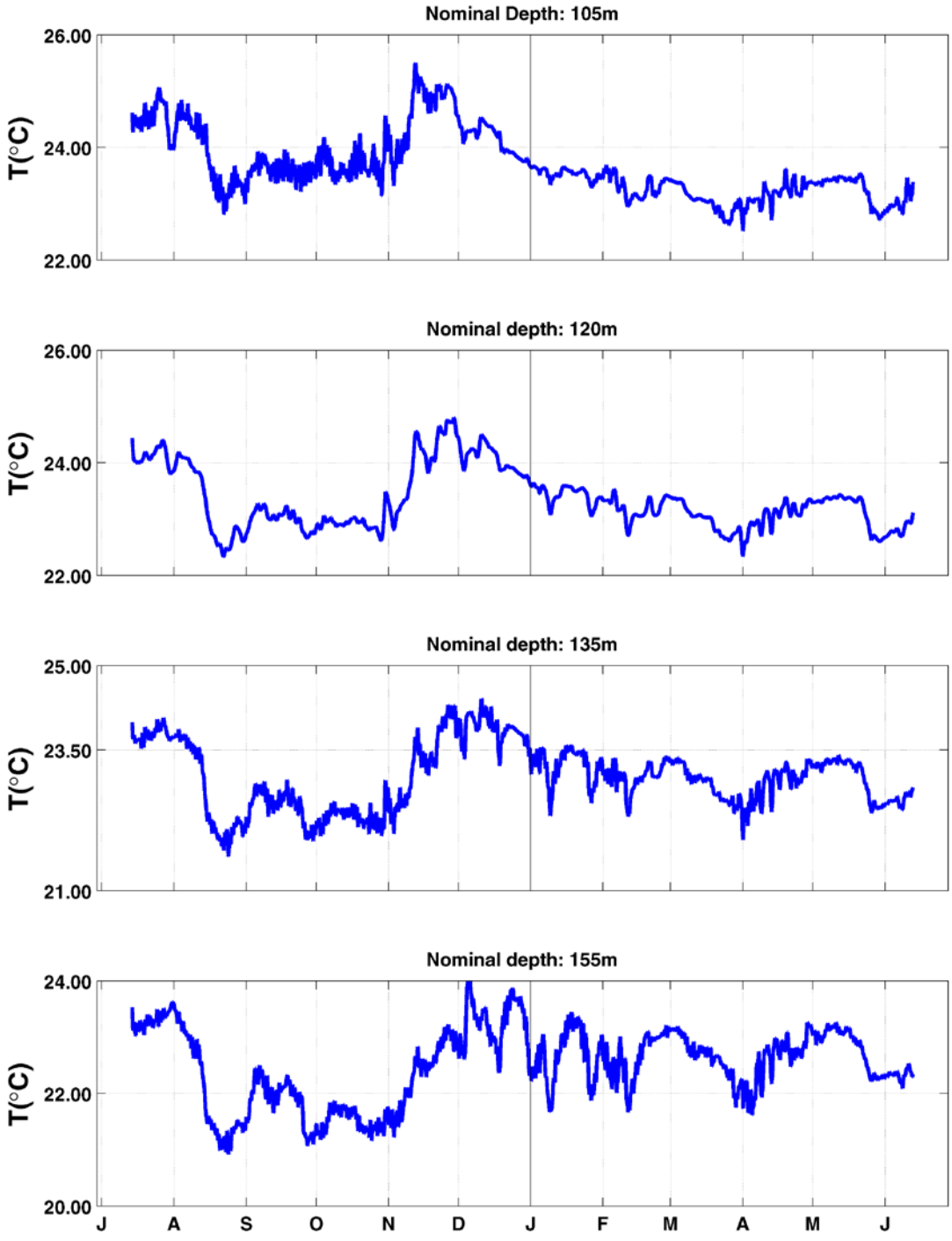

Figure 6-14. Same as in Figure 6-11, but at 105, 120, 135, and 155 m.

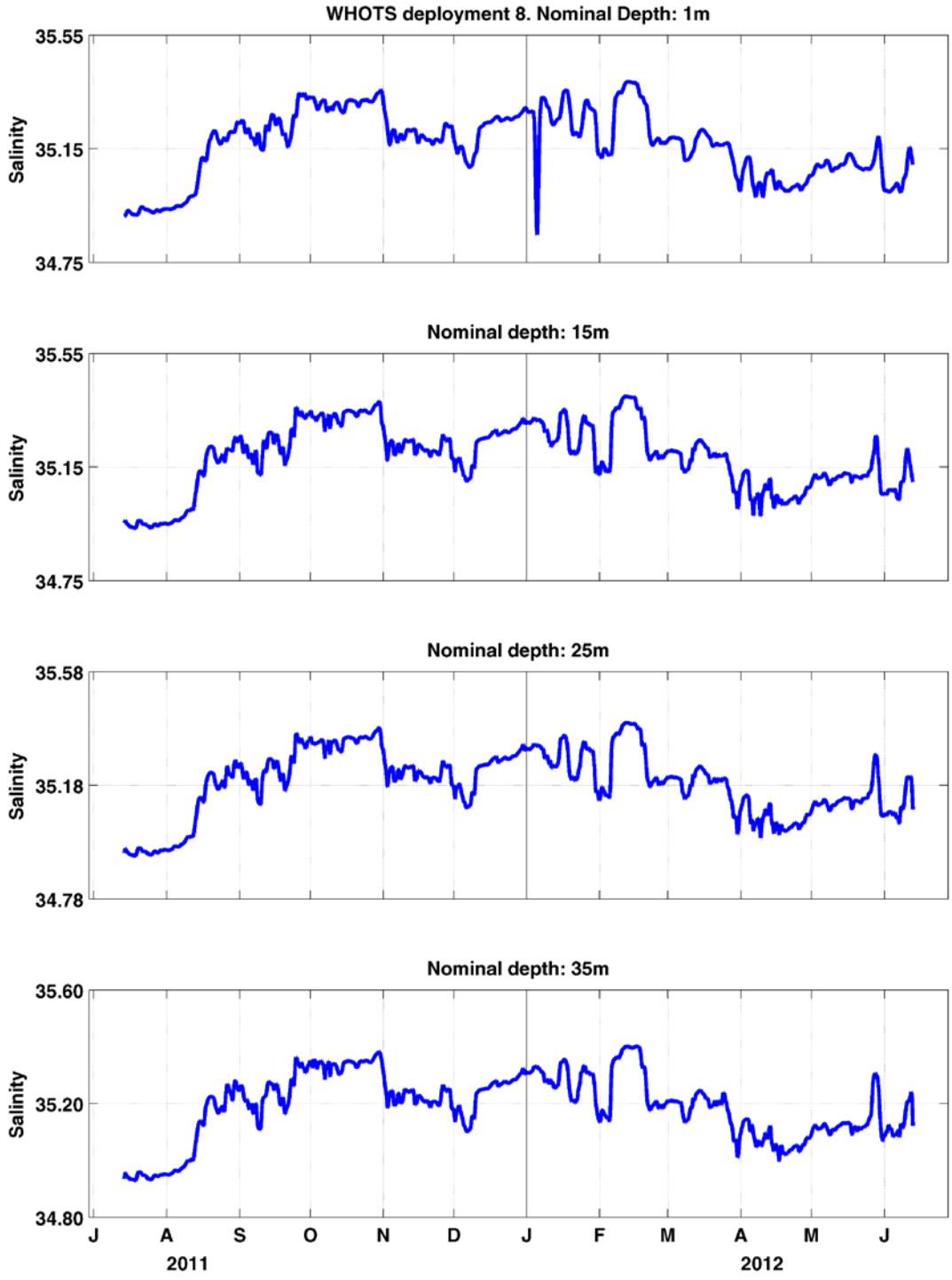

Figure 6-15. Salinities from MicroCATs during WHOTS-8 deployment at 1, 15, 25, and 35 m.

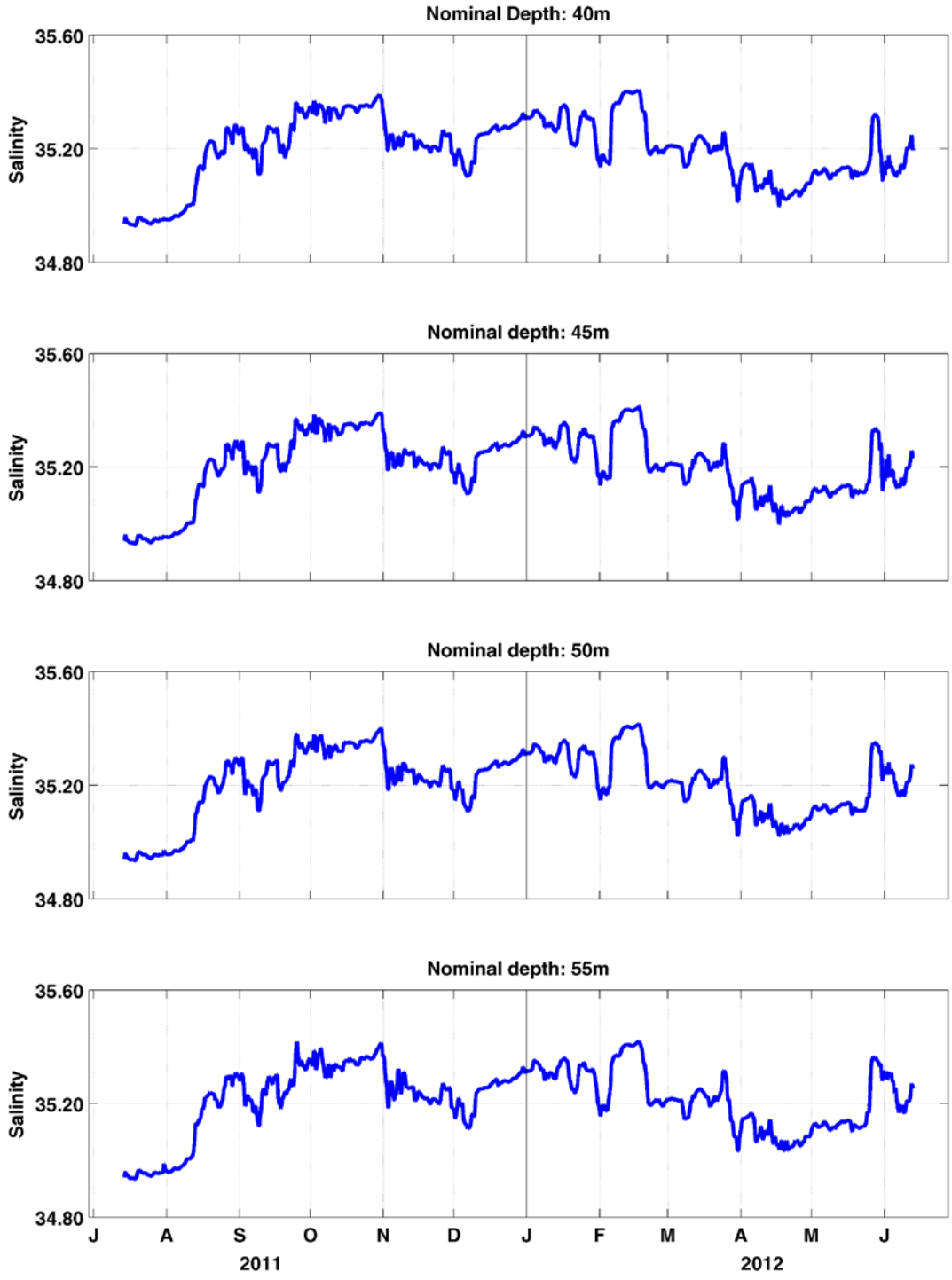

Figure 6-16. Same as in Figure 6-15, but at 40, 45, 50, and 55m.

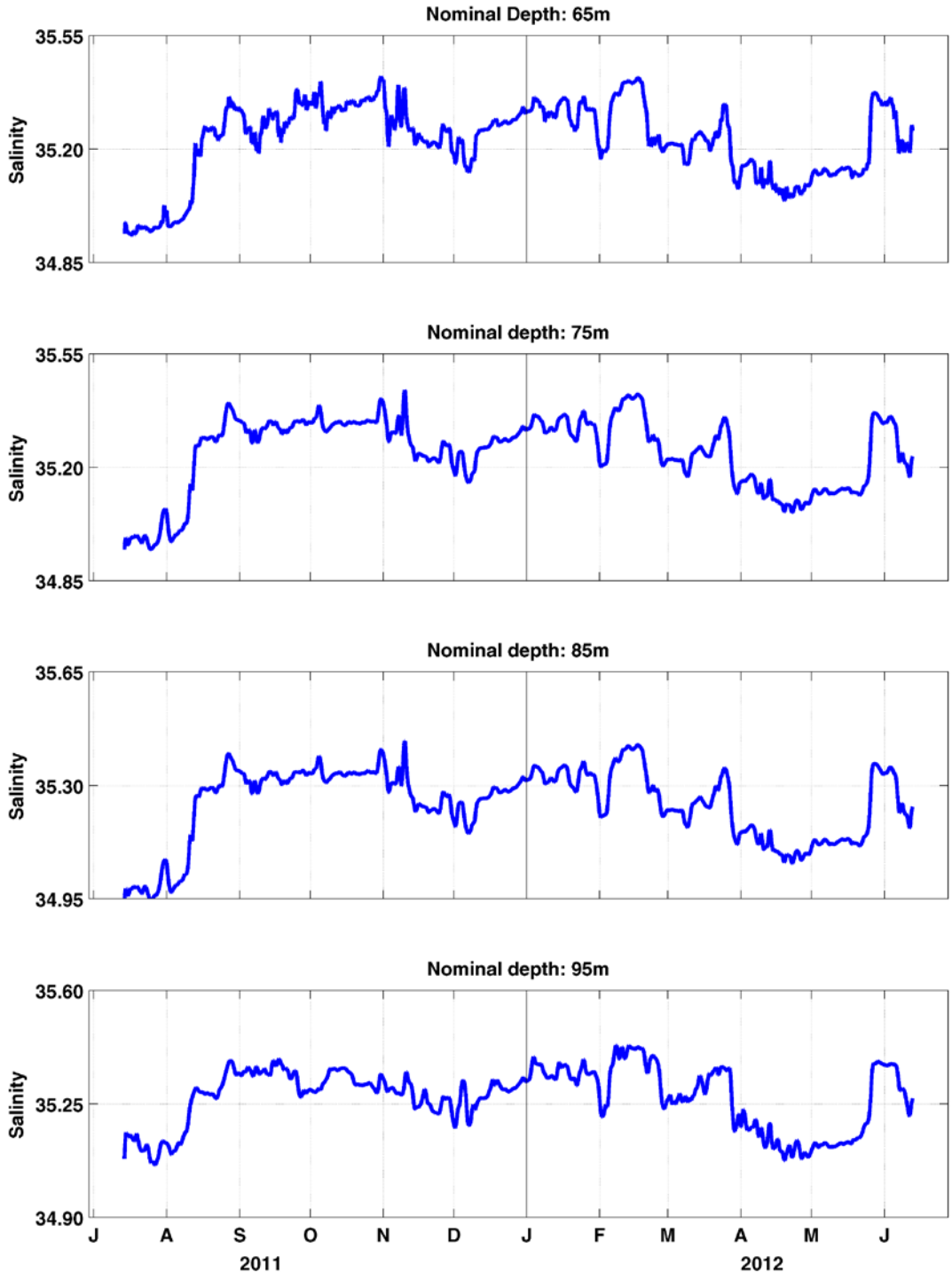

Figure 6-17. Same as in Figure 6-15, but at 65, 75, 85, and 95m.

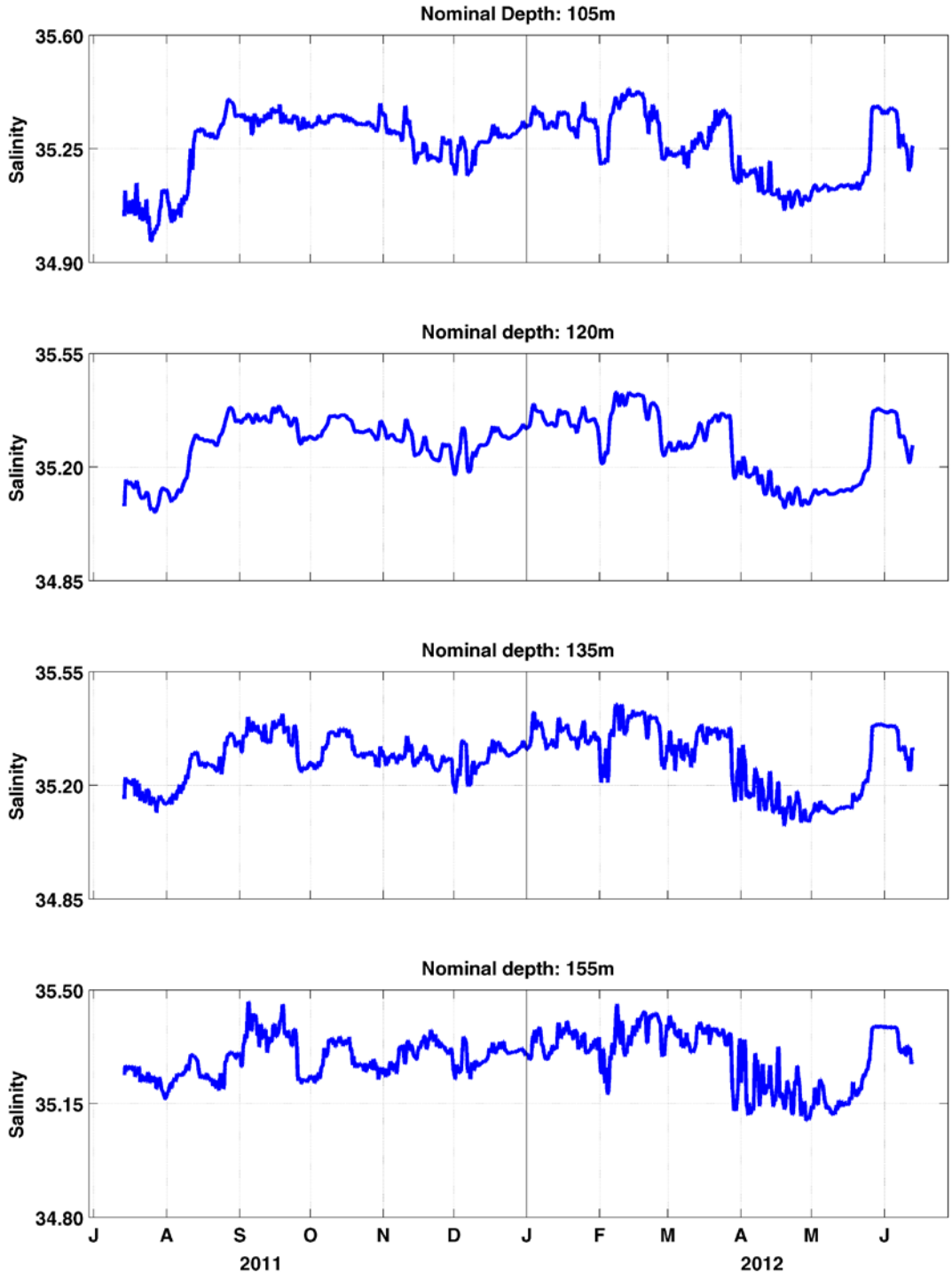

Figure 6-18. Same as in Figure 6-15, but at 105, 120, 135, and 155 m.

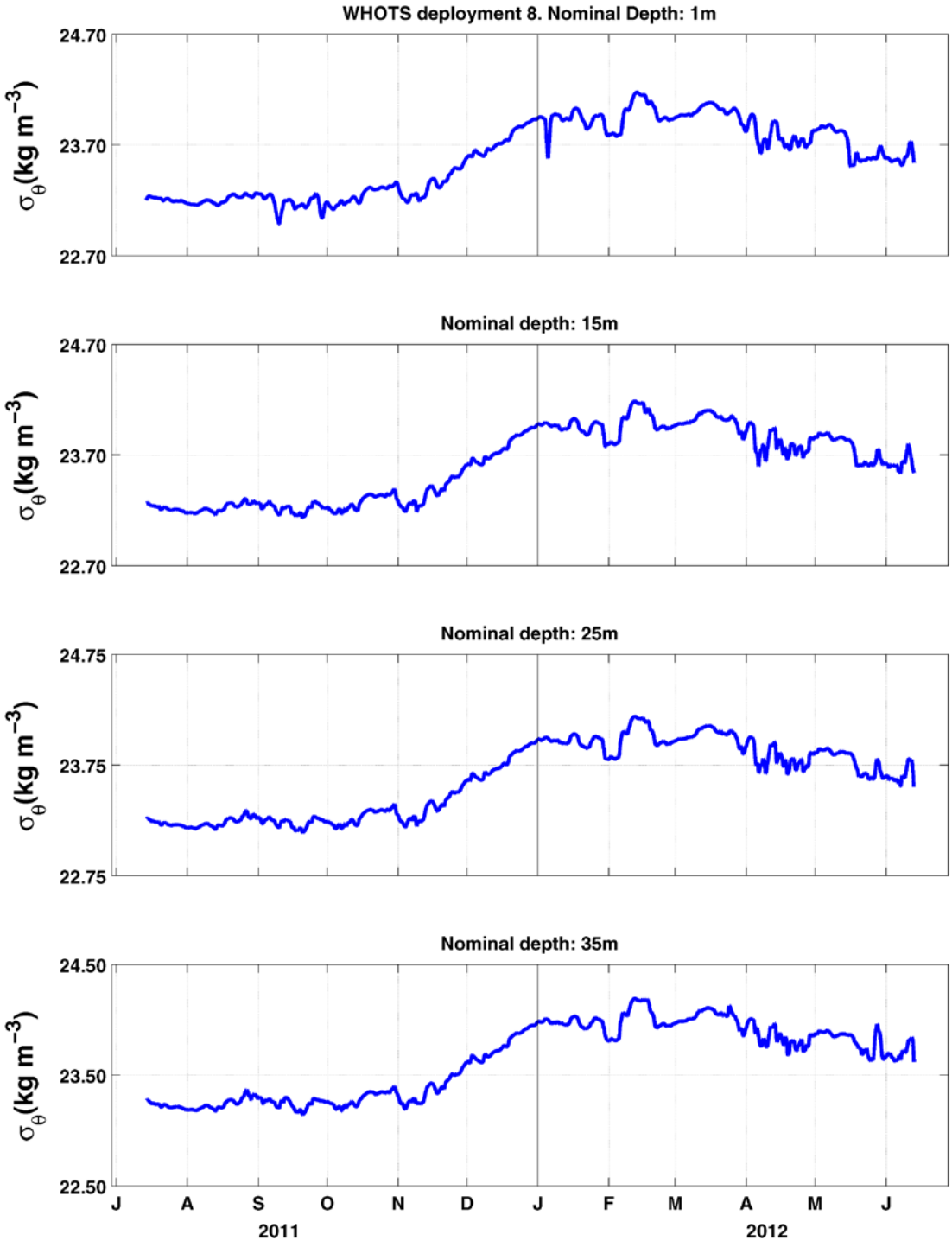

Figure 6-19. Potential density (σ_θ) from MicroCATs during WHOTS-8 deployment at 1, 15, 25, and 35 m.

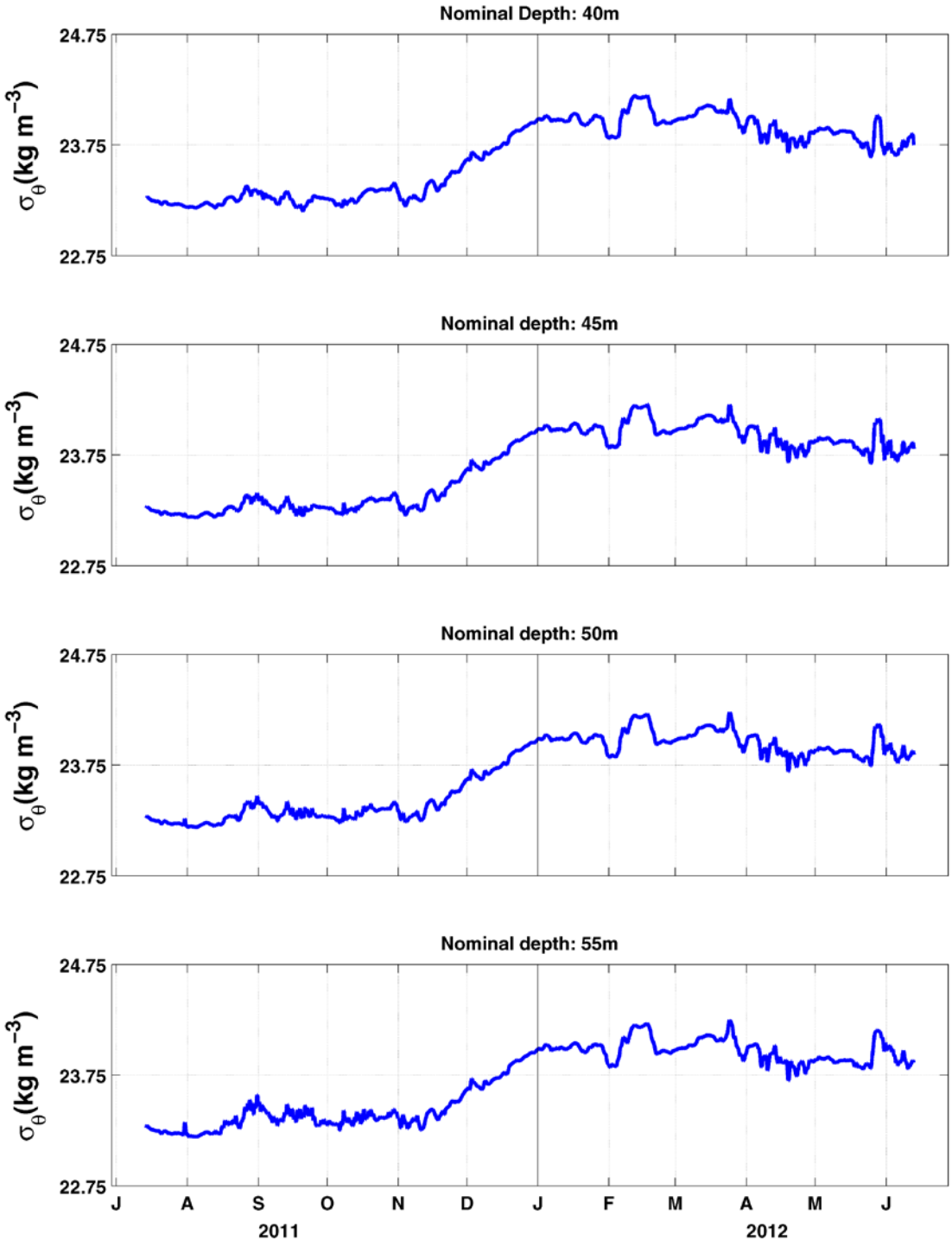

Figure 6-20. Same as in Figure 6-19, but at 40, 45, 50, and 55 m.

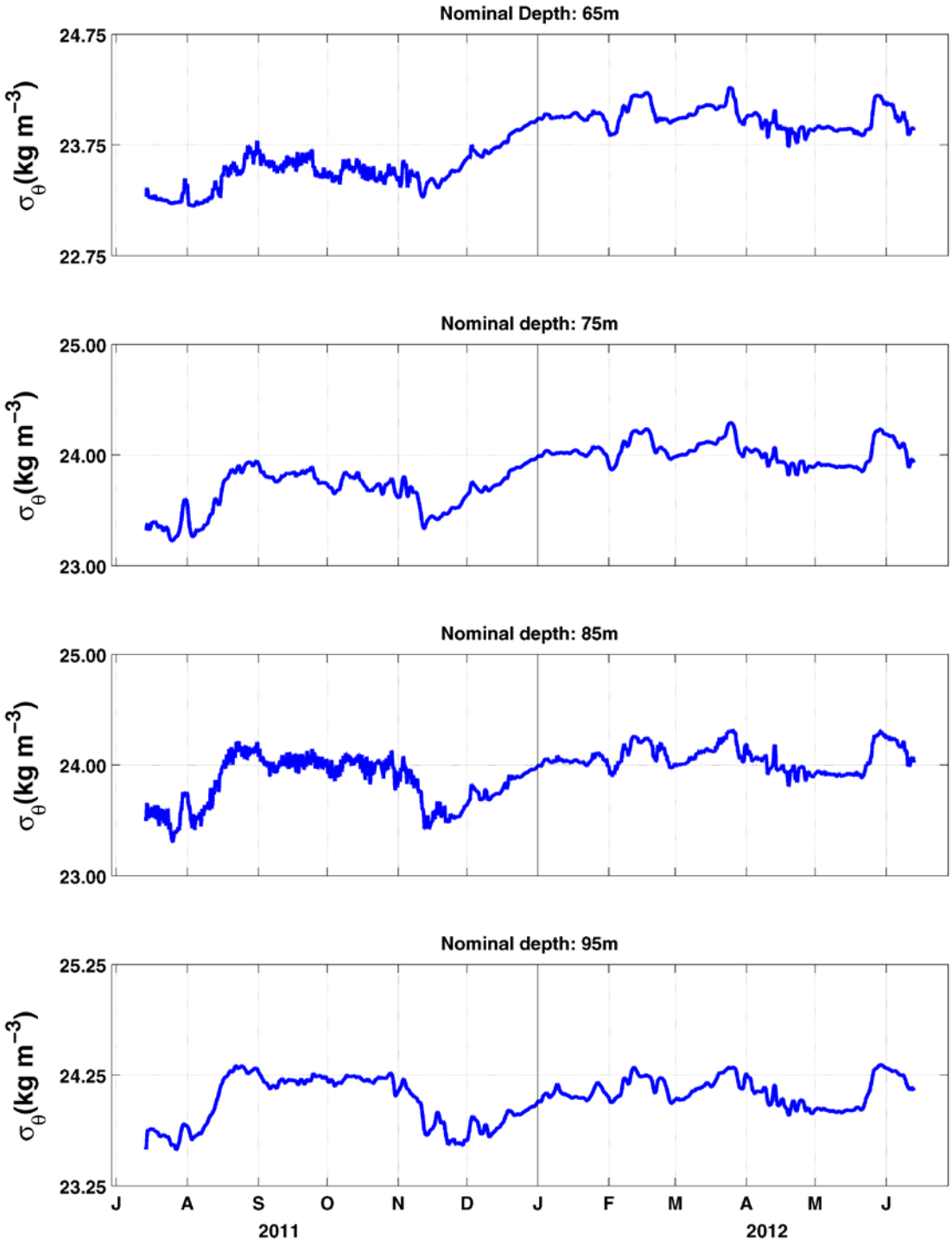

Figure 6-21. Same as in Figure 6-19 but at 65, 75, 85, and 95 m.

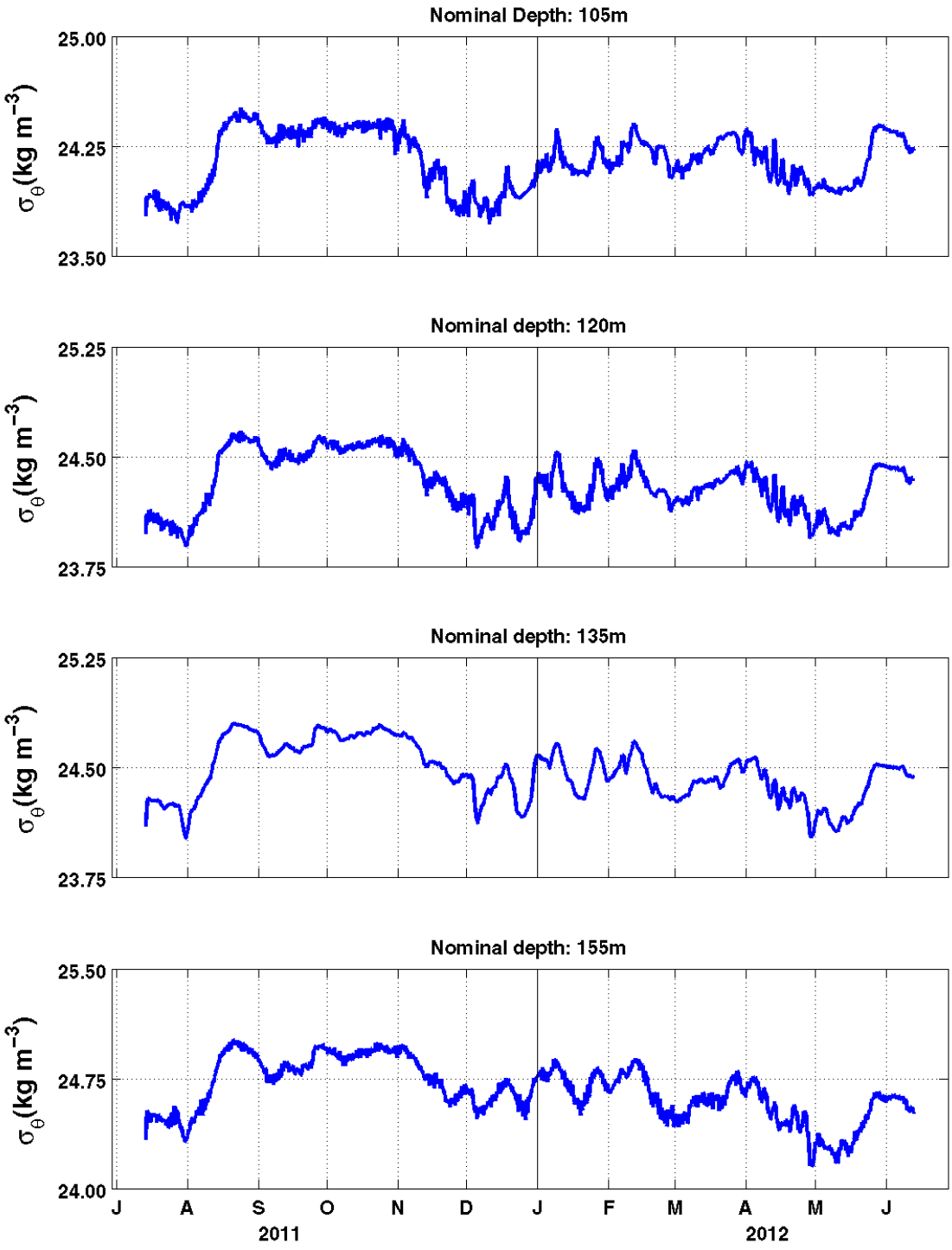

Figure 6-22. Same as in Figure 6-19 but at 105, 120, 135, and 155m.

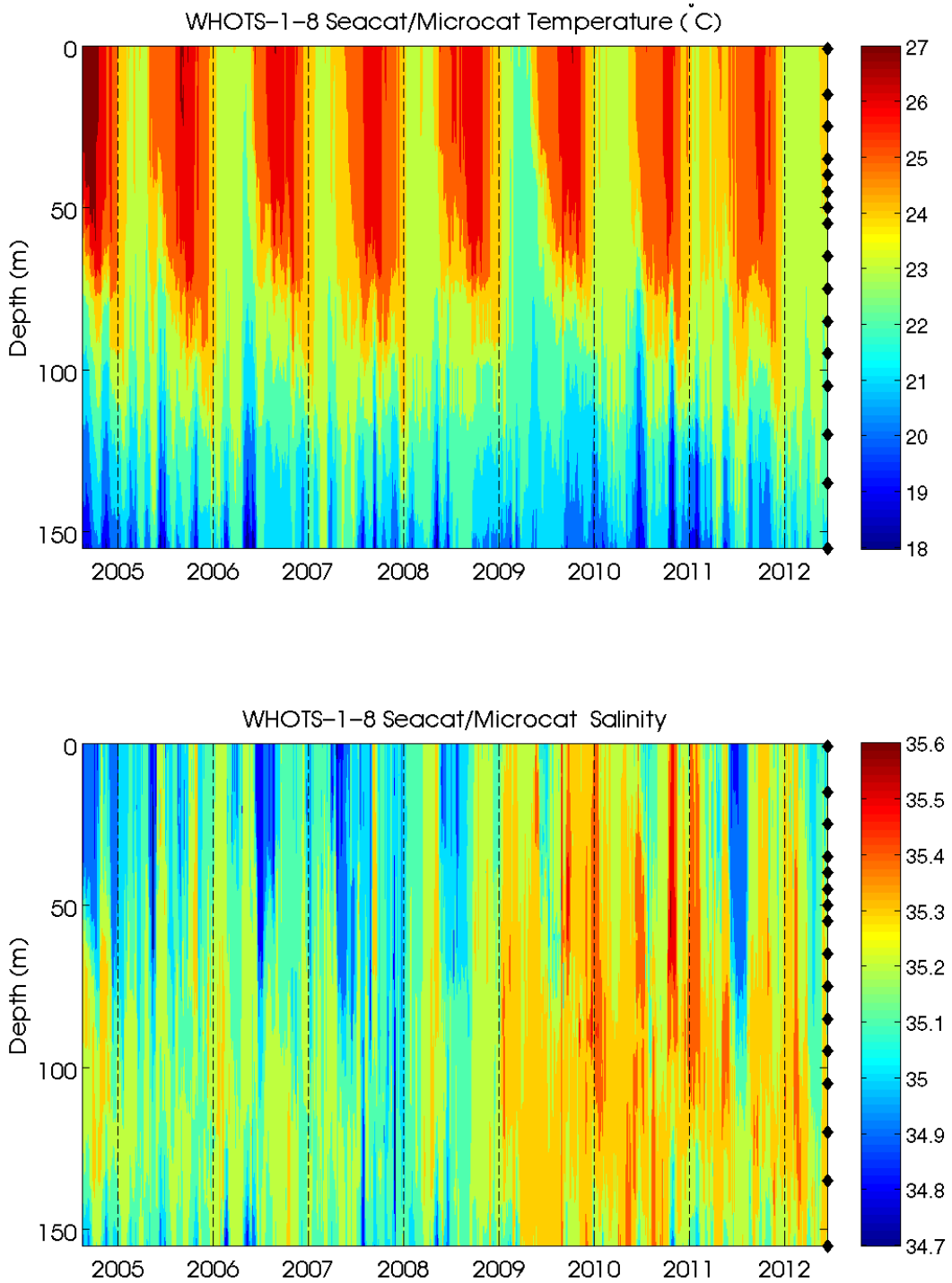

Figure 6-23. Contour plots of temperature (upper panel), and salinity (lower panel) versus depth from MicroCATs during WHOTS-1 through WHOTS-8 deployments. The diamonds along the right axis indicate the instruments depths.

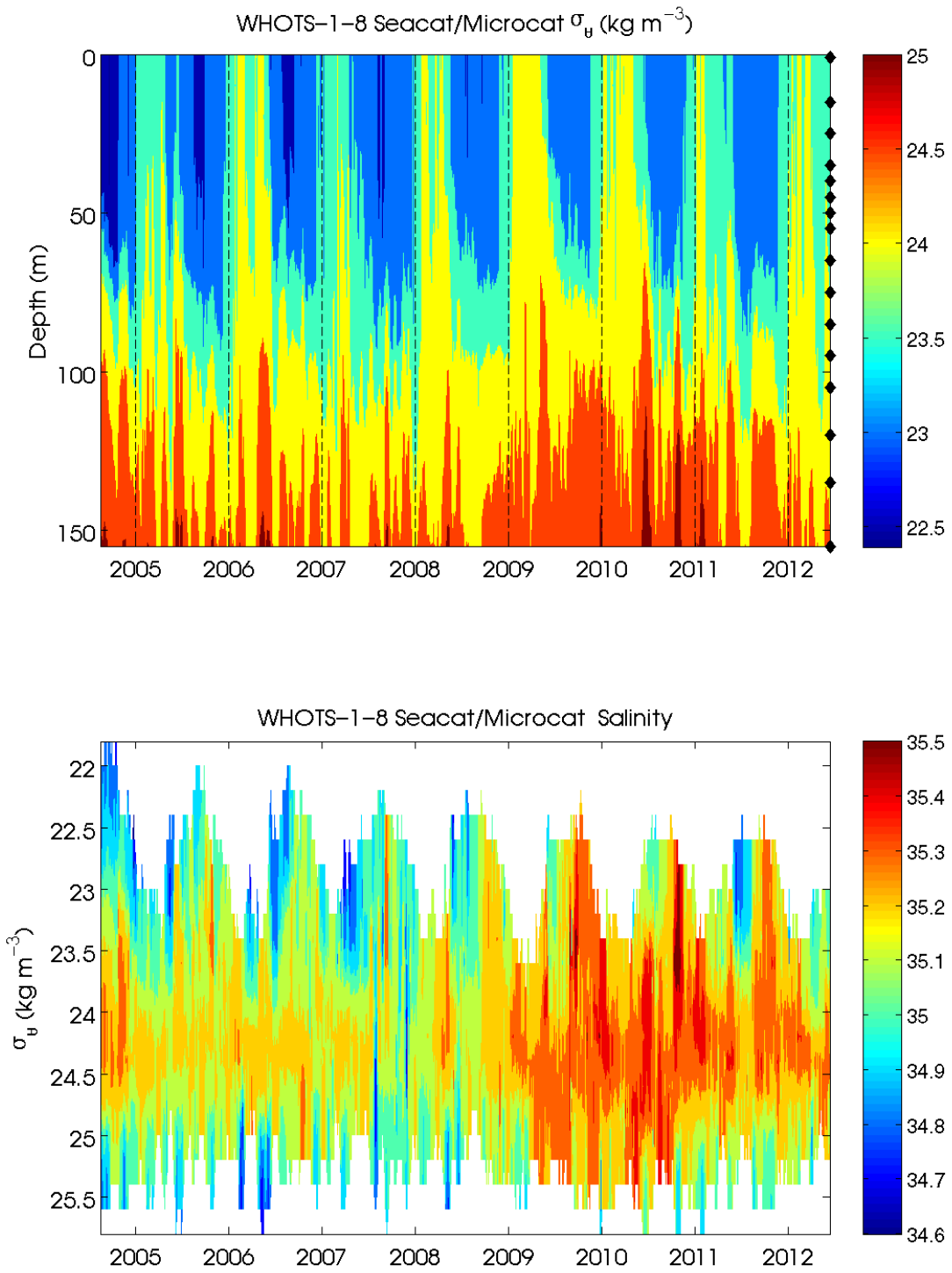

Figure 6-24. Contour plots of potential density (σ_θ , upper panel), versus depth, and of salinity versus σ_θ (lower panel) from MicroCATs during WHOTS-1 through WHOTS-8 deployments. The diamonds along the right axis in the upper figure indicate the instruments depths.

D. Moored ADCP data

Contoured plots of smoothed horizontal and vertical velocity as a function of depth during the mooring deployments 1 through 9 are presented in Figure 6-25 to Figure 6-27. A staggered time-series of smoothed horizontal and vertical velocities are shown in Figure 6-28 to Figure 6-30. Smoothing was performed by applying a daily running mean to the data and then interpolating the data on to an hourly grid.

Contours of east and north velocity components from the Ship Hi'ialakai's Ocean Surveyor broadband 75 kHz shipboard ADCP, and the moored 300 kHz ADCP from the WHOTS-8 deployment as a function of time and depth, during the WHOTS-8 deployment cruise are shown in Figure 6-31 and Figure 6-32.

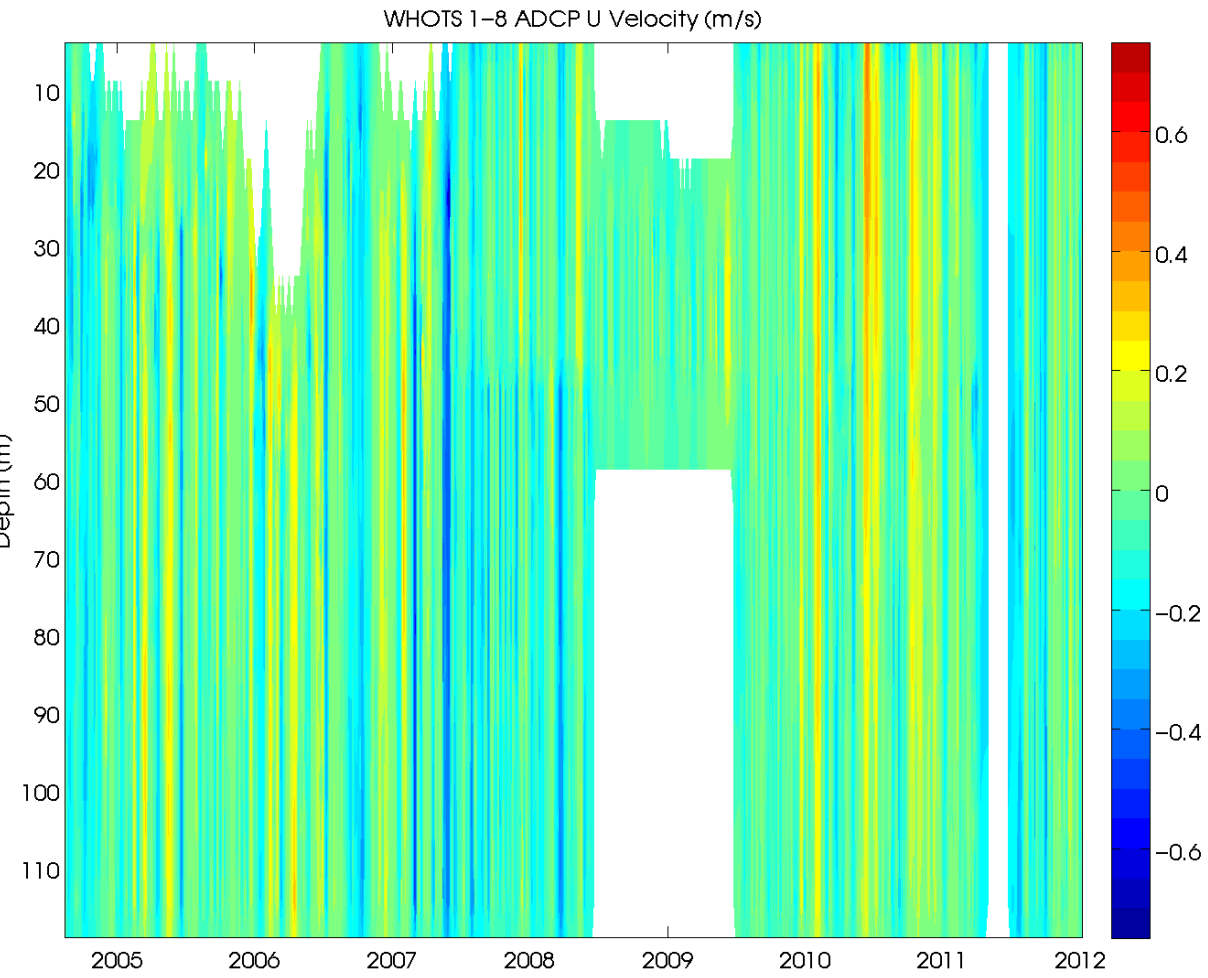

Figure 6-25. Contour plot of east velocity component (m s^{-1}) versus depth and time from the moored ADCPs from the WHOTS-1 through 8 deployments.

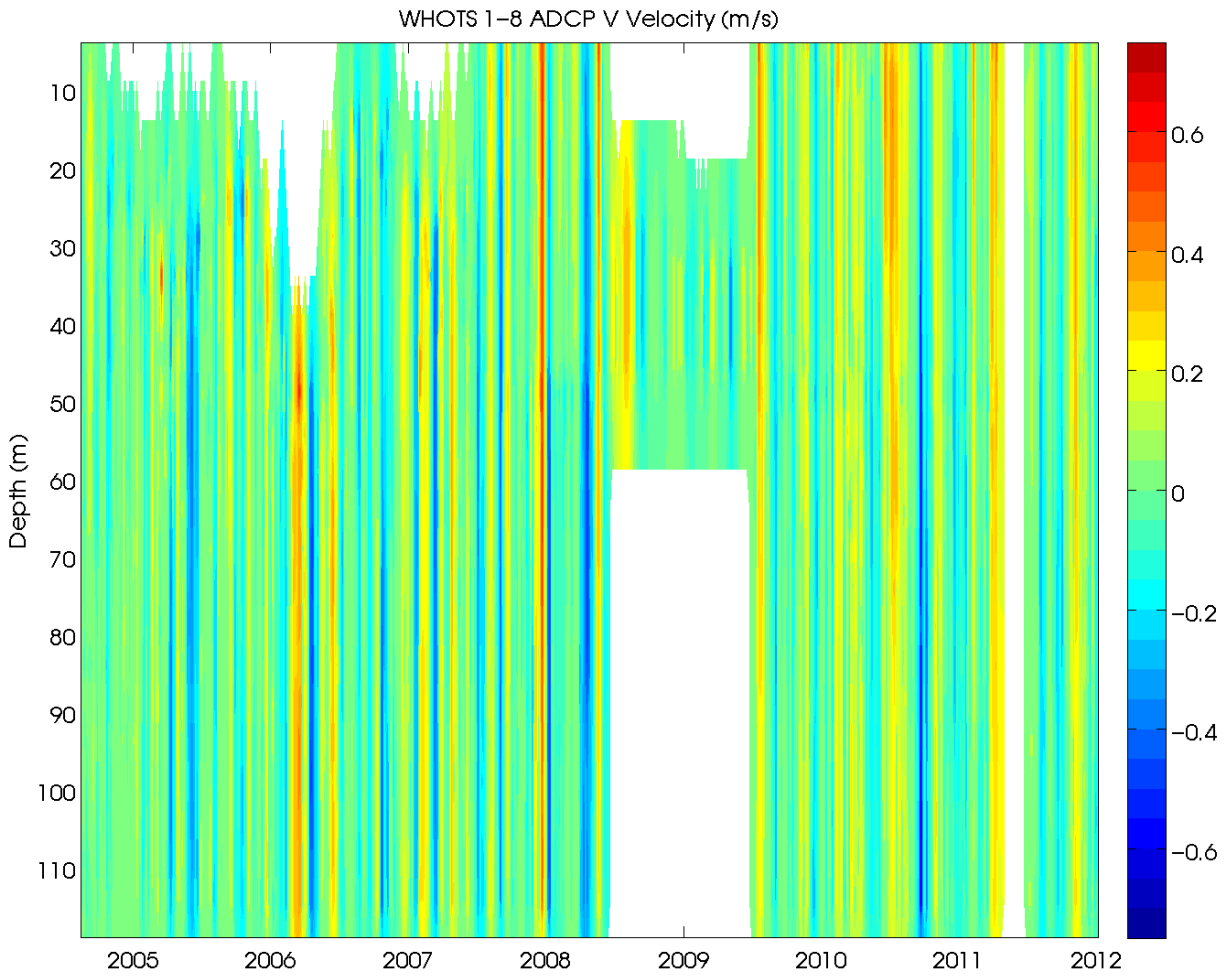

Figure 6-26. Contour plot of north velocity component (m s^{-1}) versus depth and time from the moored ADCPs from the WHOTS-1 through 8 deployments.

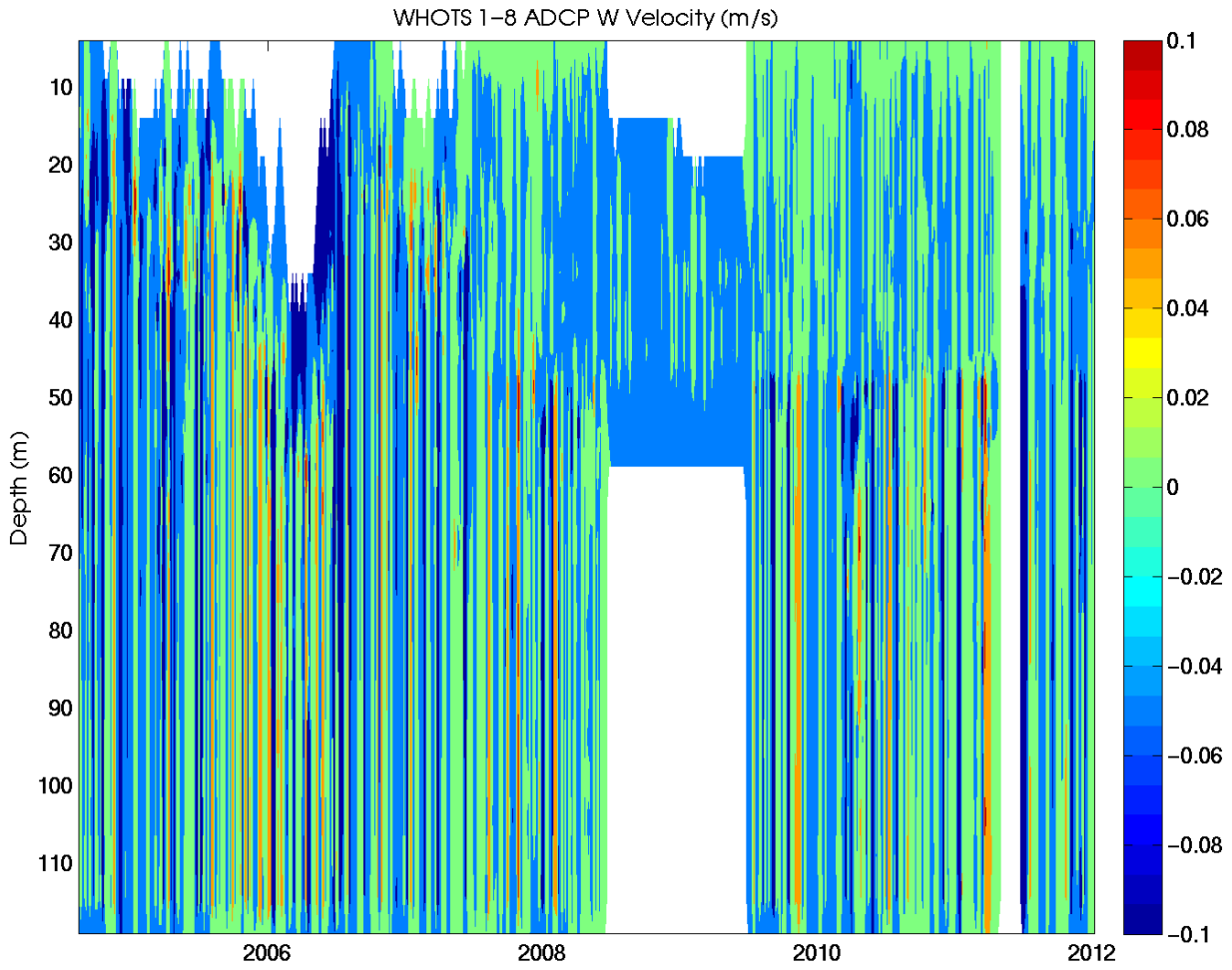

Figure 6-27. Contour plot of vertical velocity component (m s-1) versus depth and time from the moored ADCPs from the WHOTS-1through 8 deployments.

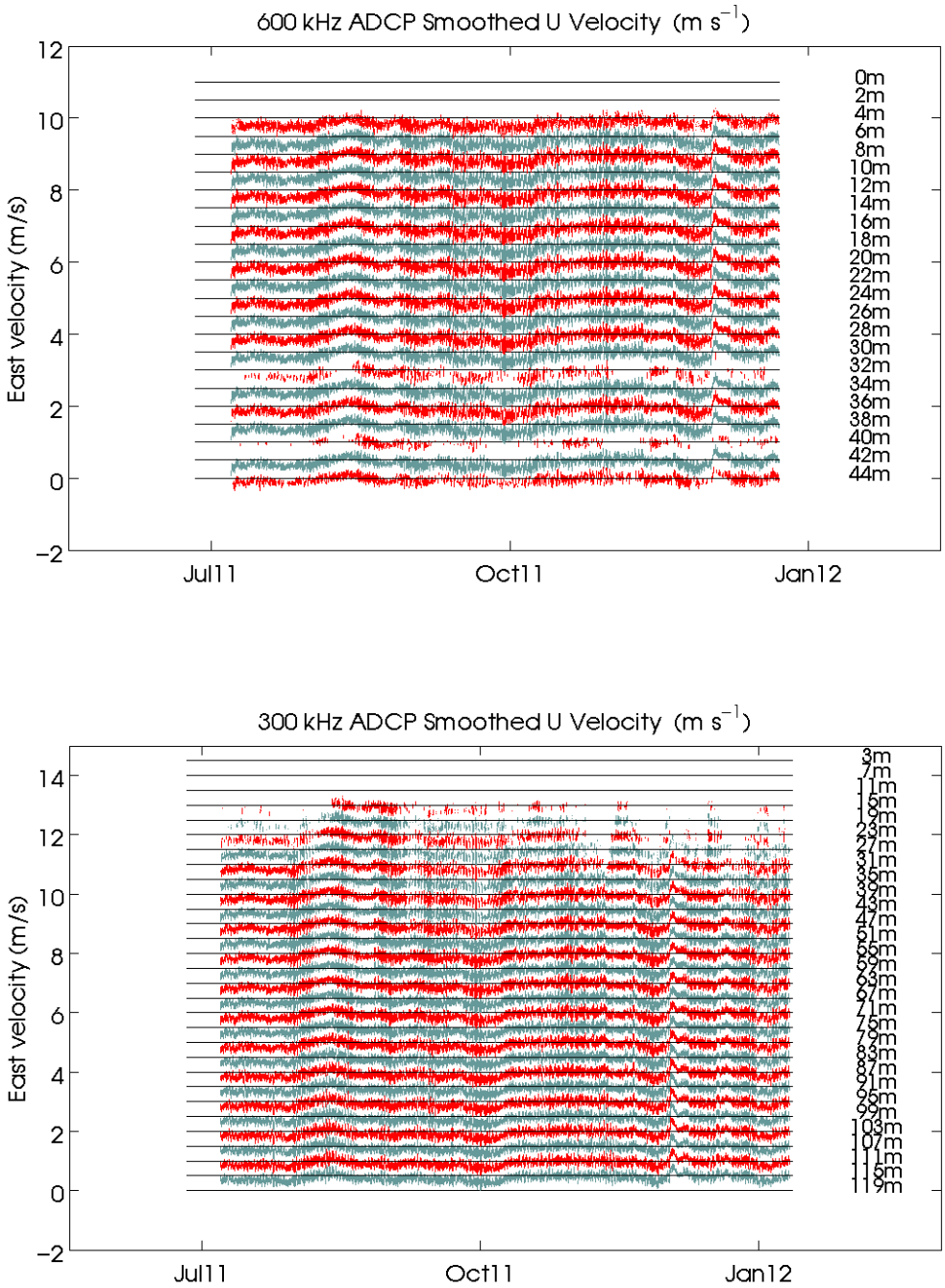

Figure 6-28. Staggered time-series of east velocity component (m s^{-1}) for each bin of the 600 kHz (upper panel), and 300 kHz (lower panel) moored ADCPs during WHOTS-8. The time-series are offset upwards by 0.5 m s^{-1}, the depth of each bin is on the right.

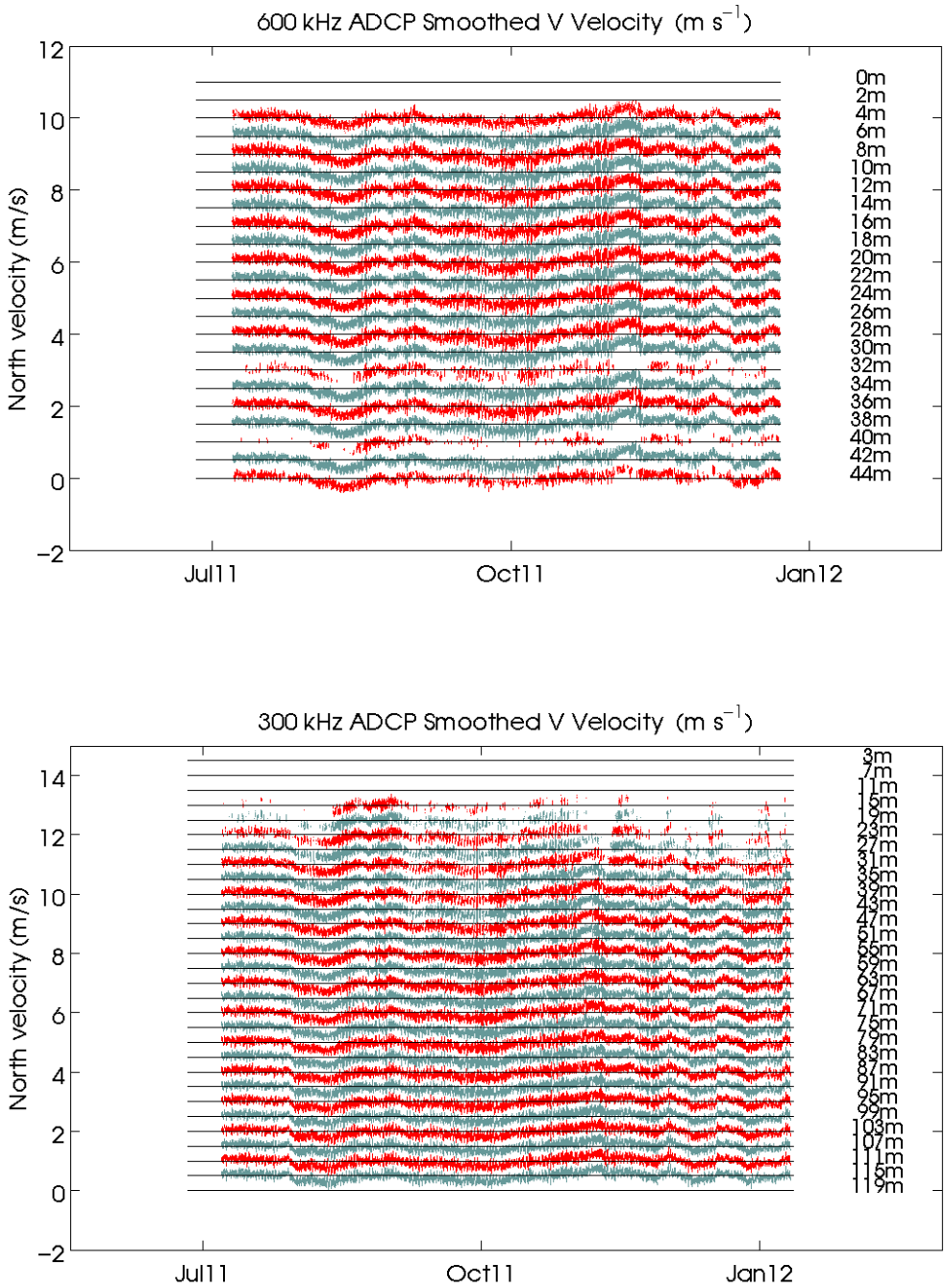

Figure 6-29. Staggered time-series of north velocity component (m s^{-1}) for each bin of the 600 kHz (upper panel), and 300 kHz (lower panel) moored ADCPs during WHOTS-8. The time-series are offset upwards by 0.5 m s^{-1}, the depth of each bin is on the right.

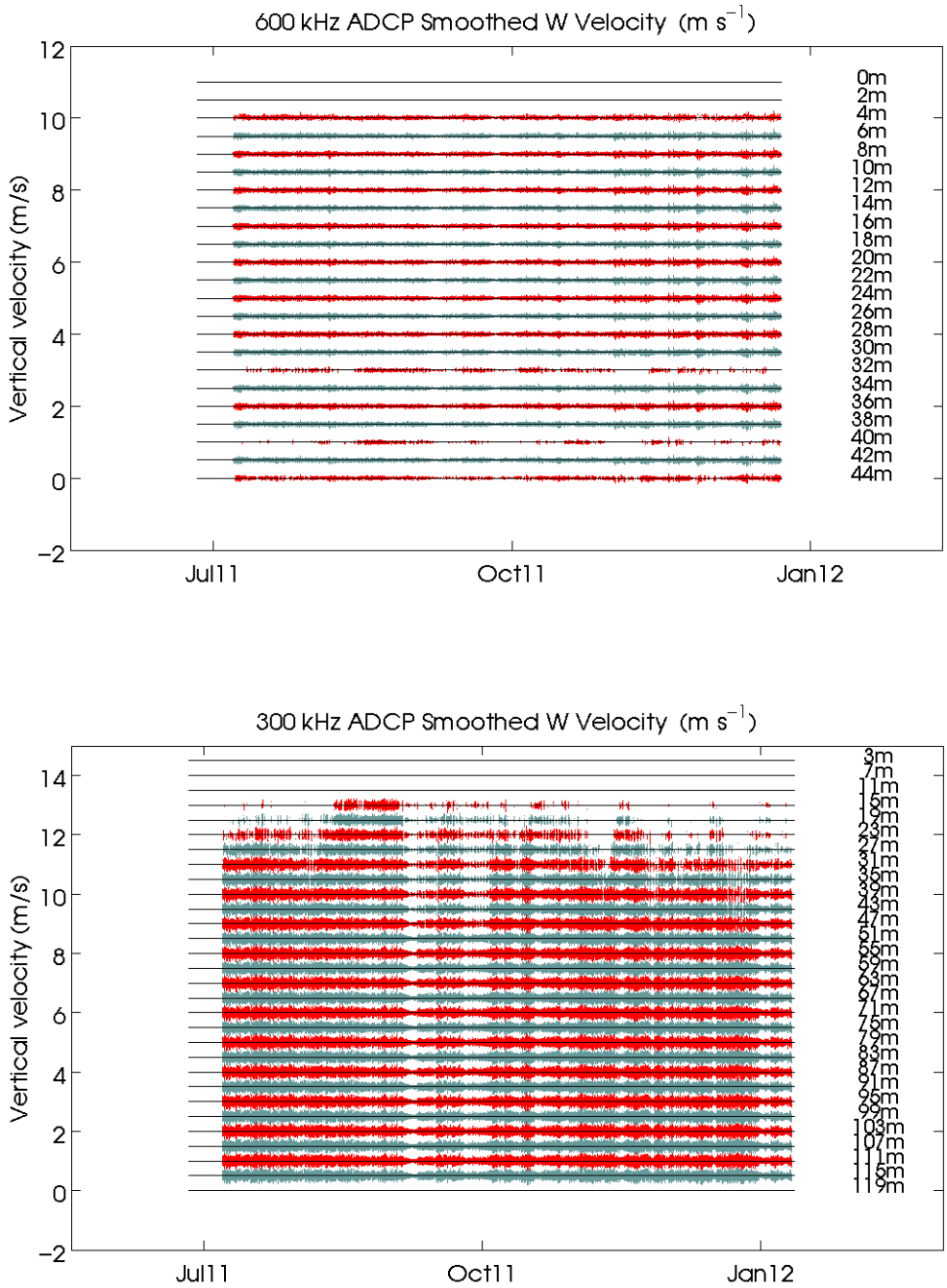

Figure 6-30. Staggered time-series of vertical velocity component (m s^{-1}) for each bin of the 600 kHz (upper panel), and 300 kHz (lower panel) moored ADCPs during WHOTS-8. The time-series are offset upwards by 0.5 m s^{-1}, the depth of each bin is on the right.

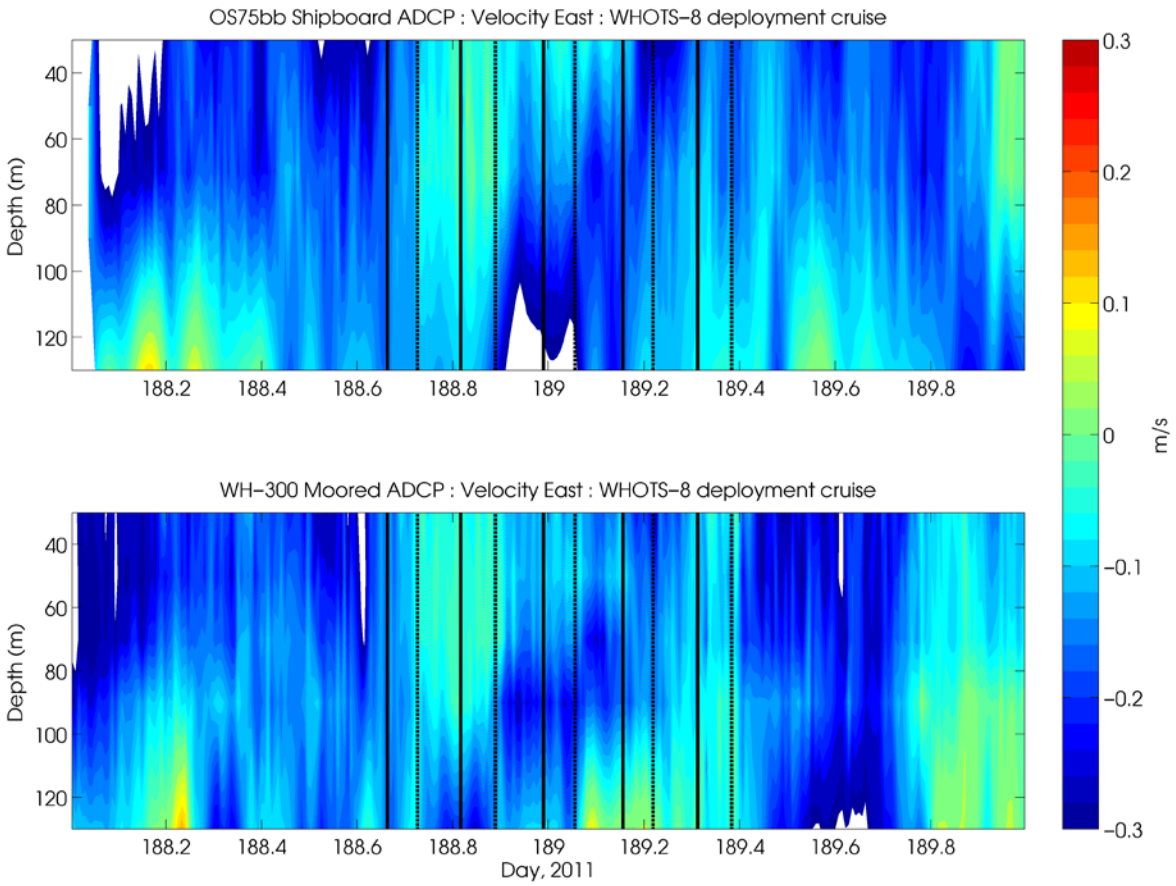

Figure 6-31. Contour of east velocity component (m s^{-1}) from the Ship Hi'ialakai's Ocean Surveyor broadband 75 kHz shipboard ADCP (upper panel), and the moored 300 kHz ADCP from the WHOTS-8 deployment as a function of time and depth, during the WHOTS-8 cruise (lower panel). Times when the CTD rosette were in the water are identified by a solid (in-water) and dashed (out-of-water) black line.

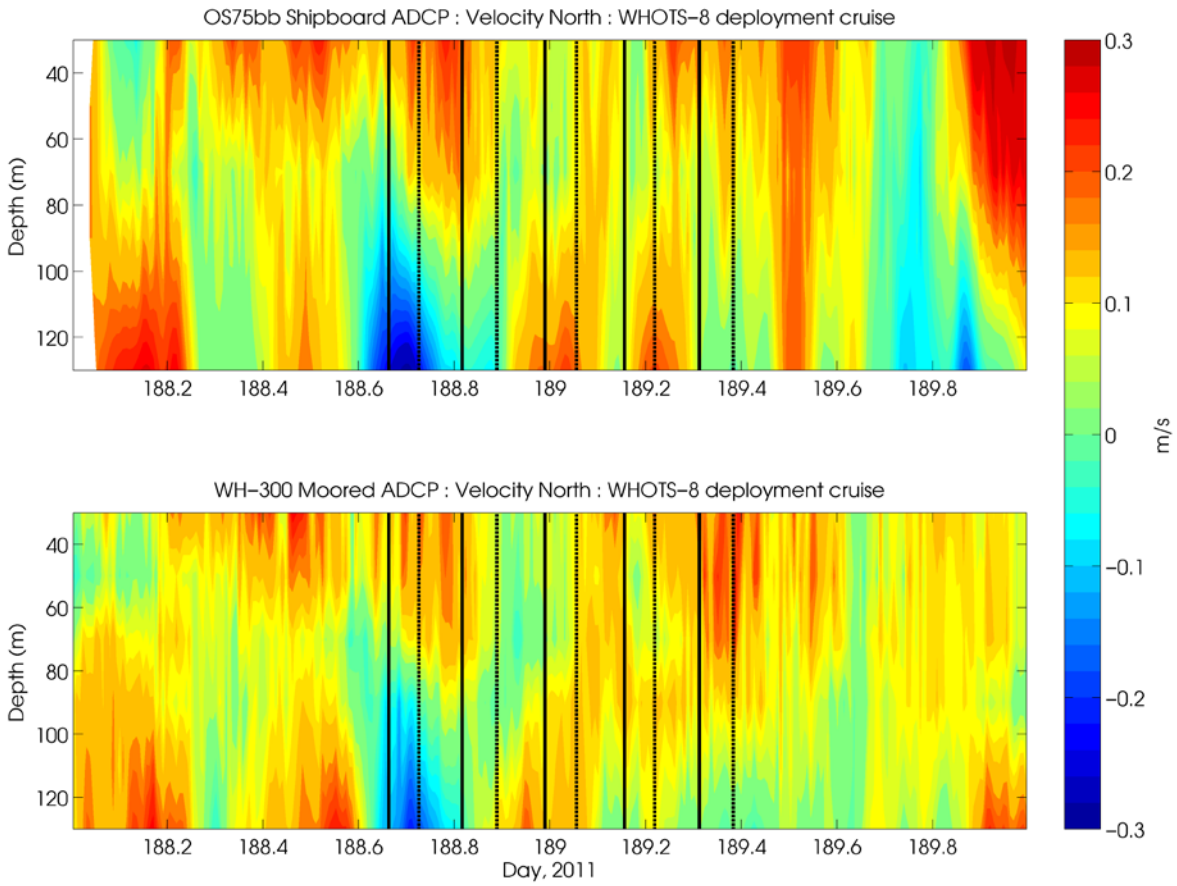

Figure 6-32. Contours of north velocity component (m s^{-1}) from the Ship Hi'ialakai's Ocean Surveyor broadband 75 kHz shipboard ADCP (upper panel), and the moored 300 kHz ADCP from the WHOTS-8 deployment as a function of time and depth, during the WHOTS-8 cruise (lower panel). Times when the CTD rosette were in the water are identified by a solid (in-water) and dashed (out-of-water) black line.

E. Moored and Shipboard ADCP comparisons

Comparisons between quality-controlled moored ADCPs during the WHOTS-8 deployment and available shipboard ADCP obtained during regular HOT cruises 233, 236, and 238 are shown in Figure 6-33 through Figure 6-35 for the 300 kHz ADCP, and Figure 6-36 through Figure 6-38 for the 600 kHz ADCP. Median and mean velocity profiles were computed during the time when HOT CTD casts were being conducted near the WHOTS mooring specifically intended to calibrate moored instrumentation (see 5.A.4). The shipboard profiles were taken when the ship was stationary, within 1 km of the mooring, and within 4 hours before the start and 4 hours after the end of the CTD cast conducted near the WHOTS mooring. Both moored ADCP's failed after HOT-238, so no comparisons were made for HOT-239 through HOT-242. Additionally, HOT-234 and HOT-235 did not feature a cast near the mooring, and HOT-237's ADCP data is unusable. The remaining HOT cruises conducted on the R/V *Kilo Moana* (HOT-233, HOT-238) had data from an RD Instruments Workhorse 300 kHz ADCP (wh300) with 4 m bin size, reaching 100 m, and averaging ensembles every 2 minutes; and from an RD Instruments

Ocean Surveyor 38 kHz operating in broad band mode (os38bb) with 12 m bin size, reaching 1200 m, with 5 minute ensemble averages, and in narrow band mode (os38nb) with 24 m bin size, reaching 1500 m and also with 5 minute ensemble averages. Data from the wh300 were used for the comparisons with the moored ADCP data, or from the os75bb if the wh300 data were not available. HOT-236 on the R/V *Ka`imikai O Kanaloa* had data from an RD Instruments Ocean Surveyor 150 kHz operating in narrow band mode (nb150) with 8 m bin size, reaching 565 m, with 5 minute ensemble averages.

The moored ADCP data were collected from the upward facing 300 kHz ADCP located at 125 m and the upward facing 600 kHz ADCP located at 47.5 m over the same time period. Each of the zonal (U), and meridional (V) current components from the shipboard and moored vertical profiles were interpolated to the profile resolution of the shipboard ADCP, and ensemble mean and median profiles were obtained for each data set to compute differences and correlation coefficients between them. Bins with less than 50% data were excluded. The correlations and the vertical mean of the differences between the ensemble median and mean for each of the U and V components are shown in Table 6-1.

Table 6-1. Correlations and differences of zonal (U), and meridional (V) ensemble median and mean currents (10 to 125 m) between WHOTS-8 moored ADCP (300 and 600 kHz) and shipboard ADCP during HOT cruises.

HOT Shipboard ADCP vs WHOTS Moored 300 kHz ADCP									
Cruise	**Ship ADCP Type**	**Ensemble Median U correlation**	**Vertical Mean of U median differences**	**Ensemble Median V correlation**	**Vertical Mean of V median differences**	**Ensemble Mean U correlation**	**Vertical Mean differences U**	**Ensemble Mean V correlation**	**Vertical Mean differences V**
HOT – 233	wh300	0.8429	-0.0184	-0.0103	-0.0340	0.5261	-0.0150	-0.2888	-0.0447
HOT – 236	nb150	-0.6653	0.0471	-0.4749	0.0131	-0.4031	0.0512	-0.8382	0.0193
HOT – 238	wh300	-0.6424	0.0451	-0.6578	0.0265	-0.7465	0.0505	-0.6320	0.0387
HOT Shipboard ADCP vs WHOTS Moored 600 kHz ADCP									
HOT – 233	wh300	0.5898	-0.0178	0.4874	-0.0112	0.6230	-0.0129	0.7104	-0.0066
HOT – 236	nb150	0.6973	-0.0057	-0.8557	-0.0533	0.7697	-0.0013	-0.8930	-0.0515
HOT - 238	wh300	-0.6545	0.0233	-0.5913	0.0673	-0.6807	0.0368	0.2123	0.0474

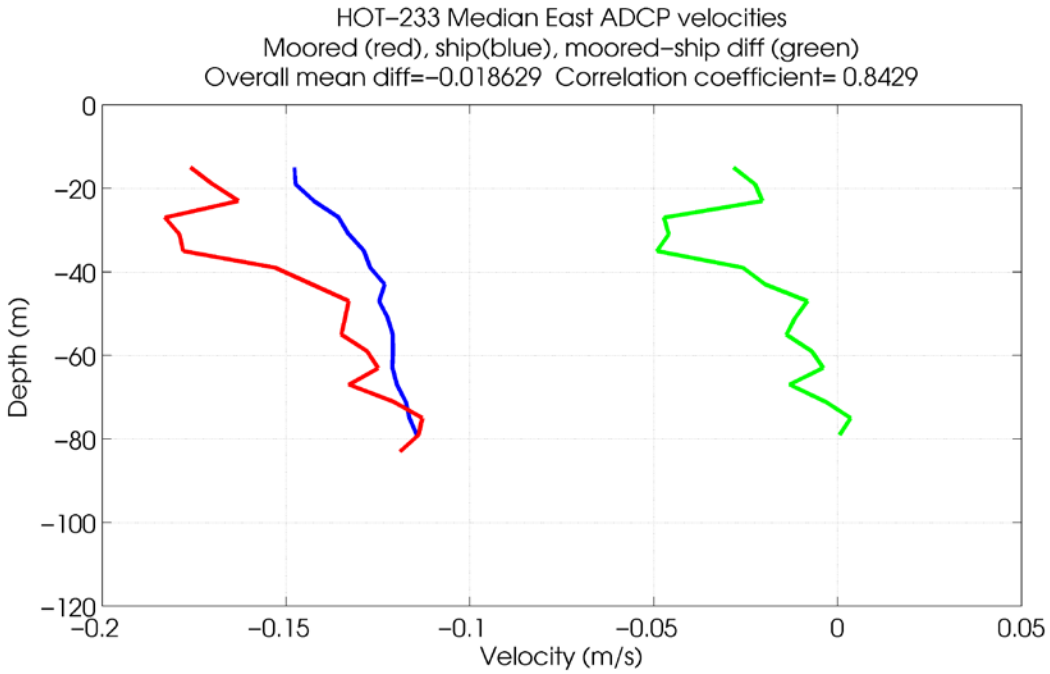

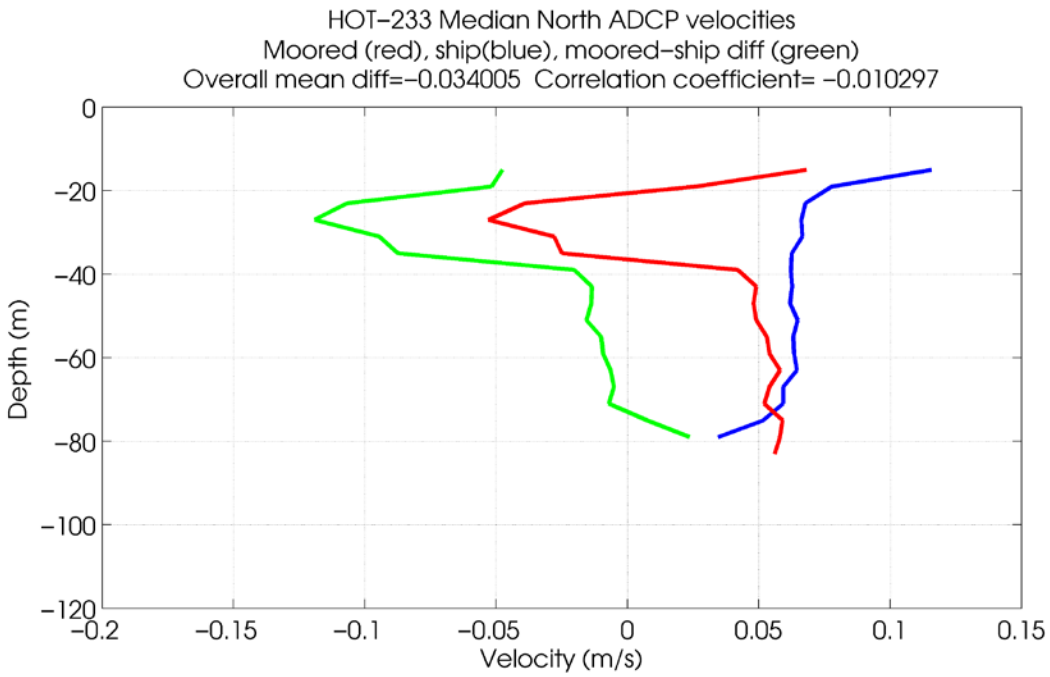

Figure 6-33. Median velocity profiles during shipboard ADCP (blue) versus moored 300 kHz ADCP (red) intercomparisons from HOT-233. Moored minus shipboard ADCP differences shown in green. Top panel shows east velocity components, bottom panel shows north velocity components.

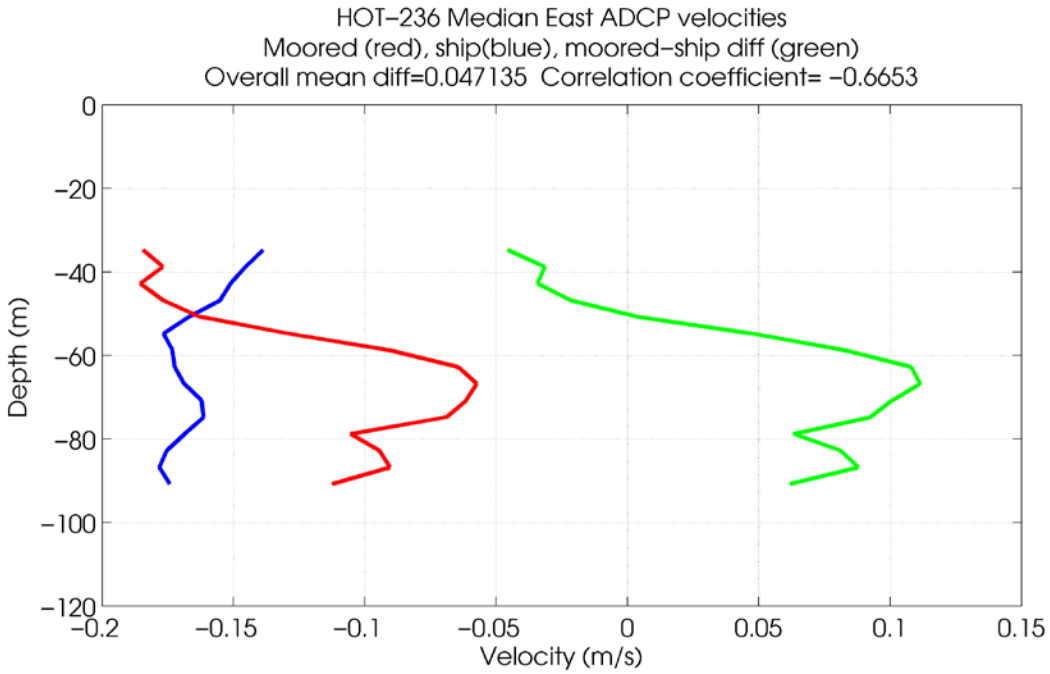

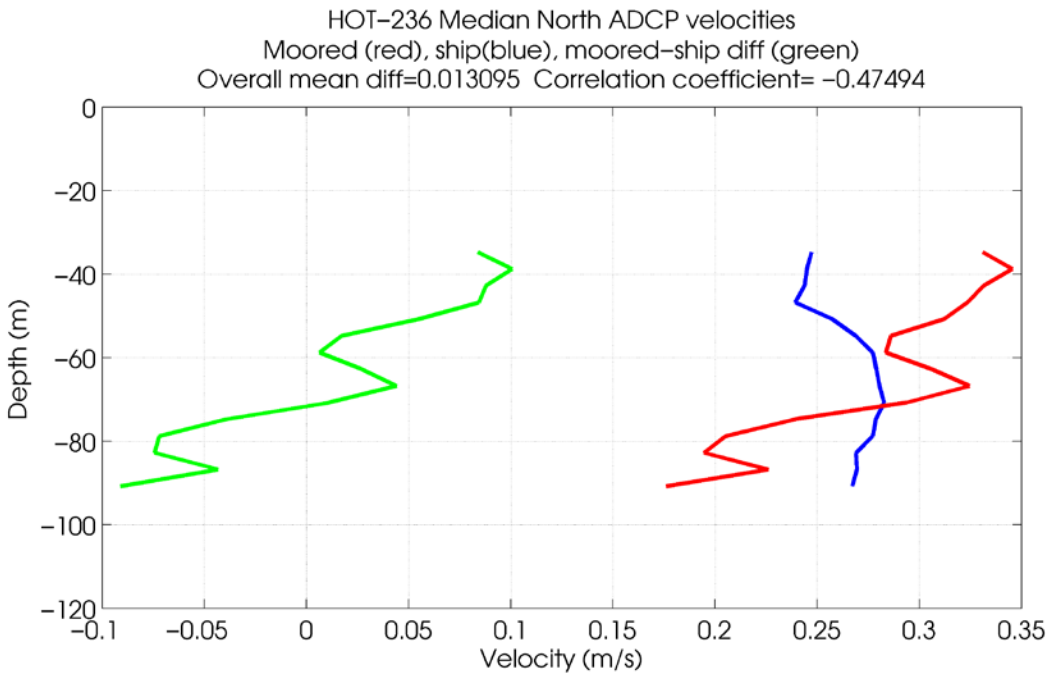

Figure 6-34. Median velocity profiles during shipboard ADCP (blue) versus moored 300 kHz ADCP (red) intercomparisons from HOT-236. Moored minus shipboard ADCP differences shown in green. Top panel shows east velocity components, bottom panel shows north velocity components.

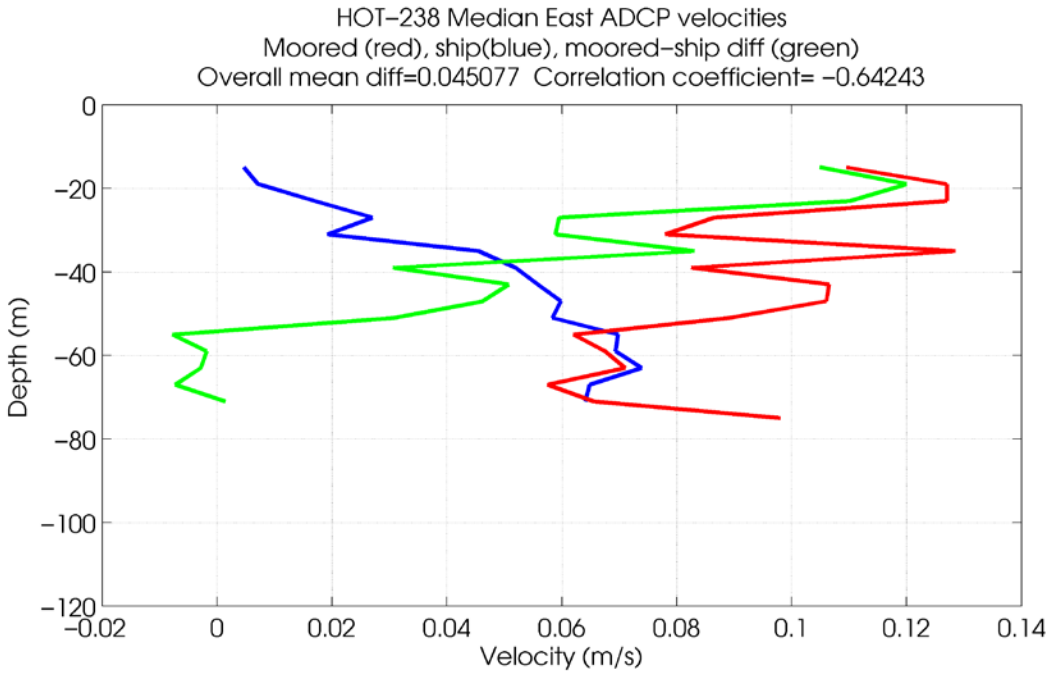

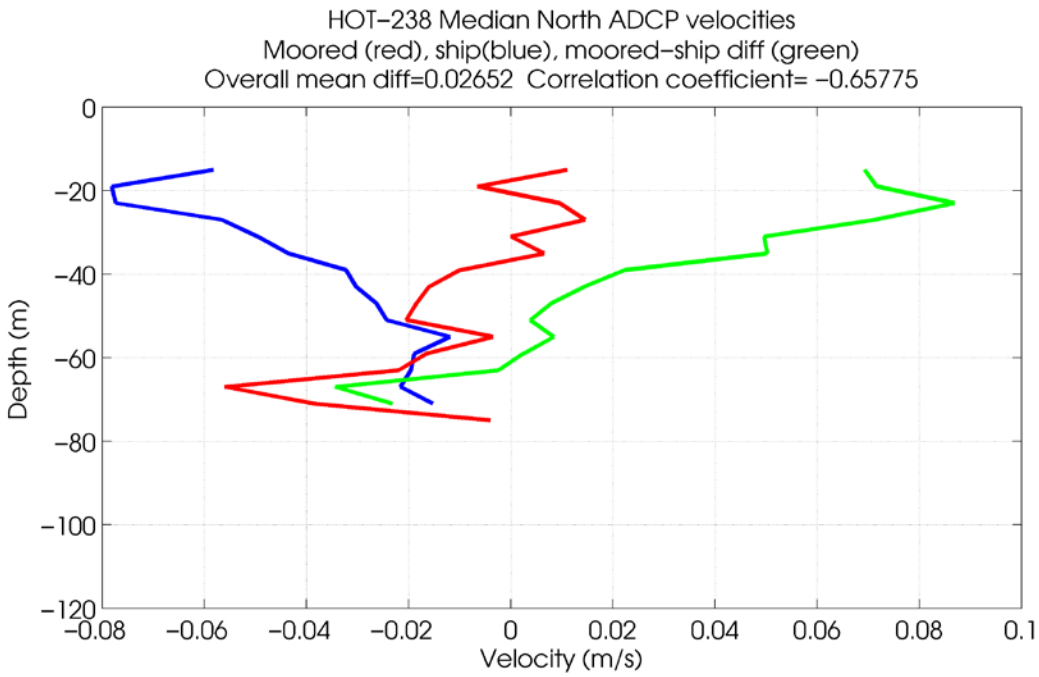

Figure 6-35. Median velocity profiles during shipboard ADCP (blue) versus moored 300 kHz ADCP (red) intercomparisons from HOT-238. Moored minus shipboard ADCP differences shown in green. Top panel shows east velocity components, bottom panel shows north velocity components.

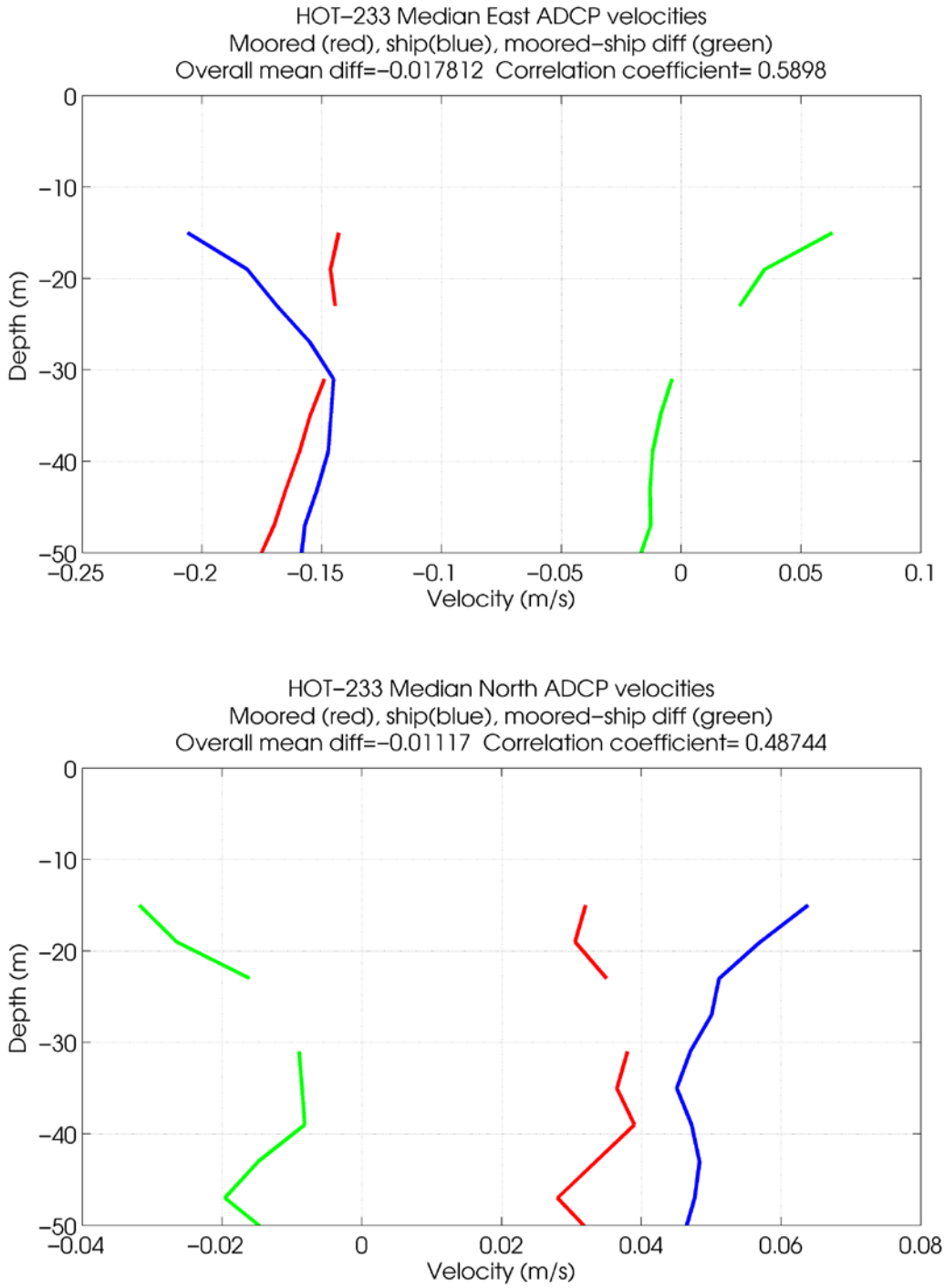

Figure 6-36. Median velocity profiles during shipboard ADCP (blue) versus moored 600 kHz ADCP (red) intercomparisons from HOT-233. Moored minus shipboard ADCP differences shown in green. Top panel shows east velocity components, bottom panel shows north velocity components.

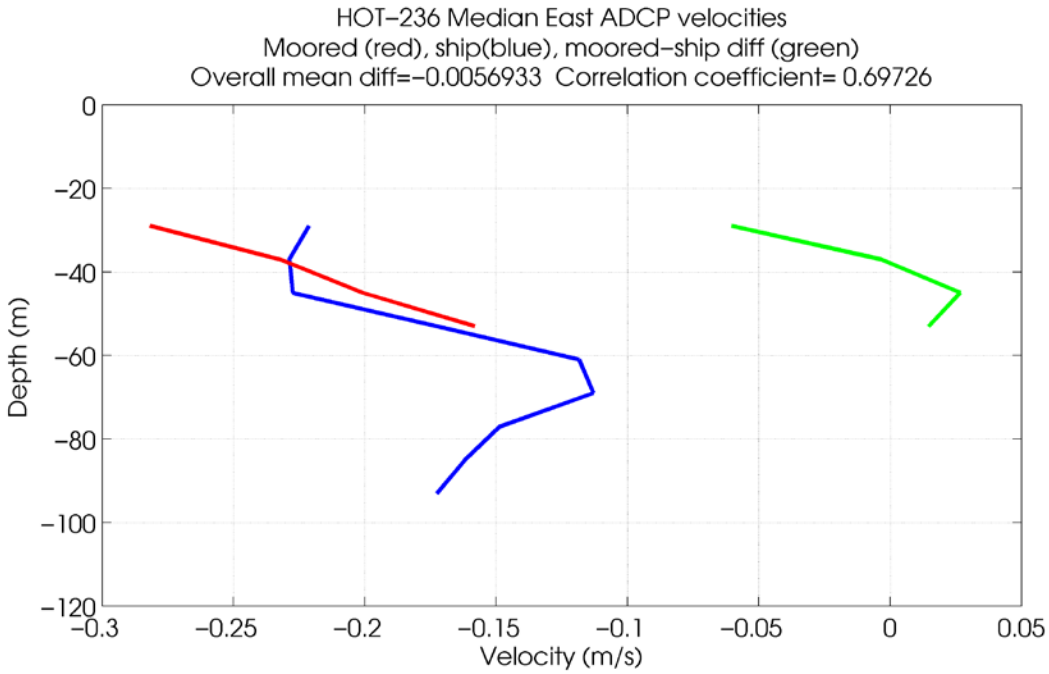

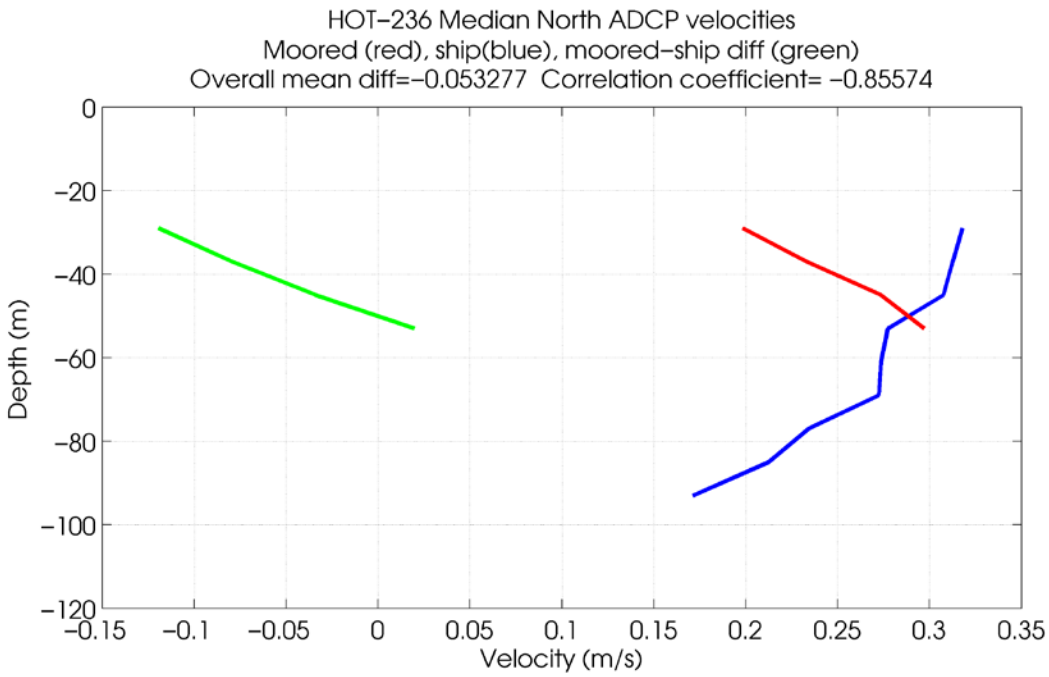

Figure 6-37. Median velocity profiles during shipboard ADCP (blue) versus moored 600 kHz ADCP (red) intercomparisons from HOT-244. Moored minus shipboard ADCP differences shown in green. Top panel shows east velocity components, bottom panel shows north velocity components.

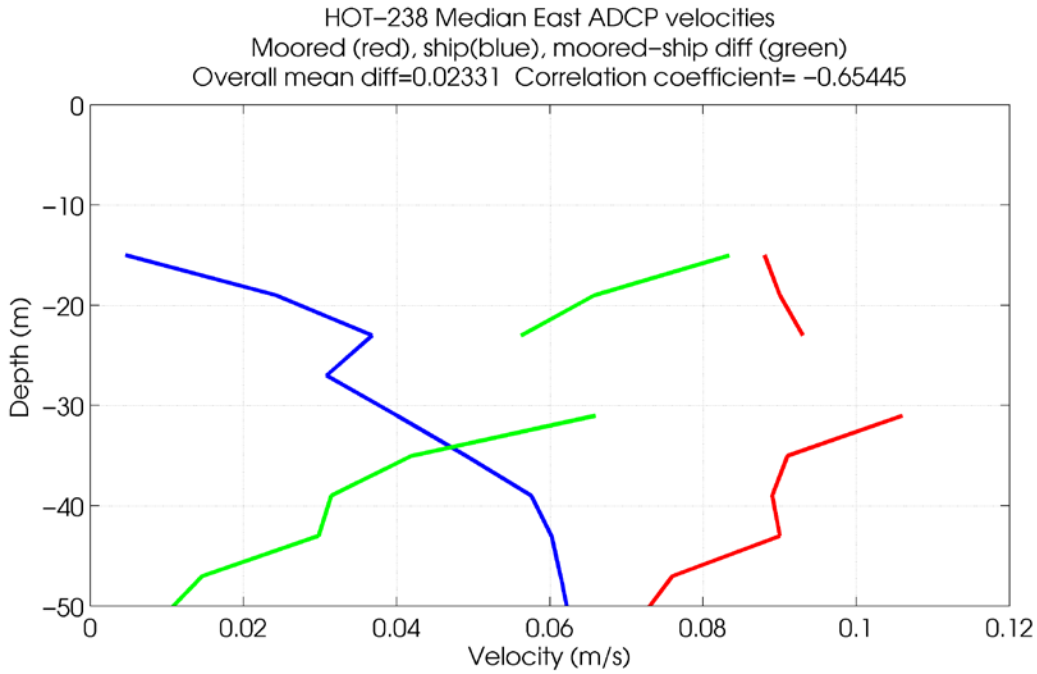

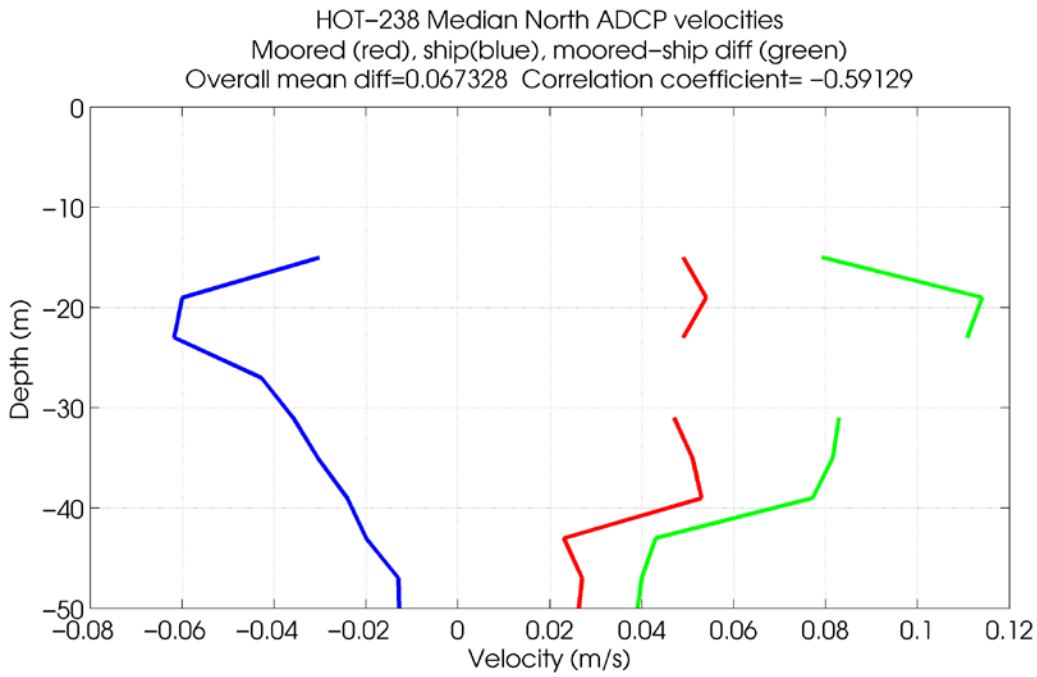

Figure 6-38. Median velocity profiles during shipboard ADCP (blue) versus moored 600 kHz ADCP (red) intercomparisons from HOT-238. Moored minus shipboard ADCP differences shown in green. Top panel shows east velocity components, bottom panel shows north velocity components.

F. Next Generation Vector Measuring Current Meter data (VMCM)

Time-series of daily mean horizontal velocity components for the VMCM current meters deployed during WHOTS-8 at 10 m and 30 m are presented in Figure 6-39.

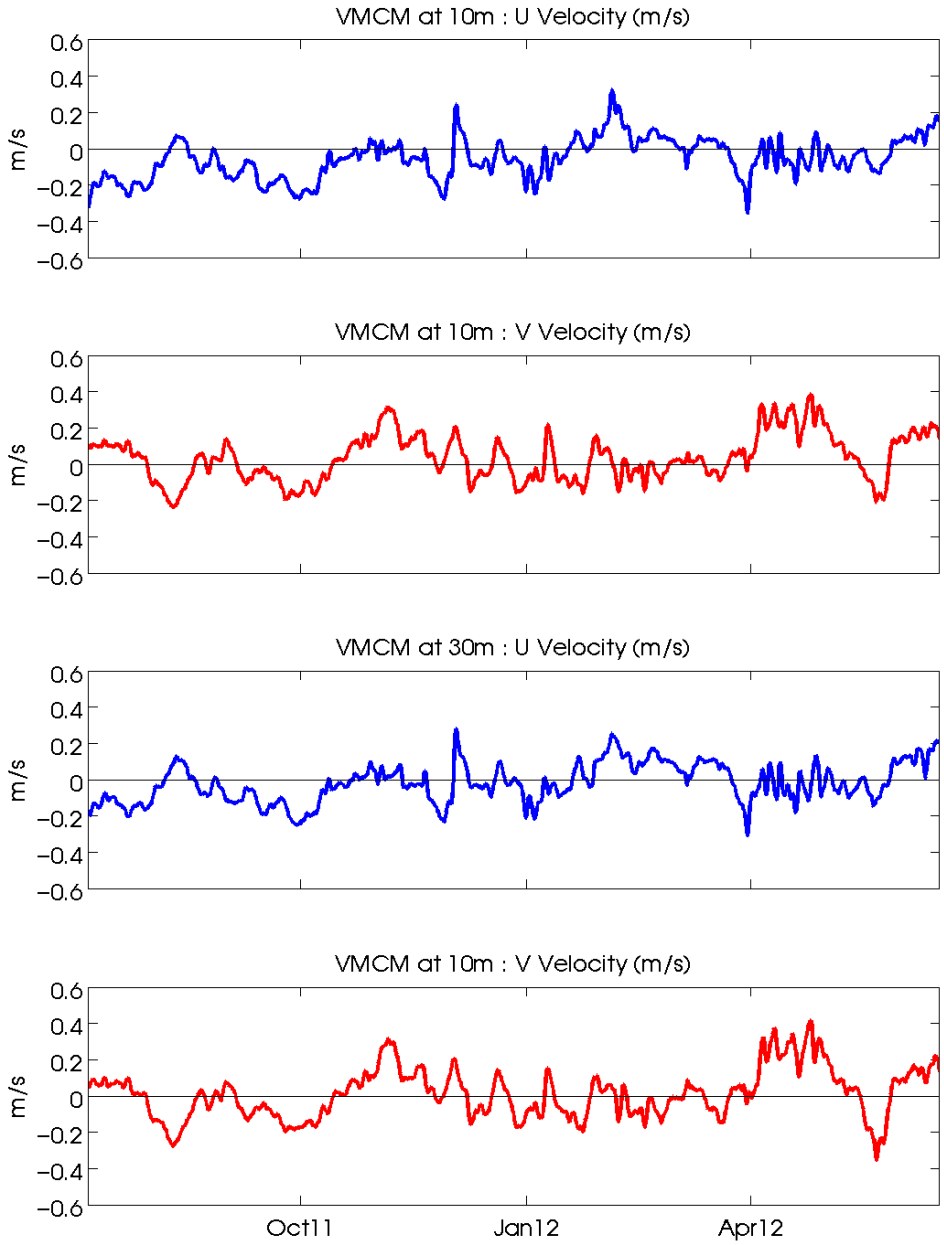

Figure 6-39. Horizontal velocity data (m/s) during WHOTS-8 from the VMCMs at 10 m depth (first and second panel) and at 30 m depth (third and fourth panel).

G. GPS data

Time-series of latitude and longitude of the WHOTS-8 buoy from GPS data are presented in Figure 6-40 and spectra of the time-series is shown in Figure 6-40.

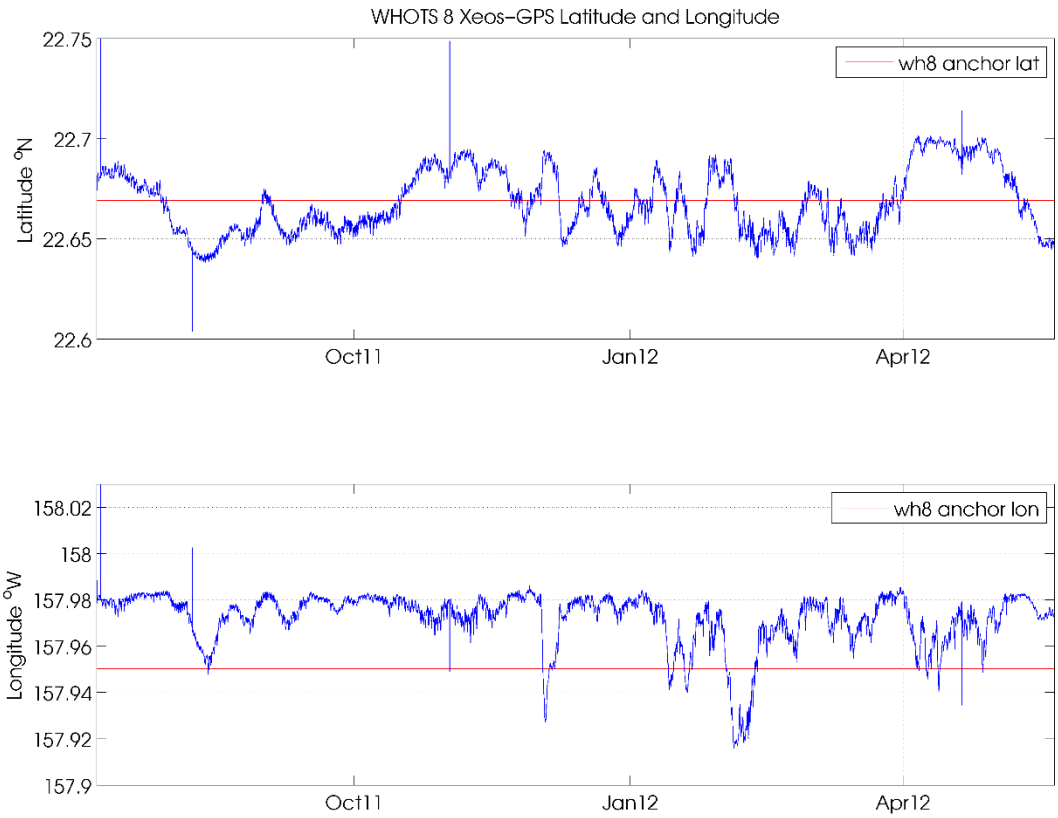

Figure 6-40. GPS Latitude (upper panel) and longitude (lower panel) time series from the WHOTS-8 deployment.

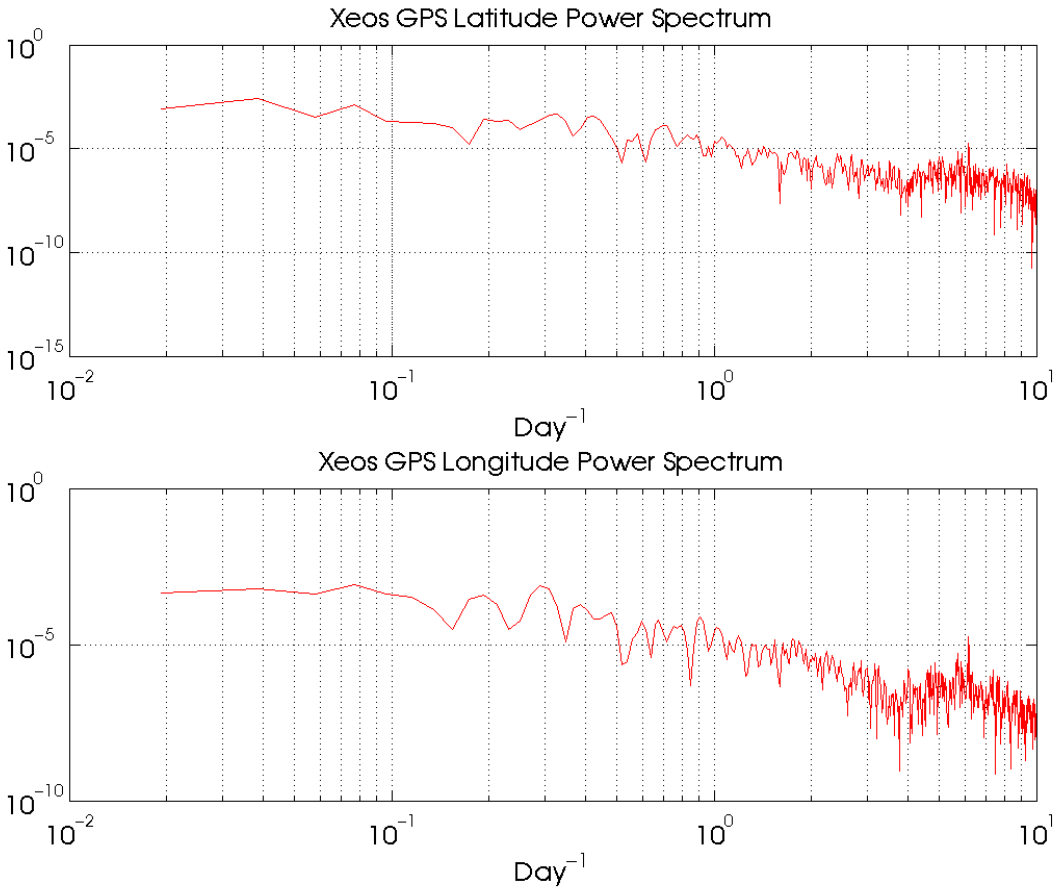

Figure 6-41. Power spectrum of latitude (upper panel) and longitude (lower panel) for the WHOTS-8 deployment.

H. Mooring Motion

The position of the mooring with respect to its anchor was determined from the ARGOS positions as shown in Section 5.D. Additional information of the mooring motion was provided by the ADCP data of pitch, roll and heading, shown in this section.

Figure 6-42 shows the ADCP data of the instrument's tilt (a combination of the pitch and roll), plotted against the buoy's distance from its anchor (derived from ARGOS positions), for both WHOTS ADCP's. The red line in the plot is a quadratic fit to the median tilt calculated every 0.2 km distance bins. The figure shows that during both deployments, the ADCP tilt increased as the distance from the anchor increased. This tilting was caused by the deviation of the mooring line from its vertical position as it was pulled by the anchor. The tilting of the line also caused the rising of the instruments attached to the line.

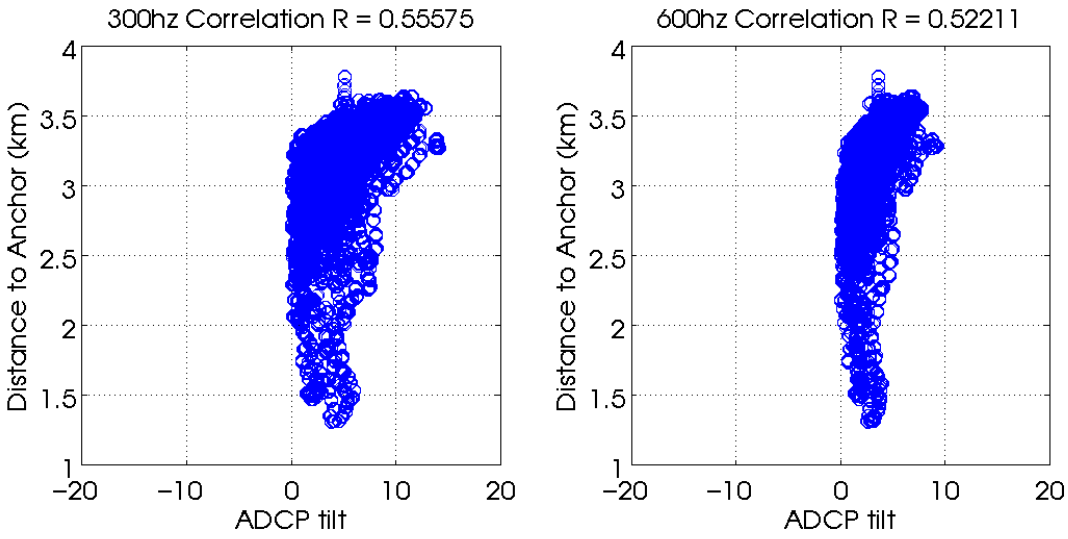

Figure 6-42. Scatter plots of ADCP tilt and distance of the buoy to its anchor for the 300 kHz (left panel), and the 600 kHz ADCP deployments (right panel, blue circles). The red line is a quadratic fit to the median tilt calculated every 0.2 km distance bins.

7. References

Colbo, K., R. Weller, 2009. Accuracy of the IMET Sensor Package in the Subtropics. J. Atmos. Oceanic Technol., 26, 1867-1890.

Firing, E., 1991. Acoustic Doppler Current Profiling measurements and navigation. In *WOCE Hydrographic Operations and Methods.* WOCE Operations Manual, WHP Office Report WHPO 91-1,WOCE Report No. 68/91, 144pp.

Freitag, H. P., M. E. McCarty, C. Nosse, R. Lukas, M. J. McPhaden, and M. F. Cronin, 1999. COARE Seacat data: Calibrations and quality control procedures. NOAA Thechnical Memorandum, ERL PMEL-115. 93 pp.

Hosom, D. R. Weller, R. Payne, and K. Prada, 1995. The IMET (Improved Meteorology) Ship and Buoy Systems. J. Atmos. Oceanic Technol., 12, 527-540.

Kara, A. B., P. A. Rochford, and H. E. Hulburt, 2000. Mixed layer depth variability and barrier layer formation over the North Pacific Ocean, J. Geophys. Res., 105, 16,803–16,821.

Larson, N. and A.M. Pederson, 1996. Temperature measurements in flowing water: Viscous heating of sensor tips. 1st International Group for Hydraulic Efficiency Measurements (IGHEM) Meeting, Montreal, Canada, June 1996.

Lueck, R. G., 1990. Thermal inertia of conductivity cells: Theory. Journal of Atmospheric and Oceanic Technology, 7, 741-755.

Lueck, R. G. and J. J. Picklo, 1990: Thermal inertia of conductivity cells: Observations with a Sea-Bird cell. Journal of Atmospheric and Oceanic Technology, 7, 756-768.

Owens, W. B. and R. C. Millard, 1985. A new algorithm for CTD oxygen calibration. Journal of Physical Oceanography, 15, 621-631.

Plueddemann, A.J., R.A. Weller, R. Lukas, J. Lord, P.R. Bouchard, and M.A. Walsh, 2006, WHOI Hawaii Ocean Timeseries Station (WHOTS): WHOTS-2 Mooring Turnaround Cruise Repor**t,** Woods Hole Oceanographic Institution, Technical Report WHOI-2006-08, 68 pp.

Plueddemann, A.J., Ryder, B. Pietro, J. Smith, C. Duncombe Rae, R. Lukas, C. Nosse, J. Snyder, L. Bariteau, S. J. Park, D. Hashisaka, E. Roth, C. Fumar, A. Andrews, and N. Seymour, 2013. WHOI Hawaii Ocean Timeseries Station (WHOTS): WHOTS-9 2012 Mooring Turnaround Cruise Repor**t,** Woods Hole Oceanographic Institution, Technical Report WHOI-2013-04, 93 pp.

Santiago-Mandujano, F., P. Lethaby, R. Lukas, J. Snyder, Weller, A. Plueddeman, J. Lord, S. Whelan, P. Bouchard, and N. Galbraith, 2007. Hydrographic Observations at the Woods Hole Oceanographic Institution (WHOI) Hawaii Ocean Timeseries (HOT) Site (WHOTS): 2004-2006. School of Ocean and Earth Science and Technology, University of Hawaii. (http://www.soest.hawaii.edu/whots/data_report1.html)

Tupas, L., F. Santiago-Mandujano, D. Hebel, R. Lukas, D. Karl, and E. Firing 1993. Hawaii Ocean Time-series Data Report 4, 1992, School of Ocean and Earth Science and Technology, University of Hawaii, 93-14, 248 pp.

Tupas, L., F. Santiago-Mandujano, D. Hebel, C. Nosse, L. Fujieki, E. Firing, R. Lukas, D. Karl, 1997. Hawaii Ocean Time-series Data Report 8, 1996, School of Ocean and Earth Science and Technology, University of Hawaii, 97-7, 296 pp.

UNESCO. 1981. Tenth Report of the Joint Panel on Oceanographic Tables and Standards. UNESCO Technical Papers in Marine Science, No. 36, UNESCO, Paris.

Whelan S., R. Weller, R. Lukas, F. Bradley, J. Lord, J. Smith, F. Bahr, P. Lethaby, J. Snyder, 2007. WHOI Hawaii Ocean Timeseries Station (WHOTS): WHOTS-3 Mooring Turnaround Cruise Report. Technical Report. Woods Hole Oceanographic Institution, WHOI-2007-03, 103 pp.

Whelan S., J. Lord, C.D. Rae, A. Plueddemann, J. Snyder, C. Nosse, R. Lukas, P. Boylan, B. Pietro, B. Ludovic, C. Sabine, S. Pezoa, 2012. WHOI Hawaii Ocean Timeseries Station (WHOTS): WHOTS-8 2011 Mooring Turnaround Cruise Report. Technical Report. Woods Hole Oceanographic Institution, WHOI-2012-04, 98 pp.

8. Appendices

A. Appendix 1: WHOTS-8 300 kHz ADCP Configuration

File Size 5,666,182 bytes

Data Structure BB/WH/OS
Ensemble Length 752 bytes

Program Version 16.31

System Frequency 300 kHz
Convex
Sensor Configuration #1
Transducer Head Attached TRUE
Orientation UP
Beam Angle 20 Degrees
Transducer 4 Beam Janus

Real Data

CPU Serial Number: 7128

False Target(WA) 70 counts
Band Width (WB) 0
Cor. Thres. (WC) 64 counts
Err Thres. (WE) 2000 mm/s
Blank (WF) 1.76 m
Min PGood (WG) 0
Ref Layer (WL) 1, 5 first bin, last bin
Mode (WM) 1
Bins (WN) 30
Pings/Ens (WP) 40
Bin Size (WS) 4.00 m

Head Align (EA) 0.00 degrees
Head Bias (EB) 9.88 degrees
Coord Xform (EX) 00011111 Earth Coordinates Using Tilts, 3 Beam Solutions, and Bin Mapping
Sens Source (EZ) 01111101 cdhprst
Sens Avail 00011101 cdhprst

Time/Ping (TP) 00:04.00

Hardware 4 Beams
Code Reps. 9
Lag Length 0.50 m
Xmt Length 4.47 m
1st Bin 6.24m

BT Pings/Ens (BP) 0
BT Ens Delay (BD) 0
BT Cor.Thres. (BC) 0 counts
BT Eval. Thres. (BA) 0 counts

BT PG Thres. (BG) 0
BT Mode (BM) 0
BT Err Thres. (BE) 0 mm/s
BT Max Range (BX) 0 dm

First Ensemble 00000001 06-Jul-2011 00:20:00
Last Ensemble 00005445 11-Jan-2012 00:59:59

B. Appendix 2: WHOTS-8 600 kHz ADCP Configuration

File Size 4,291,515

Data Structure BB/WH/OS
Ensemble Length 652 bytes

Program Version 16.31

System Frequency 600 kHz
Convex
Sensor Configuration #1
Transducer Head Attached TRUE
Orientation UP
Beam Angle 20 Degrees
Transducer 4 Beam Janus

Real Data

CPU Serial Number: 70122

False Target(WA) 70 counts
Band Width (WB) 0
Cor. Thres. (WC) 64 counts
Err Thres. (WE) 2000 mm/s
Blank (WF) 0.88 m
Min PGood (WG) 0
Ref Layer (WL) 1, 5 first bin, last bin
Mode (WM) 1
Bins (WN) 25
Pings/Ens (WP) 80
Bin Size (WS) 2.00 m

Head Align (EA) 0.00 degrees
Head Bias (EB) 9.88 degrees
Coord Xform (EX) 00011111 Earth Coordinates Using Tilts, 3 Beam Solutions, and Bin Mapping
Sens Source (EZ) 01111101 cdhprst
Sens Avail 00011101 cdhprst

Time/Ping (TP) 00:02.00

Hardware 4 Beams
Code Reps. 9
Lag Length 0.25 m
Xmt Length 2.23 m

1st Bin 3.12 m

BT Pings/Ens (BP) 0
BT Ens Delay (BD) 0
BT Cor.Thres. (BC) 0 counts
BT Eval. Thres. (BA) 0 counts
BT PG Thres. (BG) 0
BT Mode (BM) 0
BT Err Thres. (BE) 0 mm/s
BT Max Range (BX) 0 dm

First Ensemble 00000001 06-Jul-2011 00:20:00
Last Ensemble 00058154 22-Dec-2012 22:40:00

C. Appendix 3: WHOTS-8 VMCM report

WHOTS 8 VMCM Processing Notes

- **Inventory**

Two VMCMs deplyed; both recorded at 1 minute

SN	Depth (m)	First mm/dd/yy h:m	Last mm/dd/yy h:m:s
16	10	7/711 03:00:00	06/16/12 17:46:00
19	30	7/711 03:00:00	06/16/12 17:46:00

- **Mooring log notes:**

VM 16: props spinning on recovery
VM 19: one broken prop on each hub on recovery

- **Recovery document notes:**

19Jun2012

VM019
Top rotor was spun 10 revolutions @ 22:44:00 utc 19Jun2012
Bottom rotor was spun 10 revolutions @ 22:45:00 utc 19Jun2012
VM time @ 22:47:00 utc 19Jun2012 was 22:47:16
Stopped @ 22:48:00 utc 19Jun2012
504168 records were used

VM016
Top rotor was spun 10 revolutions @ 22:52:00 utc 19Jun2012
Bottom rotor was spun 10 revolutions @ 22:53:00 utc 19Jun2012
VM time @ 22:55:00 utc 19Jun2012 was 22:57:08
Stopped @ 22:57:00 utc 19Jun22
504179 records were used

- **Data Conversion**

Intel Type-II cards were dumped using a Linux laptop. Binary 'dat' files were converted to Matlab on a Mac intel laptop (Ocelot), with do_vmcms.m, which uses (recent) standard UOP routine get_vmcm.m

- **Raw Data return**

SN	Total records	Deployed records	Start	End date
16	504179	497799	05-Jul-2011 20:00:15	16-Jun-2012 17:46:15
19	504168	497799	05-Jul-2011 20:00:45	16-Jun-2012 17:46:45

- **Timing marks**
    - **VMCM 16**

Pre-deployment spin indicates that the clock was nearly correct; Post-recovery spin indicates VMCM 16 clock is 2 minutes too fast at end of deployment

i. Pre-deployment

This is a 'bands off' note on the mooring log; because this is not done in the lab., the times may not be exact.
VMCM 16 bands off: July 6, 2011 at 18:28

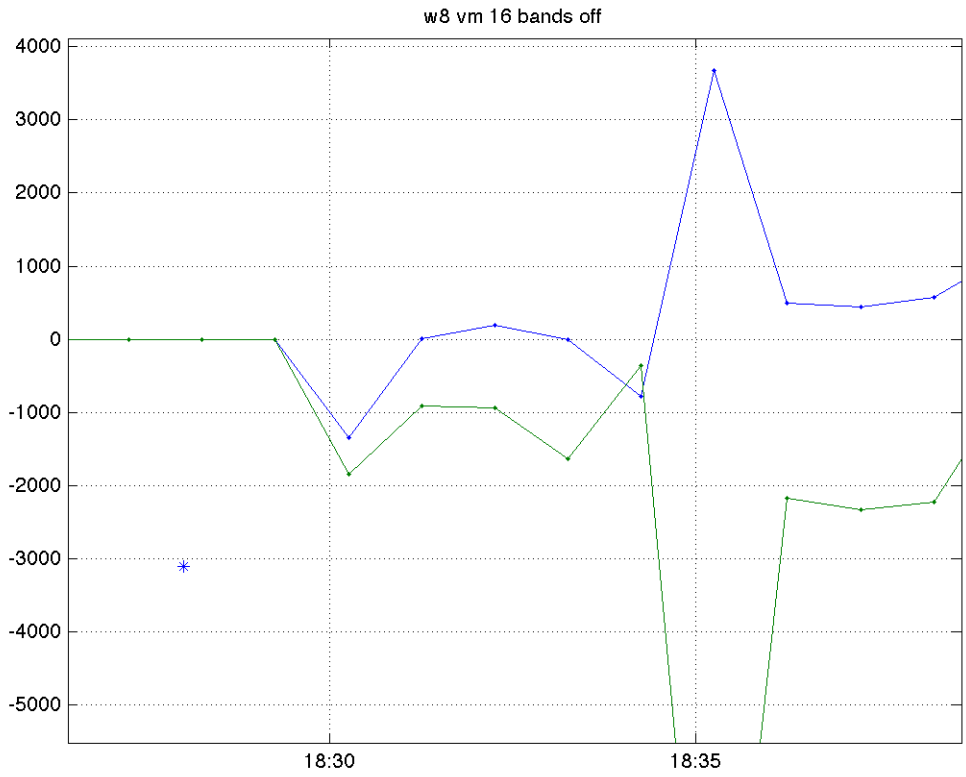

i. Post-recovery

For a more reliabel post-recovery mark, rotors were spun in the lab after recovery; also time is noted when instruments are powered down.

Top rotor 16 spun 10 revolutions @ 22:52:00 utc 19 Jun 2012
Bottom rotor 16 spun 10 revolutions @ 22:53:00 utc 19 Jun 2012
VM time @ 22:55:00 utc 19 Jun 2012 was 22:57:08
Stopped @ 22:57:00 utc 19 Jun 2012

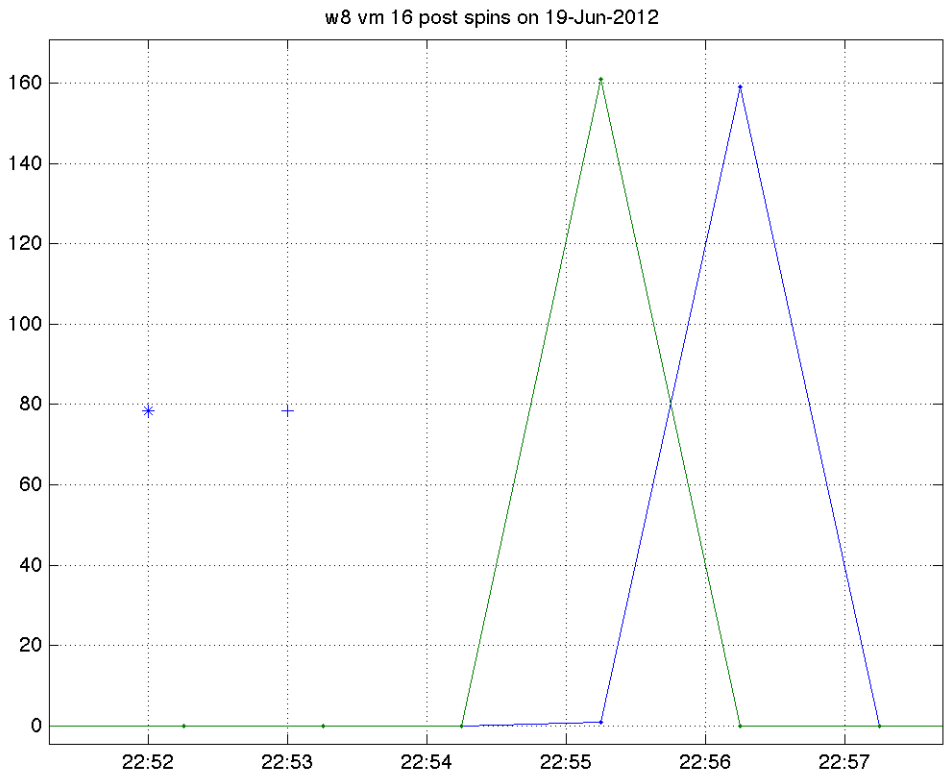

- **VM019:**

Both pre-deployment and post-recovery timing mark plots confirm the instrument tech's notes, that the clock is correct.

i. Pre-deployment

Pre-deployment timing mark is a 'bands off' note on the mooring log; because this is not done in the lab., the times may not be exact.
VMCM 19: Bands off July 6, 2011 at 18:17

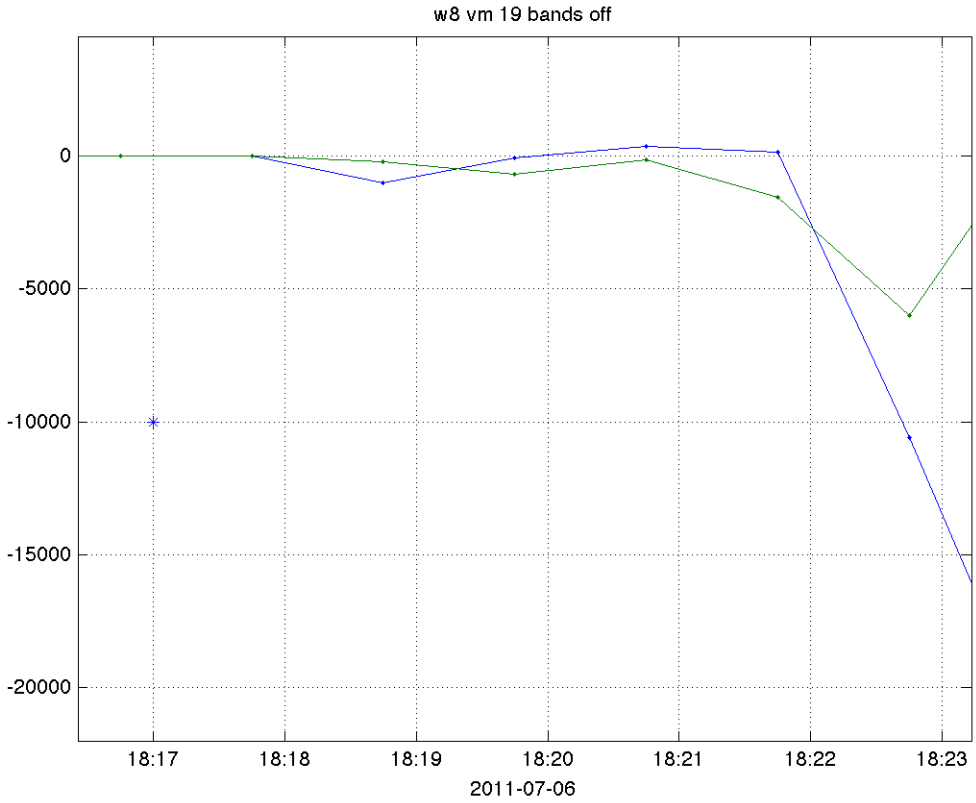

ii. Post-recovery

Top rotor was spun 10 revolutions @ 22:44:00 utc 19Jun2012
Bottom rotor was spun 10 revolutions @ 22:45:00 utc 19Jun2012
VM time @ 22:47:00 utc 19Jun2012 was 22:47:16
Stopped @ 22:48:00 utc 19Jun2012

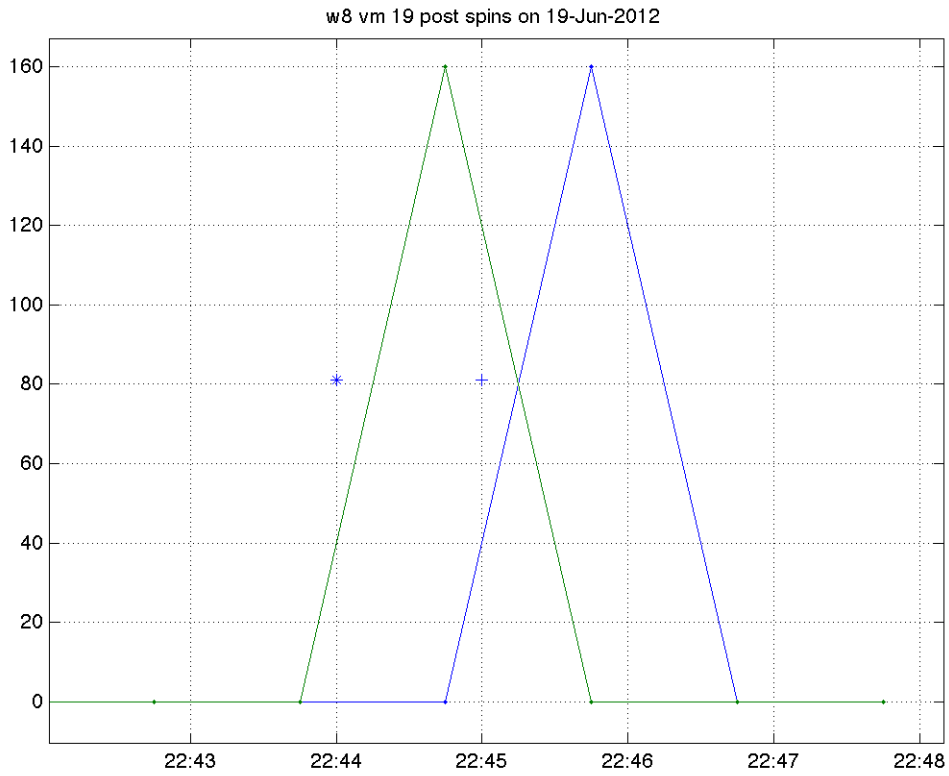

- **Post-processing**

The clock on VMCM 16 was corrected, as above (2 minutes too fast), and all variables were checked with a first difference filter using Kealn Huang's script get_vmcm_wtimecorr.m, which also truncates the data. Metadata was restructured to UOP standard with script publish_vmcm.m.